LA-UR- 11-04877

Approved for public release; distribution is unlimited.

Title: "Turbulence By Design": LDRD-DR # 20090058: Closeout Review - August 24, 2011

Author(s): Malcolm J. Andrews

Intended for: LDRD-DR Final Review Presentation
University House
Los Alamos National Laboratory
August 24, 2011

Los Alamos NATIONAL LABORATORY
EST. 1943

"Turbulence By Design": LDRD-DR # 20090058: Closeout Review - August 24, 2011

Malcolm J. Andrews

Abstract

This presentation reviews the three years of research performed under the LDRD-Directed Research titled "Turbulence By Design". The presentation was given as a "closeout" to the DR project on August 24, 2011.

"Turbulence By Design": LDRD-DR # 20090058 Closeout Review - August 24, 2011

- Title: "Turbulence By Design"
- Start Date: October 1, 2008
- Finish Date: September 30, 2011
- PI: Malcolm Andrews (XCP-4), Z-138959, 6-1430
- Co-PI's: Daniel Livescu (CCS-2), Z-179815 (DNS)
  Kathy Prestridge (P-23), Z-149289 (RM Experiments)
  Fernando Grinstein (XCP-4), Z-660029 (ILES)
  Raymond Ristorcelli (XCP-4), Z-143749 (Theory)
- Collaborating University: Texas A&M (the RT Water Tunnel)
- Post-doc's: B. Rollin, T. Wei, S. Balasubramanian, A. Gowardhan
- GRA's: A.J. Wachtor, N. Hjelm, S. Reckinger

LDRD-Directed Research "Turbulence By Design"

Carefully chosen initial perturbations can be used to control turbulent transport and mixing effectiveness

- **Liquid disintegration,**
- **Degradation of ICF capsules, Climate,**
- **Formation of oil trapping salt domes,**
- **Super-Nova Remnants (SN1987A),**
- **Boundary layer control (catastrophic loss of lift),**
- **The Eagle Nebula**

LANL Shock Tube, Prestridge, 2009, P-23

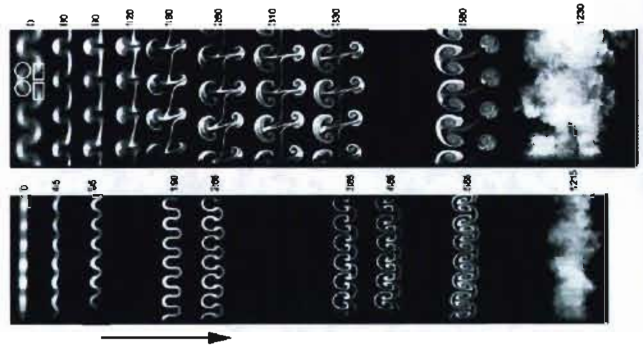

Changing initial conditions can strongly affect late-time turbulence

ILES Shock Tube, Grinstein, 2010, XCP-4

Andrews, 2008, CCS-2, P-23

Ranjan, 2010, TAMU

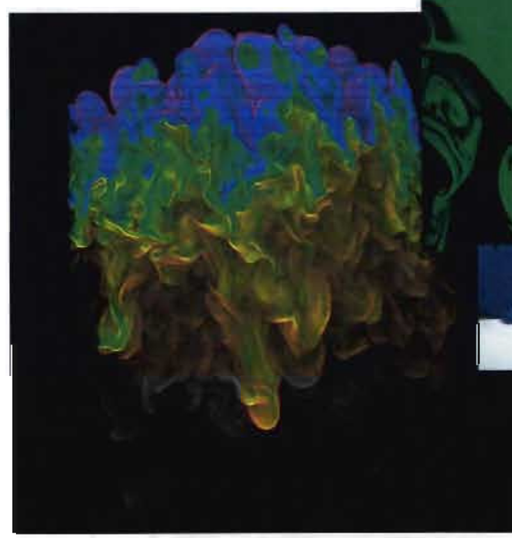

Livescu et al., 2009, CCS-2

RoadRunner DNS and experiment are used to explore IC effects on Rayleigh-Taylor (RT) Turbulence

Some Dramatic Effects of Initial Conditions

M.J. Andrews, TAMU water channel experiment

Long wavelength initial conditions

Short wavelength initial conditions

Richtmyer-Meshkov (RM) Transitions From Different Initial Conditions

(from the LANL Gas Shock Tube – K. Prestridge)

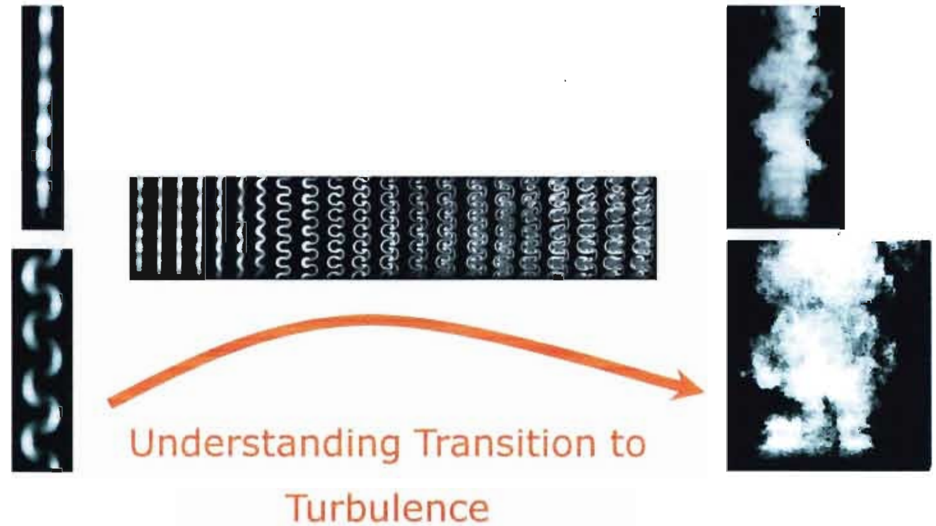

Credit: Hjelm & Ristorcelli (LBM simulations)

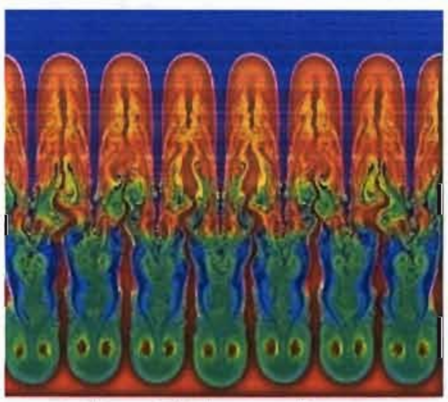

No IC noise

With IC noise

Turbulence "Control" via Initial Conditions

Hypothesis:

Carefully prescribed initial conditions could be used to control "late-time" turbulent transport and mixing effectiveness.

Motivation:

Provide a rational basis for setting up initial conditions in turbulence models for Richtmyer-Meshkov and Rayleigh-Taylor driven mixing

Overall Objective:

Predict profiles of relevant variables before the fully turbulent regime and use them as initial conditions for a (BHR) turbulence model.

Advisory Charge

- *You are the advisory panel for our final report*

Please send your advisory comments to Dr. James Hammerberg (jeh@lanl.gov)

Outline

- Project overview (goals, activities, tasks, achievements)
- Richmyer-Meshkov (RM)
- Rayleigh-Taylor (RM)
- Closing Remarks (Integrated?, validation of the hypothesis?, next steps)

Summary of Project Goals Over 3 Years

- **Our overarching scientific goal is to explore, and make use of, large-structures embedded in the initial conditions – *memory of initial conditions is NOT lost*.**
- **Our practical goal is to describe birth to full development of turbulent mixing – so enabling prediction and design.**
- **Main objectives:**
  - **Enhance the predictive capability** of Turbulence Models by demonstrating how initial conditions can be properly accounted.
  - **Demonstrate the ability to "design"** late-time turbulence.
  - **Extend our understanding of "transitions" to turbulence**, and how they can be controlled and employed to advantage.
  - **Show how under-resolved computational simulations** can correctly incorporate initial condition information.
  - **2nd Year review adjustment:** Metrics for material mix development

Overview of Research Schedule

Year 1: Single-mode & two-mode

Year 2: Multi-mode and mode-coupling

Year 3: Multi-mode/Multi-Physics

Overview

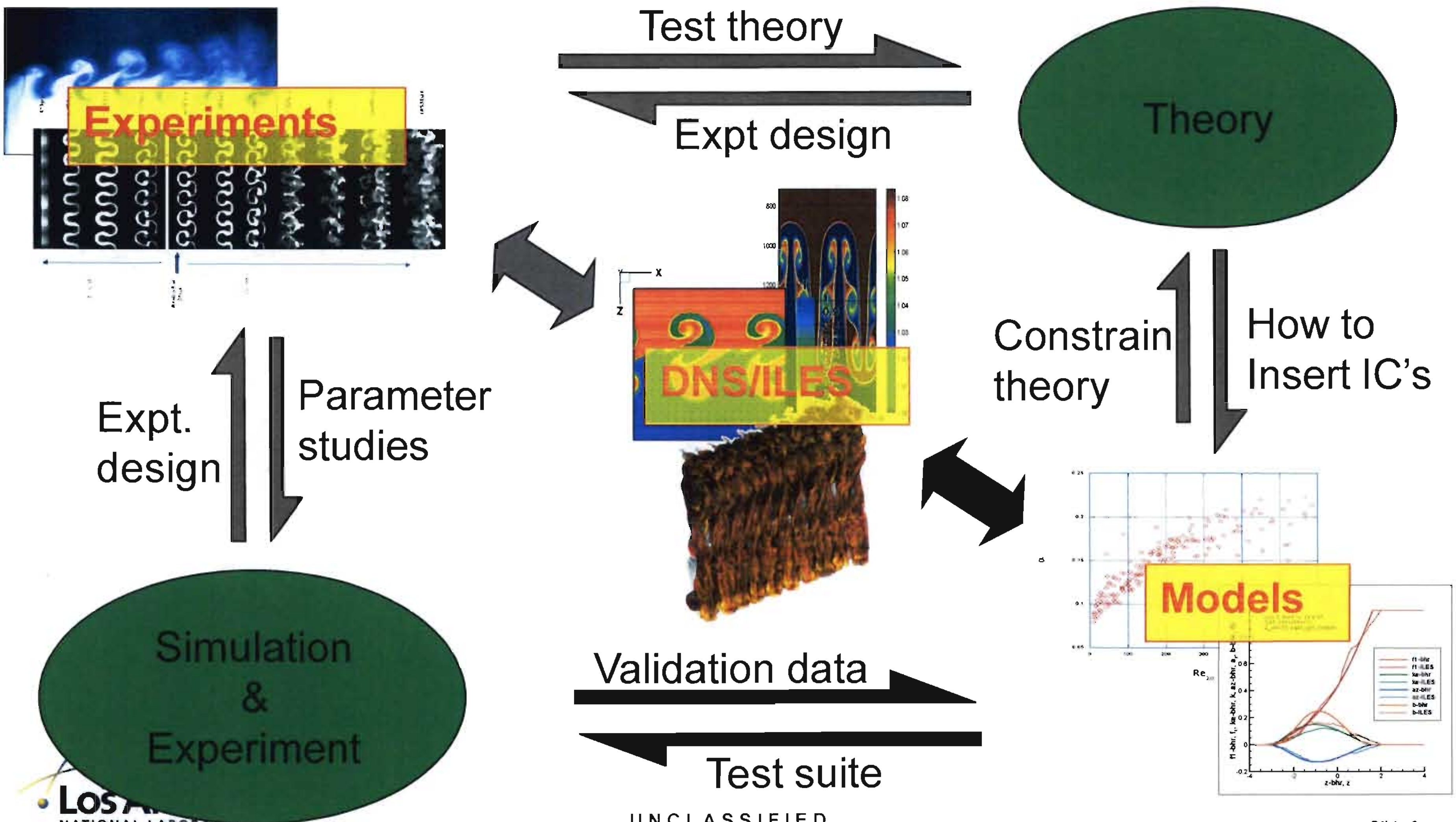

Experiments
Test theory
Expt design
Theory
DNS/ILES
Expt. design
Parameter studies
Constrain theory
How to Insert IC's
Models
Simulation & Experiment
Validation data
Test suite

Project Tasks by PI, co-PI – Summary of Completion Status

Yr	Main Tasks	Main Deliverables	% Complete
Andrews – Deterministic theory			**A(ndrews)**
1	Uncoupled ballistic model.	Model for broad-band experiments, without mode coupling and suitable for single and multi-mode experiments.	100%
2	Incorporate mode-coupling.	Validated model for TbD engineering designs and related to on-going experiment. Also, to include mode-coupling terms from Haan.	100%
3	Incorporate molecular mixing.	Validated model for miscible & immiscible RT and RM to use as a design tool to validate TbD – **"miscible" not done in favor of "metrics"**	100%
2/3	**"Metrics"**	New task after 2nd year review: Metrics for RT and RM transition and turbulence model use (replaced "Molecular mixing")	100%
Ristorcelli – Turbulence theory			**R**
1	Investigate self similar statistical solutions for variable density (VD) RT & RM.	Obtain solutions and VD self similar scalings; initiate validation with experiment and engineering models.	100%
2	Using self similar VD solution synthesize reduced order model.	Link to Andrews bottom-up engineering model, and derive link to ICs.	100%
3	V&V with expt. data, ILES and perhaps DNS.	Demonstrate predictability outside of V&V, and demonstrate links to ICs and TbD.	100%

Project Tasks by PI, co-PI – cont.

Yr	Main Tasks	Main Deliverables	% Complete
	Prestridge/Andrews (TAMU) – RM & RT Experiments		**P/A**
1	Single-mode experiments	Provide ICs for ILES at Mach 1.2, and one set of ICs data from the TAMU experiments.	100%/ 100%
2	Develop multi-mode ICs using three different gas curtains in the GST.	Instantaneous velocity and density fields for model/code validation and to give Reynolds stresses, turbulence KE and molecular mixing parameters for model validation. To include error estimates and suggestions for future work. This would be the 1st such data, and will validate TbD.	100%/ 100%
3	Varying Ma experiments for the GST, Atwood and Shear for TAMU.	Three full data sets under different conditions and as in the previous deliverable, and TbD validation. Ma and Shear experiments dropped in favor of "metrics" work	100%/100 %
2/3	"Metrics" exploration	Developed κδ metric and multi-mode initial conditions	100%
	Livescu/Grinstein – DNS/ILES Simulations		**L/G**
1	ICs for TGV, RM and single-mode RT.	ICs-design ILES: a) TGV ILES V&V w/theory; b) RM ILES w/expts.;c) V&V w/single-mode RT data.	100%/ 100%
2	Compressible TGV, RM mixing; multi-mode RT (with Andrews).	Validated ILES data & ICs guidelines for TbD in RM and single-mode miscible RT expts.	100%/ 100%
3	RM/RT driven mixing; V&V with expts. and theory.	Validated ILES data & ICs guidelines for TbD in multi-mode expts.	100%/ 100%

Summary of Significant Achievements

- Prestridge et al.
  - ✓ Measurement of 3-D characteristics of IC's to constrain simulations
  - ✓ Implementation of longer test section and Stereo-PIV system
  - ✓ Evolution of three different initial conditions (density fields)
  - ✓ Characterization of transition mixing at reshock with an appropriate metric
  - ✓ Studies of bipolar behavior of gas curtain initial conditions

- Grinstein + Gowardhan + Wachtor
  - ✓ NS-Boussinesq 3D gas-curtain to serve as ICs for RM studies
  - ✓ 3D Shocked Gas-Curtain RM; IC design for TbD & BHR
  - ✓ ILES-XRage RM V&V (vs. expts. & previous LES); bipolar behavior of ICs
  - ✓ Reshock effects can be emulated from first shock
  - ✓ Gas curtain studies for bipolar behavior (a new V&V test problem)

- Ristorcelli + all:
  - ✓ Devised new linear stochastic theory
  - ✓ Applied to RT to get ICs on moments for BHR model
  - ✓ Determined RM and possible RT metric for late-time development from different Ics; application to RM and RT

Summary of Significant Achievements – cont.

- Livescu+ Wei
  - ✓ Computational proposals for time on large supercomputers and DNS code set-up for incompressible R-T
  - ✓ Single mode simulations (effect of amplitude & diffusion)
  - ✓ Two mode simulations (phase shifts, asymmetric ejections)
  - ✓ 3-D DNS spectral shape studies for initial density perturbations

- Andrews + Rollin:
  - ✓ Implementation of Goncharov ODE solver
  - ✓ 1-D BHR for RT (test bed for theories)
  - ✓ Binary perturbation comparison with expt.
  - ✓ Multi-mode ODE solver + mode coupling
  - ✓ Use of 2-fluid formulas for IC's (why quadratic profiles work)
  - ✓ Use against RT and RM mixing

Publications & Awards

22 International Journal Publications (18 Appeared), e.g.:

- Grinstein, F.F., "On integrating large eddy simulation and laboratory turbulent flow experiments", Trans. R. Soc. A 2009 367, 2931-2945.
- Livescu, D. and Ristorcelli, J.R. "Mixing asymmetry in variable density turbulence," Advances in Turbulence XII, Editor Bruno Eckhardt, Springer, Berlin, Vol. 132 Springer Proc. In Physics, 2009.
- Banerjee, A., and Andrews, M.J., "3D Simulations to investigate initial condition effects on the growth of Rayleigh–Taylor mixing," International Journal of Heat and Mass Transfer, Vol.52, iss.17-18, p.3906-3917, 2009.
- B.J. Balakumar, K.P. Prestridge, G. Orlicz, S. Balasubramanian, C. Tomkins, 2009. High resolution experimental measurements of Richtmyer-Meshkov turbulence in fluid layers after reshock using simultaneous PIV-PLIF. Shock Compression of Condensed Matter-2009, CP1195, American Institute of Physics.

63 Conference Publications/Presentations

9 Posters

Recognition: 1st place LDRD Day, September, 2009

Initial Conditions for Moments and Mix Growth Collapse with a Taylor Reynolds Number Scaling (Ristorcelli & Hjelm)

Single mode interface: $x_s(x_2, x_3, t) = a_0 e^{i(\kappa_2 x_2 + \theta_2)} e^{i(\kappa_3 x_3 + \theta_3)} e^{\sigma t}$

$$\mathrm{Re}_k = \frac{\sqrt{k}\,h}{\nu} \ \textit{at centerline}$$

Mean interfacial thickness: $\delta^2 = \langle x_s x_s \rangle = a_0^2 e^{2\sigma t}$

Mean zero crossing wavelength: $\lambda_0^2 = \dfrac{\langle x_s x_s \rangle}{\langle x_{s,k} x_{s,k} \rangle} = \dfrac{1}{\kappa_2^2 + \kappa_3^2} = \dfrac{1}{\kappa^2}$

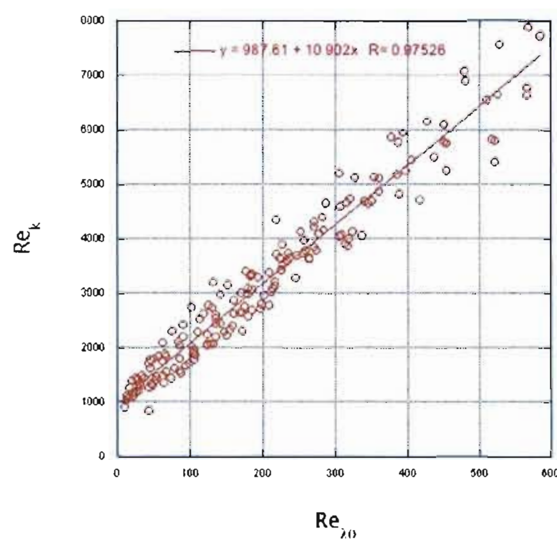

Multi-mode: $\delta^2 = \langle x_s x_s \rangle = \sum_n a^2{}_n \qquad (\kappa\delta)^2 = \langle x_{s,j} x_{s,j} \rangle = \sum_n a^2{}_n \kappa^2{}_n$

Insert into moment definitions to get initial values, e.g.:

$$k_0 = \tfrac{1}{2} A g \delta (\kappa\delta)[1 + \tfrac{2}{3}(\kappa\delta)^2 + ...]$$

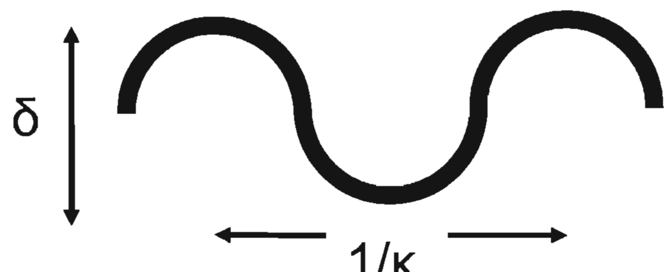

$$\mathrm{Re}_{\lambda 0} = \sqrt{\frac{A g \delta^3}{\nu^2 \kappa \delta}}$$

"κδ" metric basis

Initial (single) material interface parameterization

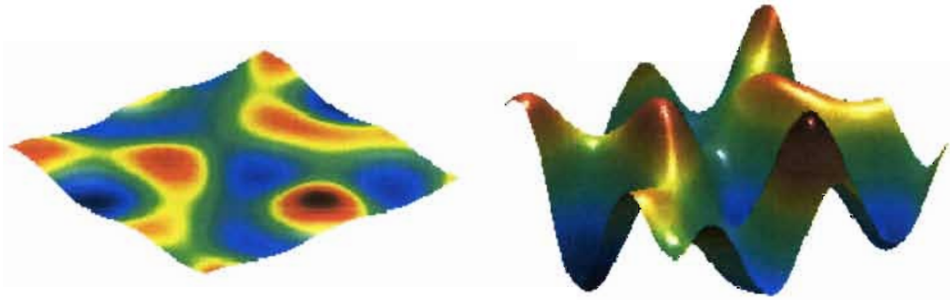

high η_0 ***class***

η_o= ***10π/12 , 10π/8, 10π/4 , 10π/2***

$$\eta_o = \kappa_o \delta_o$$

$$\sim \left\langle \nabla X_s \nabla X_s \right\rangle^{1/2}$$

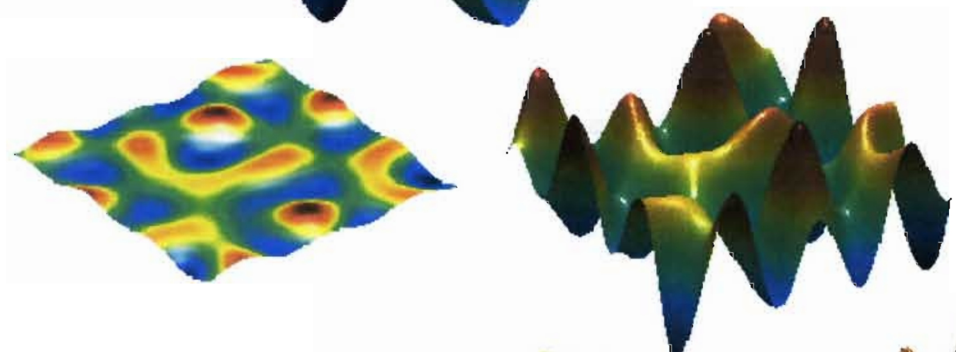

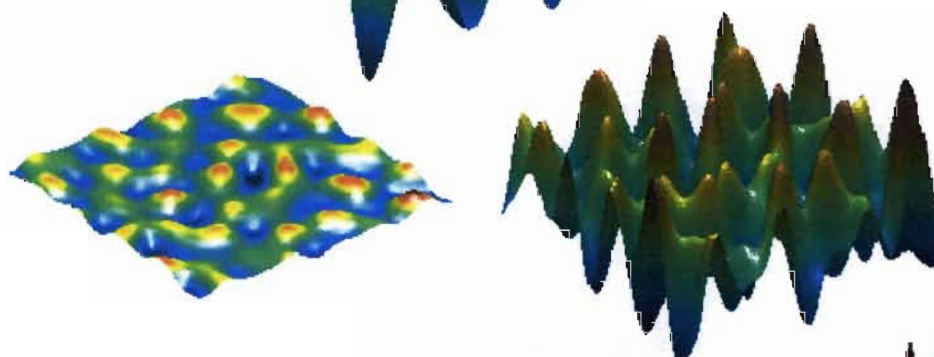

low η_0 ***class***

η_o= ***π/12 , π/8 , π/4 , π/2***

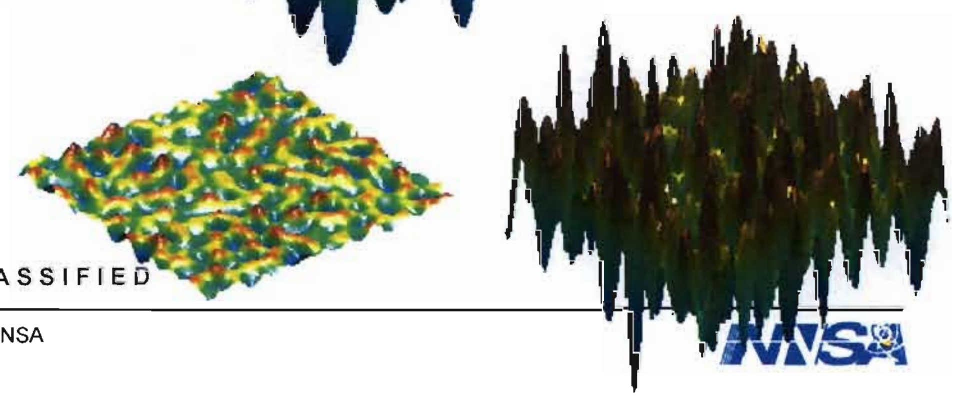

Richtmyer-Meshkov Experiments at P-23 (Prestridge et al.)

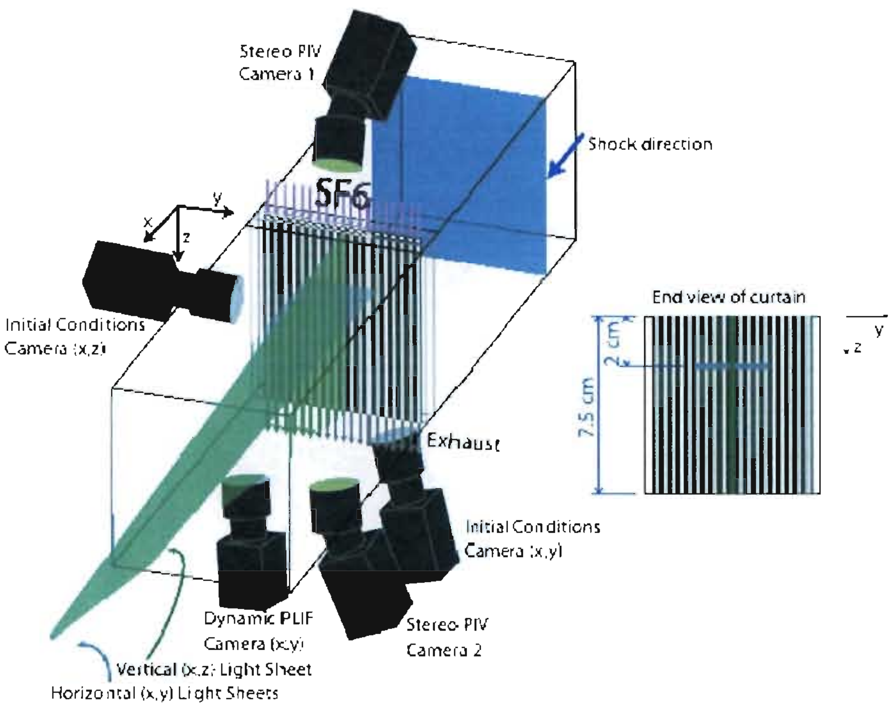

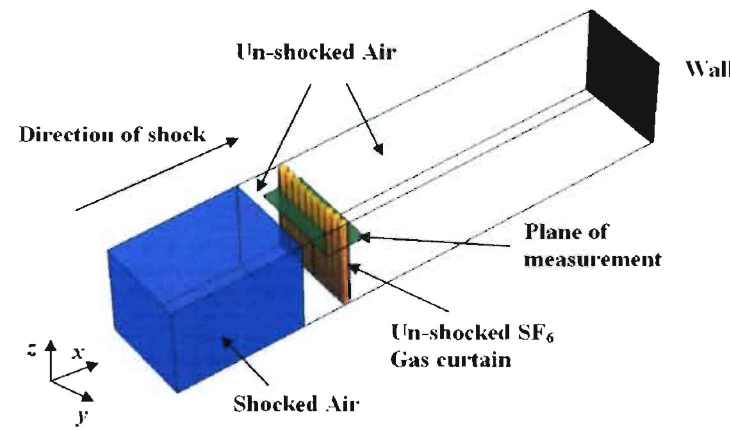

$$\eta = \kappa\delta \quad \text{where} \quad \kappa = \frac{\pi(z_c)}{y}$$

z_c is the no. of zero crossings

y is the spanwise length

If you shock a more complex interface, the flow mixes more rapidly

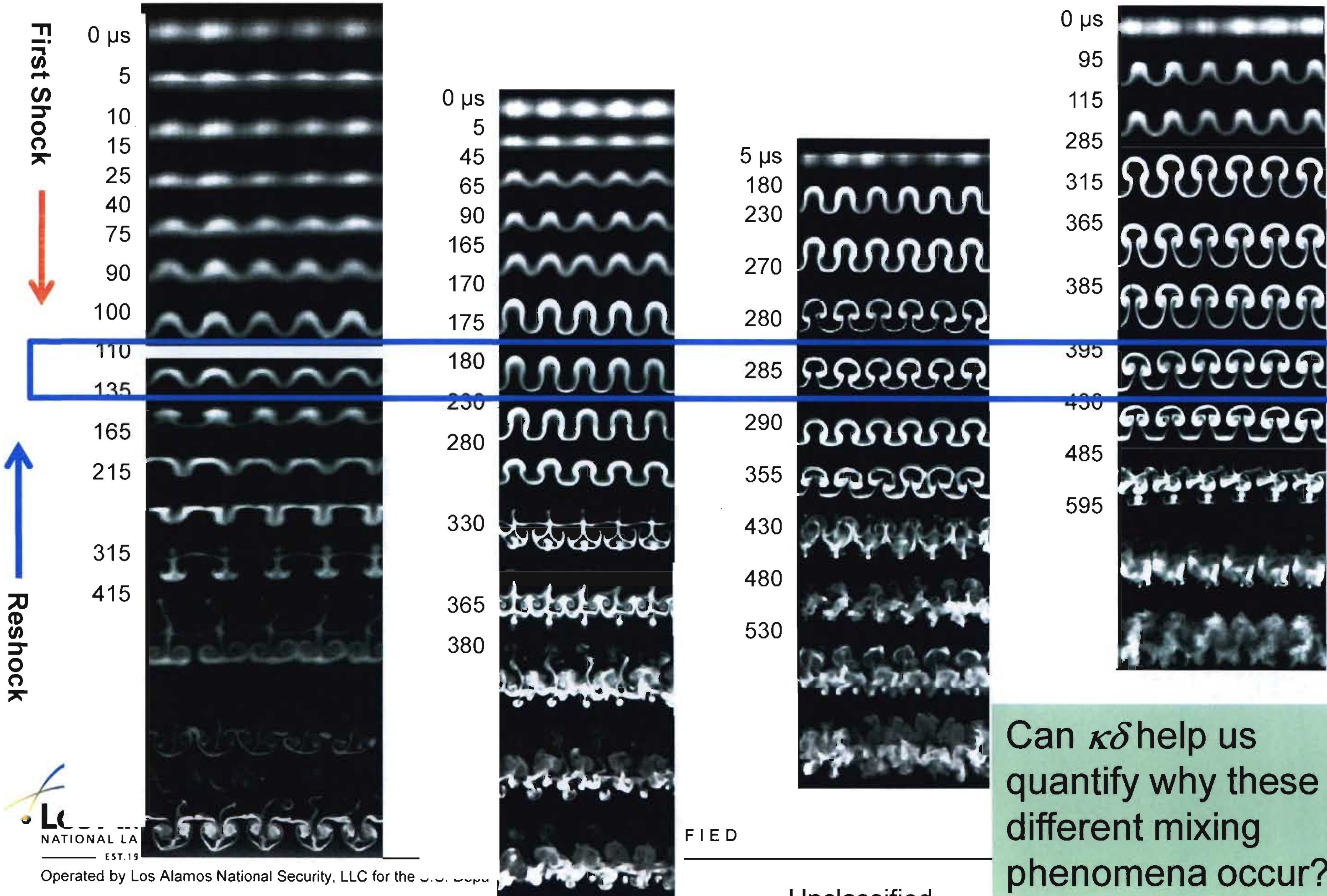

Can $\kappa\delta$ help us quantify why these different mixing phenomena occur?

κδ indicates the complexity of the initial conditions

$$\eta = \kappa\delta \quad \text{where} \quad \kappa = \frac{\pi(z_c)}{y}$$

z_c is the no. of zero crossings

y is the spanwise length

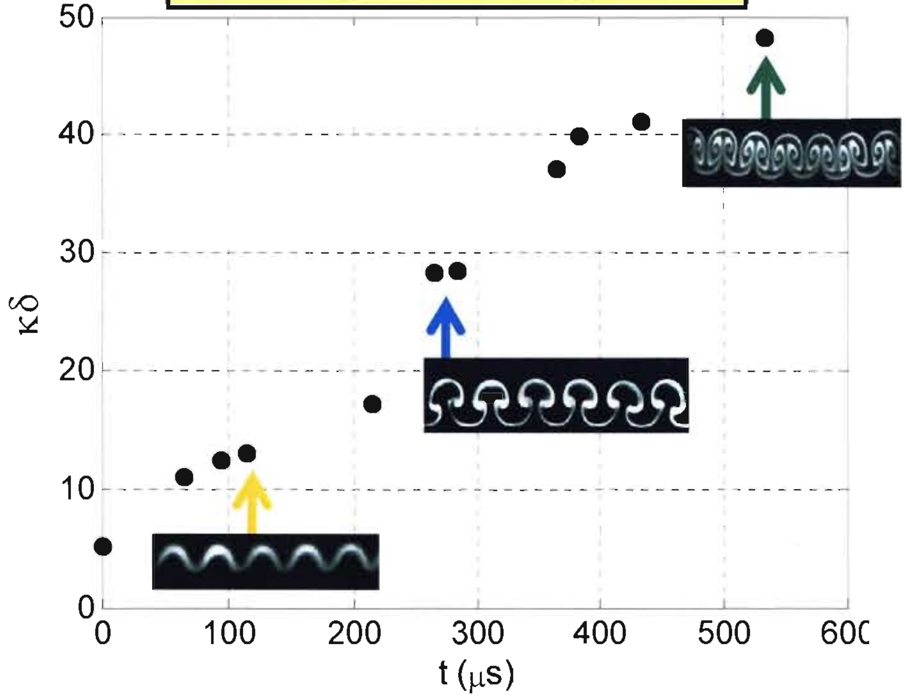

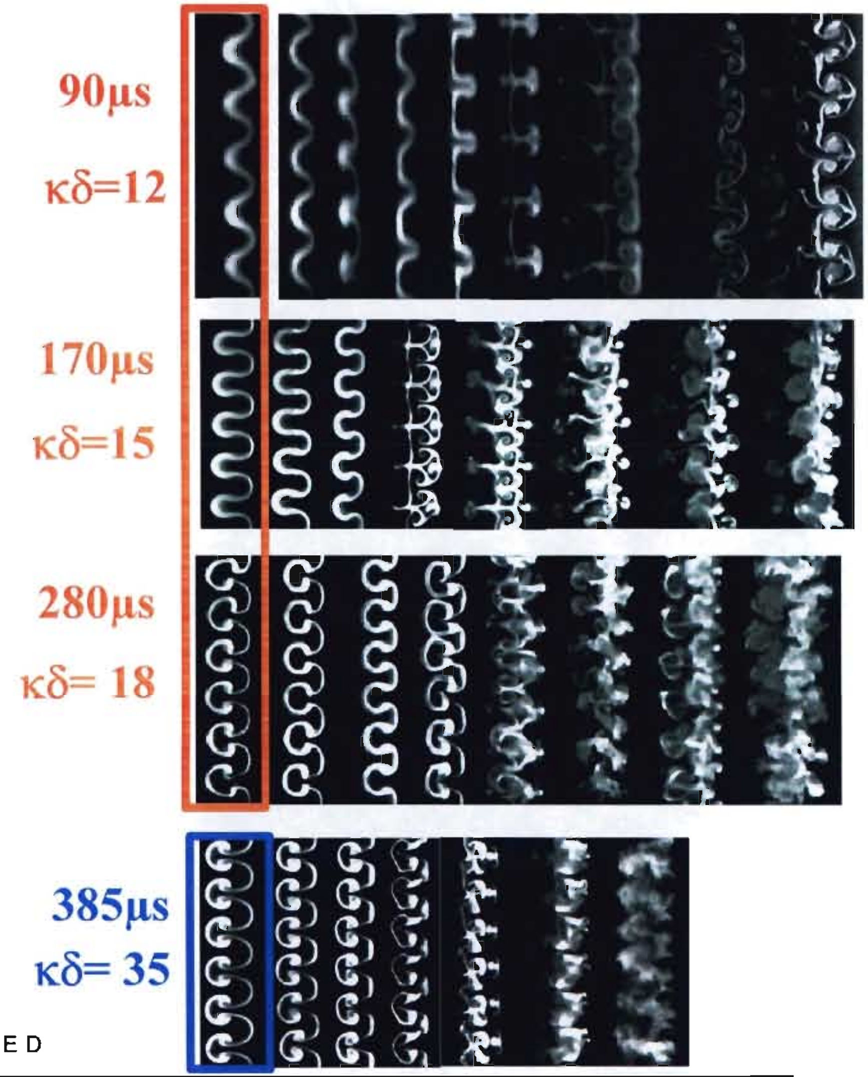

As modes present in initial conditions increase in complexity, the value of $\kappa\delta$ increases. Discontinuities at 300 and 600 μs, indicate possible changes in mixing behavior upon shock.

With similar starting amplitudes, different wavelengths in the initial conditions produce dramatic mixing differences

Incident Shock wave →

Single mode short wavelength

$\kappa\delta = 5.2$

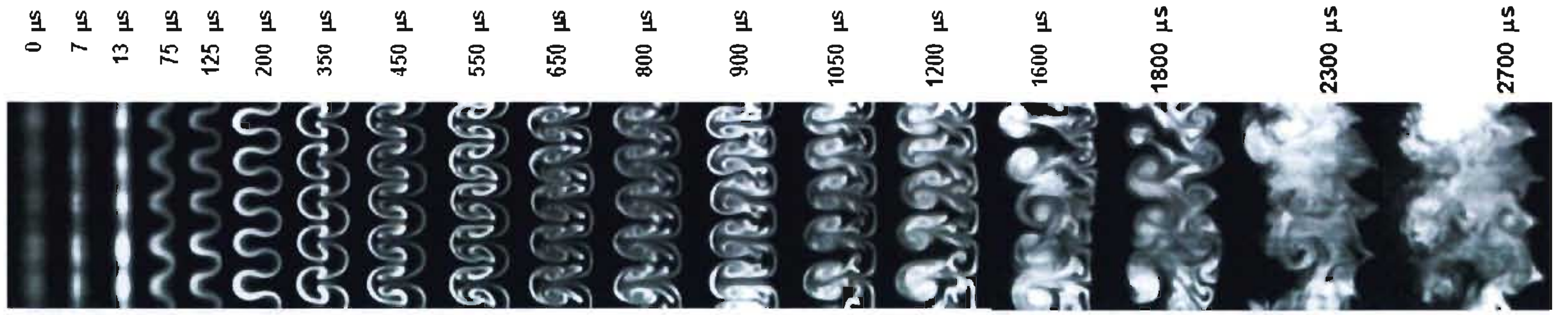

Single mode long wavelength

$\kappa\delta = 2.6$

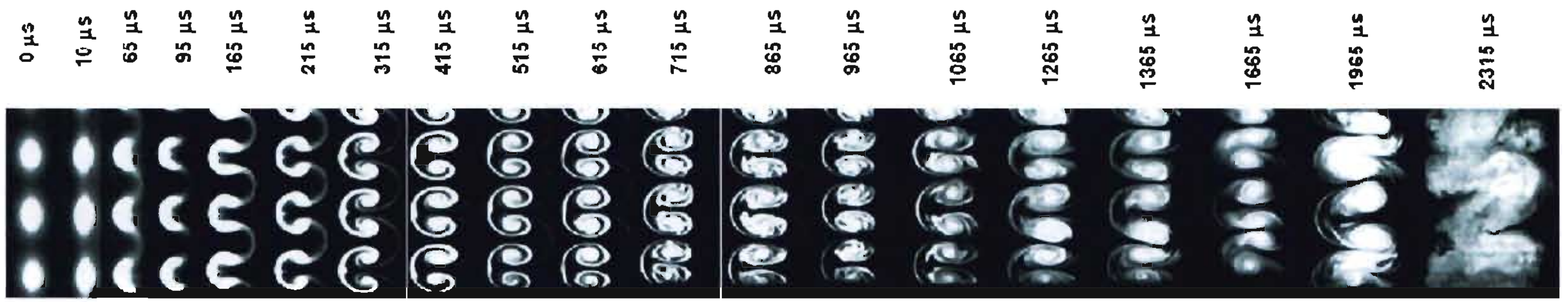

Multi mode

$\kappa\delta = 4.1$

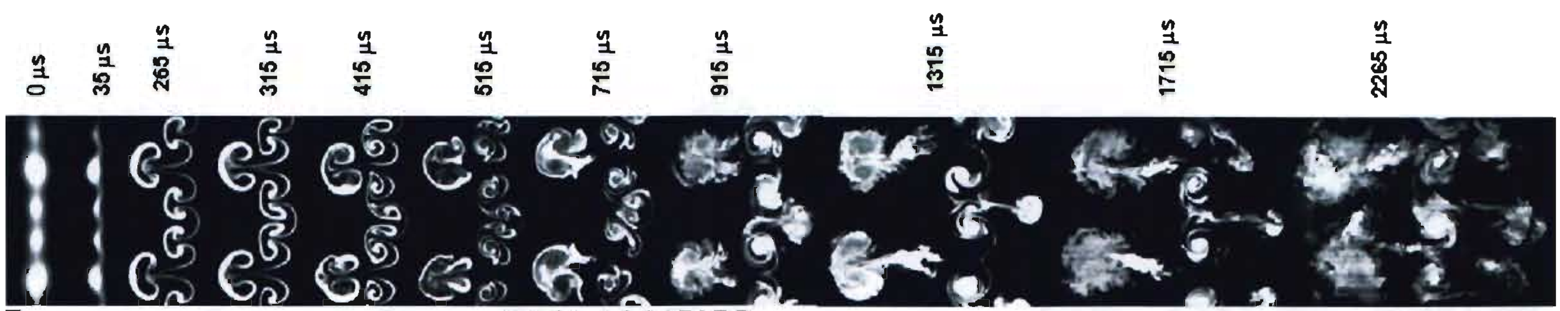

Even a simple initial condition with low κδ will transition to a highly-mixed state at late times

Shocked once, κδ=2.6
These insights into the time evolution of the density field will help us to develop a metric for when and how to initialize turbulence models such as BHR.

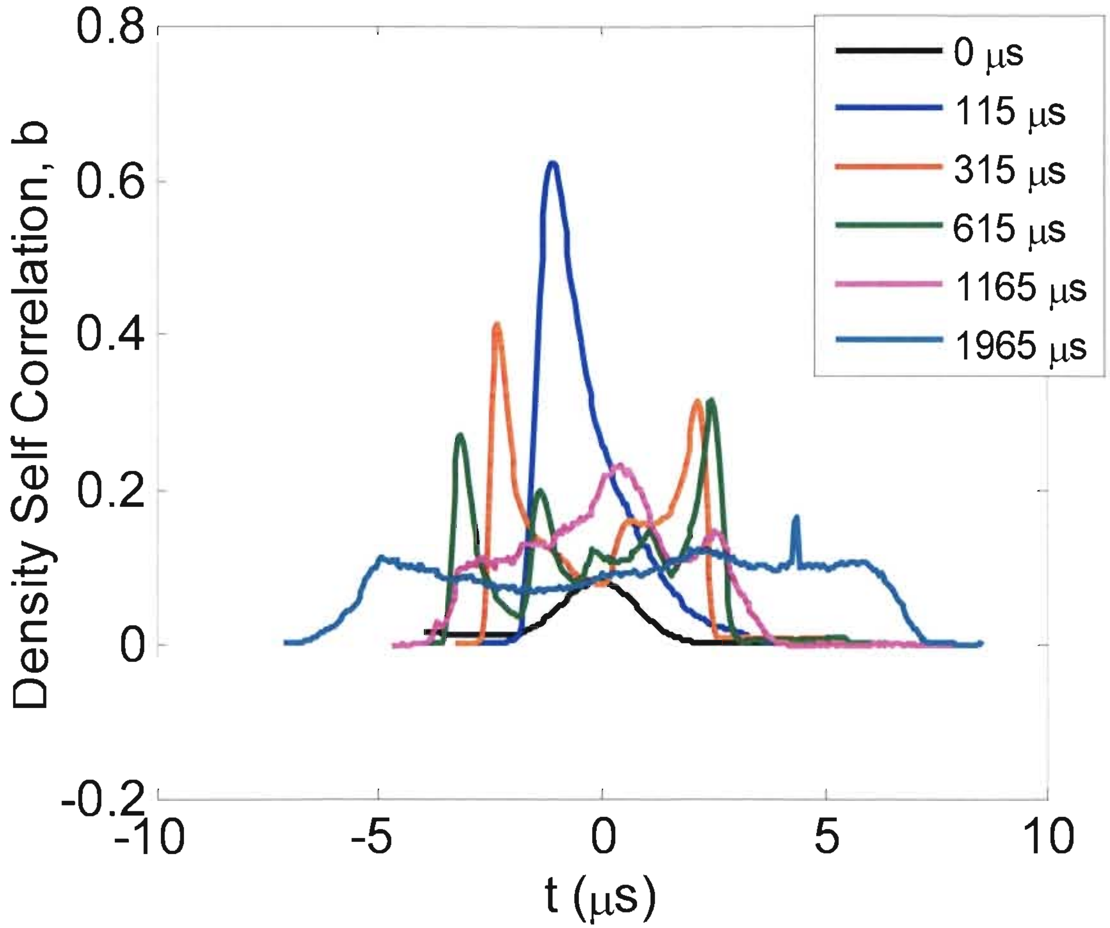

LDRD

Simulations of Initial Condition Effects on Shock-Driven Turbulent Mixing

Fernando F. Grinstein (XCP-4), Akshay A. Gowardhan (D-4: post-doc), Adam J. Wachtor (XCP-4: GRA student), J. Ray Ristorcelli (CCS-2)

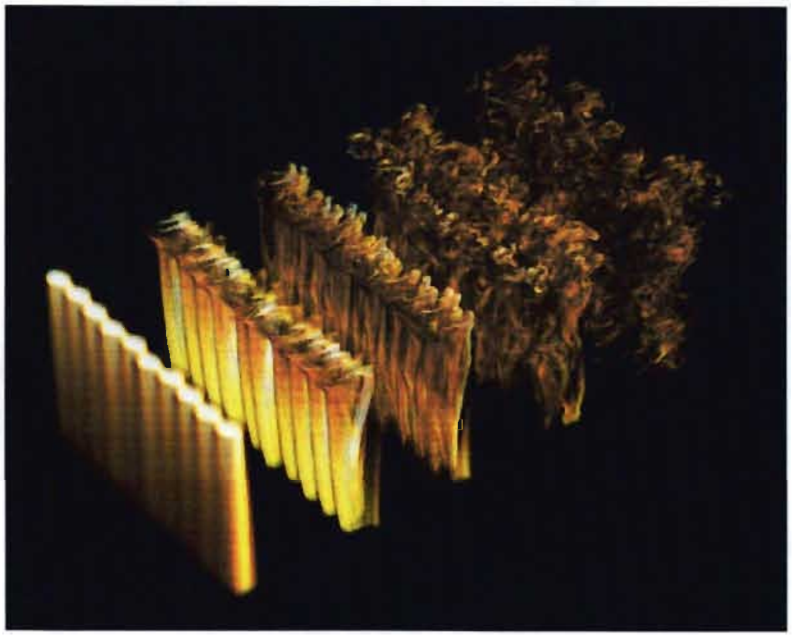

The (single-interface) planar RM experiment

- Challenges to Moment Closures: *the bipolar RM behavior*
- Can reshock effects occur on first-shock ?

The (double-interface) Gas Curtain RM experiment

- Initial 3D GC characterization and modeling
- Sensitivity of turbulence characteristics to ICs
- Data reduction and bipolar RM behavior

Initial (single) material interface parameterization

high η_0 *class*

$\eta_o = 10\pi/12,\ 10\pi/8,\ 10\pi/4,\ 10\pi/2$

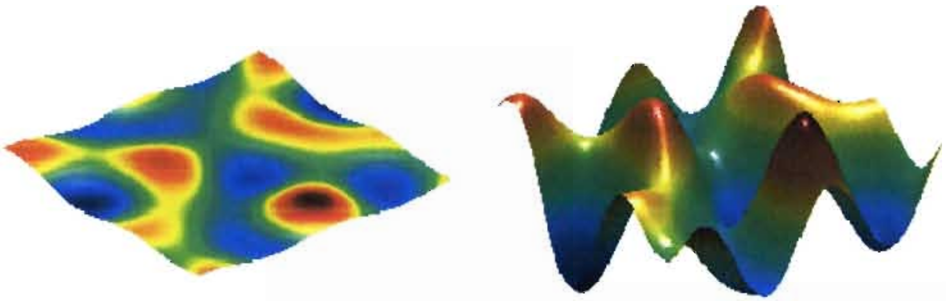

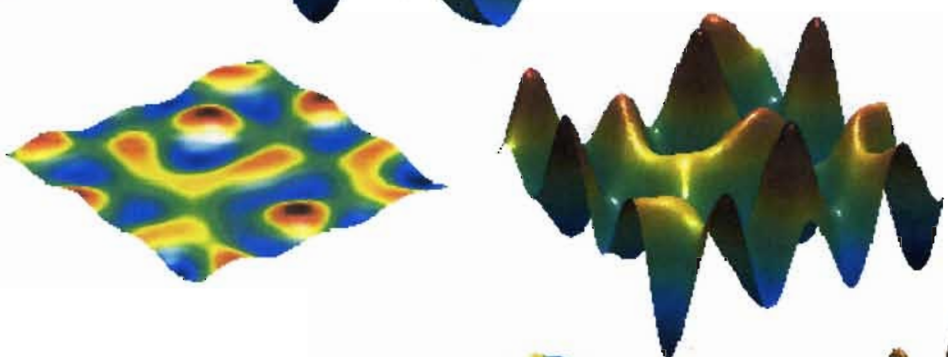

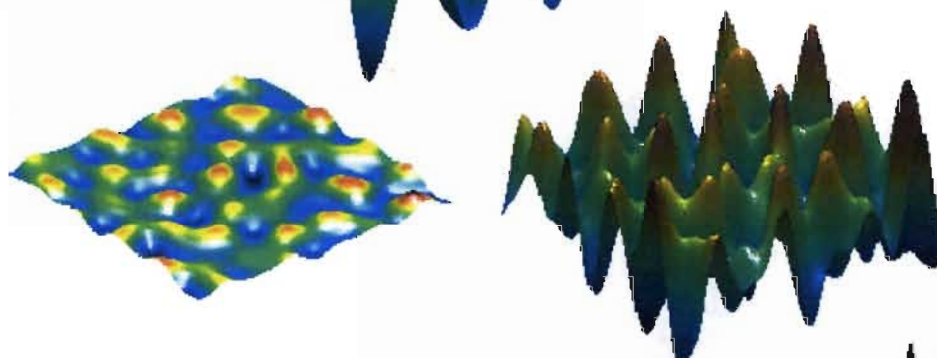

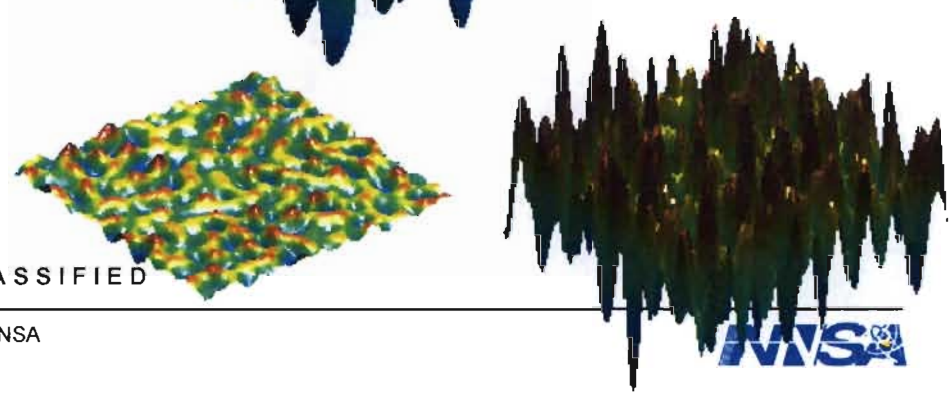

low η_0 *class*

$\eta_o = \pi/12,\ \pi/8,\ \pi/4,\ \pi/2$

Unclassified

ILES RAGE of planar Richtmyer-Meshkov:

Ma=1.5 shocked air/SF_6 – **no** egg-crate in ICs

Gowardhan, Ristorcelli and Grinstein; *PoF* Letters, 2011

Impact of *rms* slope $\eta_o = \kappa_o \delta_o$ of Initial Material Interface

Beyond Richtmyer (growth = constant × η_o):

- → ***bipolar RM behavior vs. IC morphology***
- → ***different instability mechanisms & late-time flow***

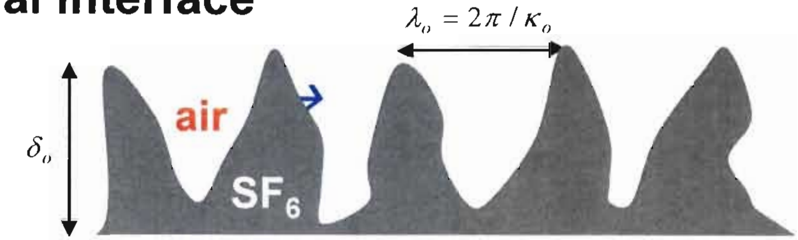

Dimensional **results**

low η_0

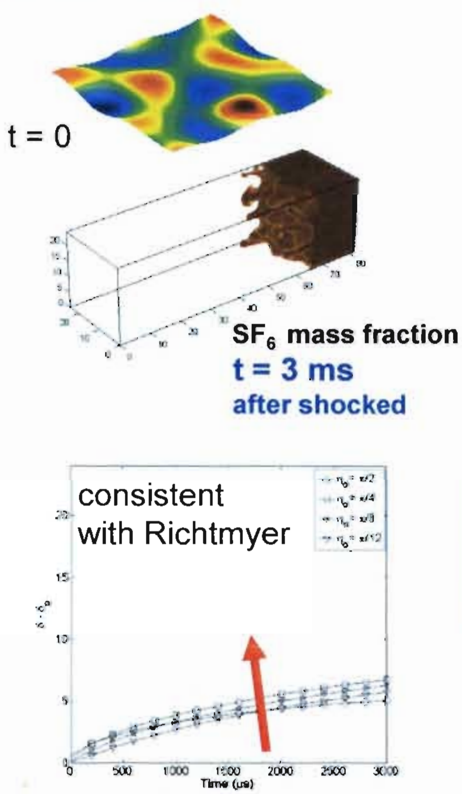

Mixing width **increases** with increasing η_o

high η_0

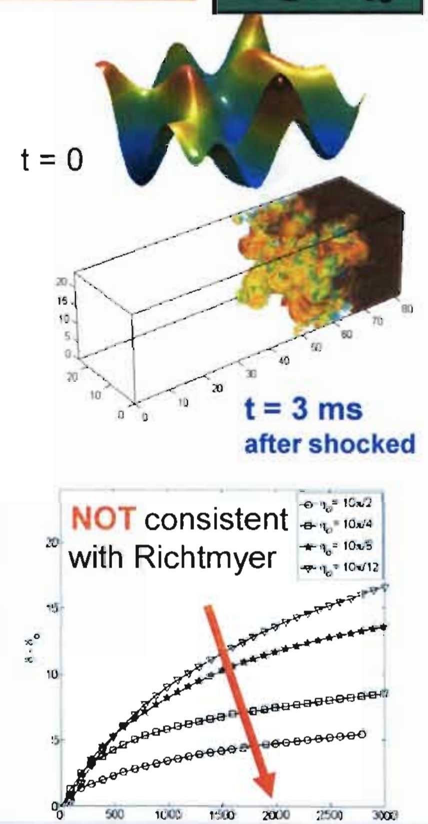

Mixing width **decreases** with increasing η_o

Non-Dimensional "Bipolar" **results**

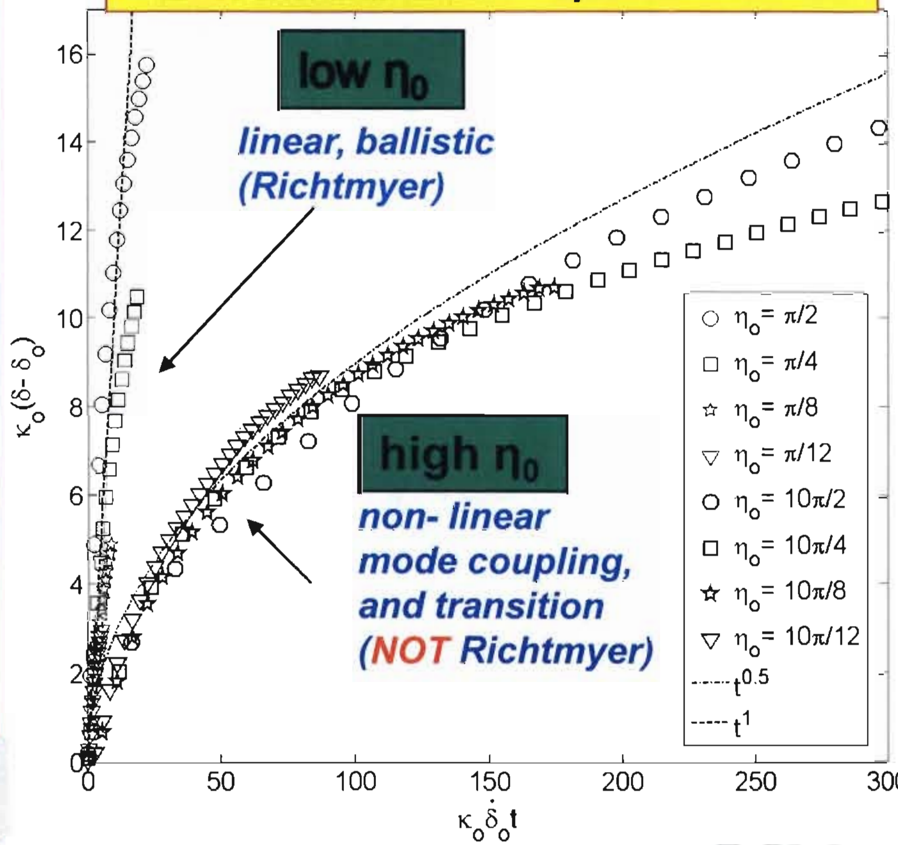

Unclassified

Consequences of Bipolar RM Behavior

(low η_o) reshock effects achieved on (high η_o) first shock

Gowardhan, Ristorcelli, Grinstein; AIAA Paper June 2011, → PoF (2011)

low η_0 ***re-shocked***

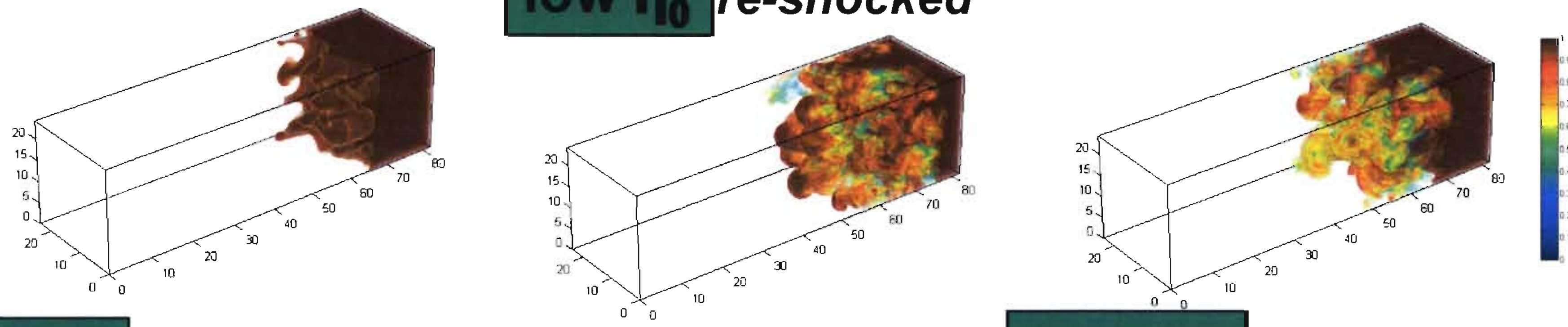

low η_0 ***first-shocked***

high η_0 ***first-shocked***

time: 3000 μs after first-shock
(or after reshock)

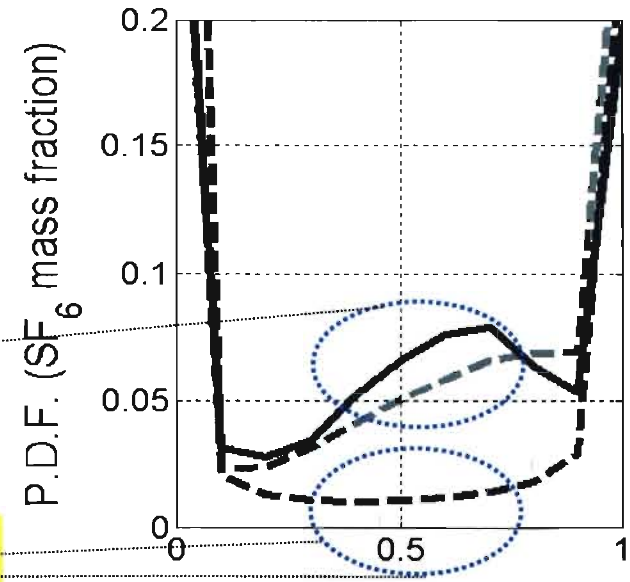

— **low η_0** ***reshocked*** **mixed**

- - - **high η_0** ***first-shocked*** **mixed**

low η_0 ***first-shocked*** **unmixed**

Planar (single interface) RM

Gowardhan, Ristorcelli and Grinstein; in preparation for *PoF* Letters, 2011

- **Initial *rms* slope η_o of the material interface controls RM evolution → bipolar RM behavior:**

low η_0 : *linear, ballistic*

high η_0 : *non-linear, mode coupling*

switch for $\eta_0 \sim 1$

→ *transition to turbulence suggested*

→ more material mixing & smaller scales

- **Reshock effects on mixing and transition can be achieved with single shock, if η_o > 1;**

- **The modeler's (initial condition) challenge**
  - **two different instabilities & growth trends**

low η_0 $\rightarrow as\ \eta_o \uparrow \quad enstrophy \uparrow \quad isotropy \uparrow \quad TKE \uparrow \quad mix-width \uparrow$

high η_0 $\rightarrow as\ \eta_o \uparrow \quad enstrophy \uparrow \quad isotropy \uparrow \quad TKE \downarrow \quad mix-width \downarrow$

Unclassified

Simulations of the Shocked (two-interface) Gas-Curtains from Prestridge

Gowardhan & Grinstein, JoT 2011, under review

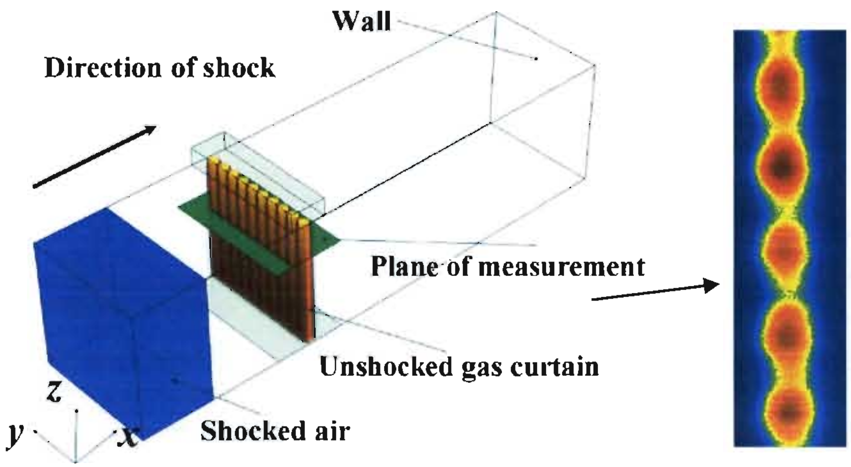

2D intensity (C / C_{max}) of SF_6 measured in a horizontal plane 2 cm from nozzle exits

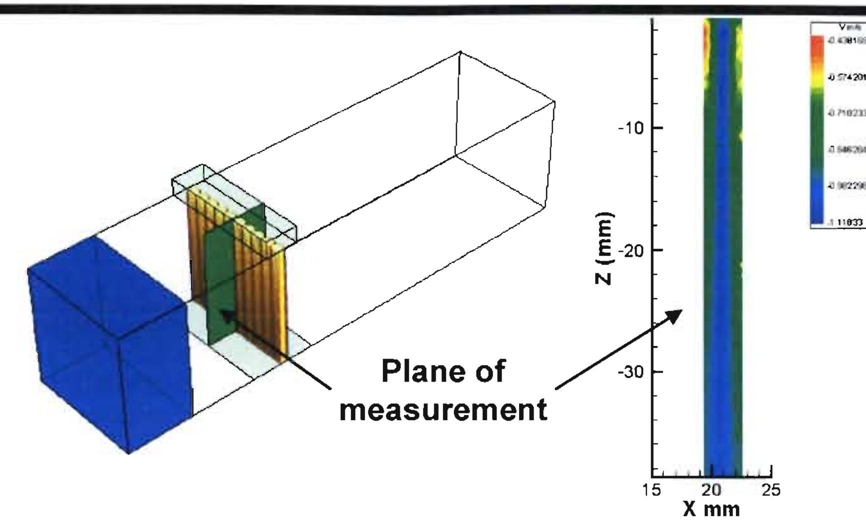

Vertical PIV @ center of GC, gives estimates of nozzle exit velocity (~100 cm/sec)

- Composition & fluctuations of SF_6 mixture at nozzle exits only estimated

  50-80% SF_6 – rest Acetone (used as a tracer for PLIF), and air;

- Uncharacterized co-flow and bottom suction used to stabilize the GC

Available info insufficient to address inherent 3D nature of GC and RM instabilities !

Simulated 3D Gas Curtain → Initial Conditions for RAGE

- Separate laminar NS-Boussinesq simulation of SF_6 falling through nozzle arrangement
- Available info from lab. expts. used to constrain 3D GC simulations

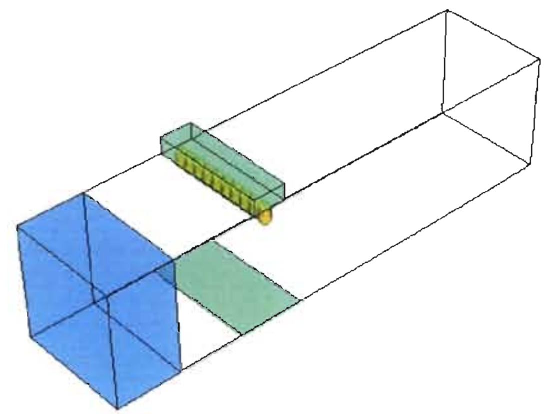

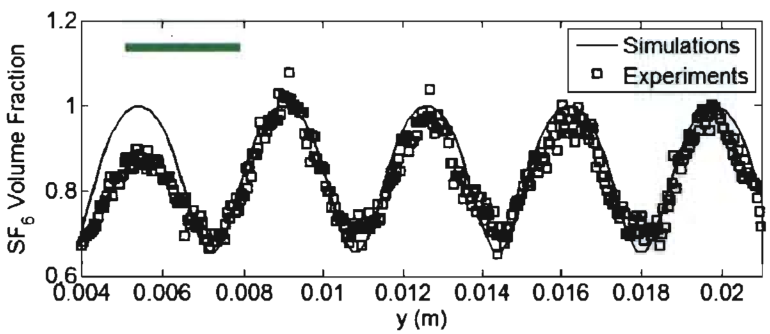

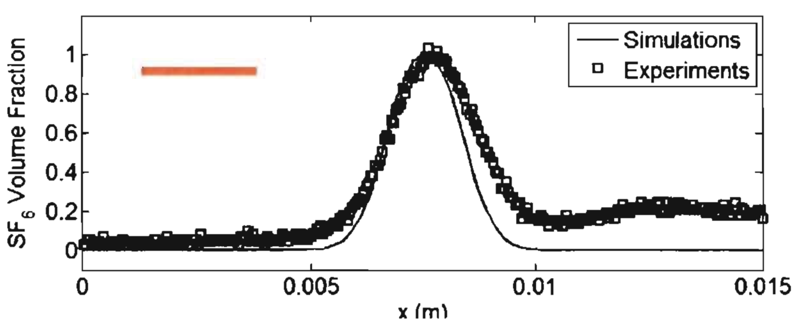

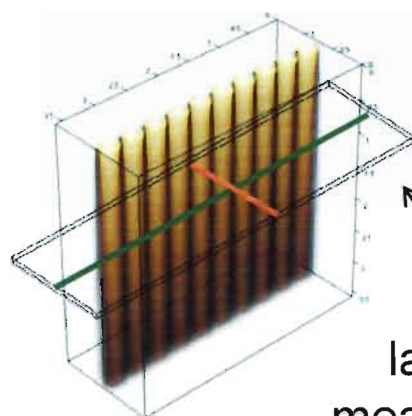

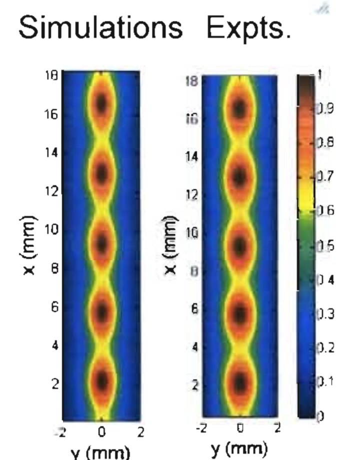

laboratory measurements plane

IC Mass-Density Variance Spectra

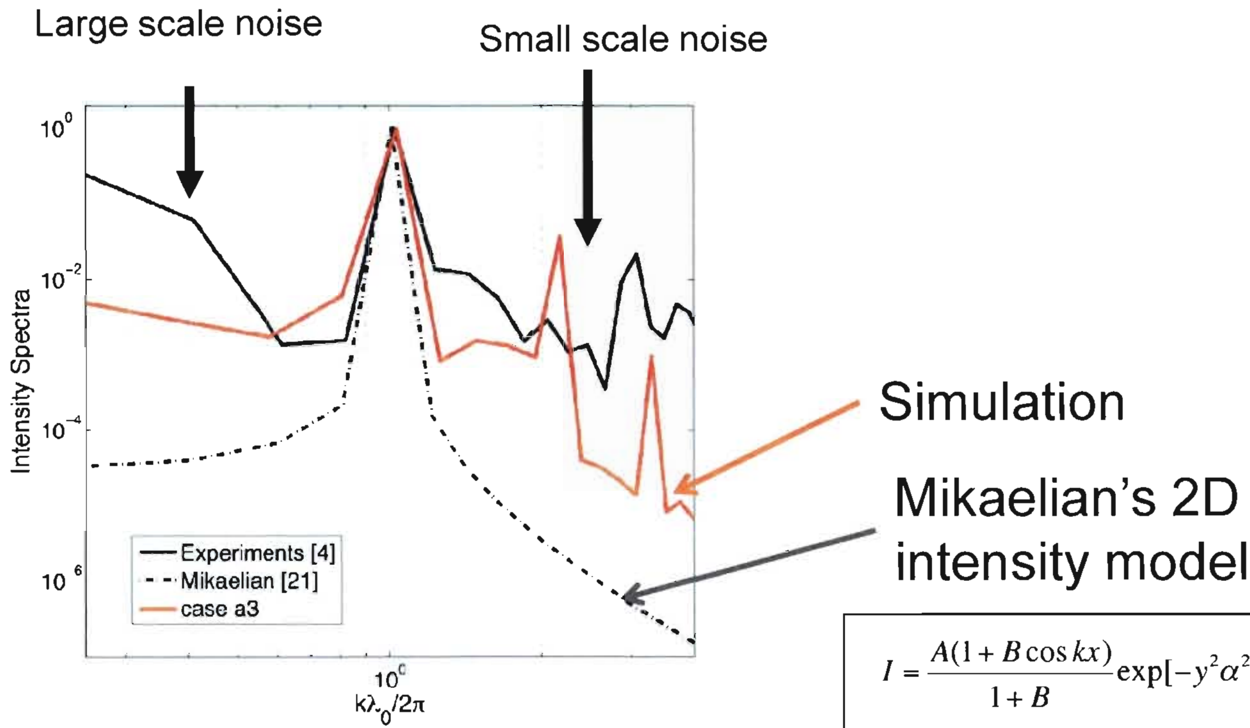

$$I = \frac{A(1+B\cos kx)}{1+B}\exp[-y^2\alpha^2/(1+\beta\cos kx)^2]$$

Mass-density variance spectra of experimental data indicates presence of *small* and *large* scale modes, in addition to 2D Mikaelian's dominant mode …

To mimic the noise present in the experiments, SF_6 concentration perturbations were added in simulation ICs

Unclassified

ILES of Shocked SF_6 Gas Curtain
RAGE V&V ; IC characterization / modeling issues

RM instability very sensitive to initial conditions (ICs)

→ insufficiently characterized ICs in lab. experiments

(e.g., SF_6 mixture composition & fluctuations, ...)

Generate initial 3D Gas Curtain (ICs for RAGE)

→ use separate 3D (NS–Boussinesq) GC code

→ superimpose multi-mode fluctuations in ICs

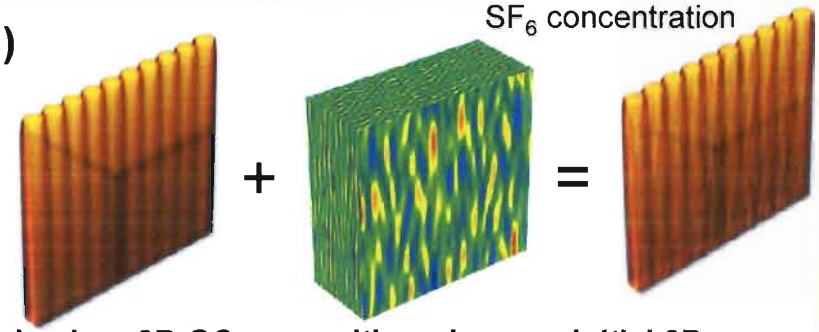

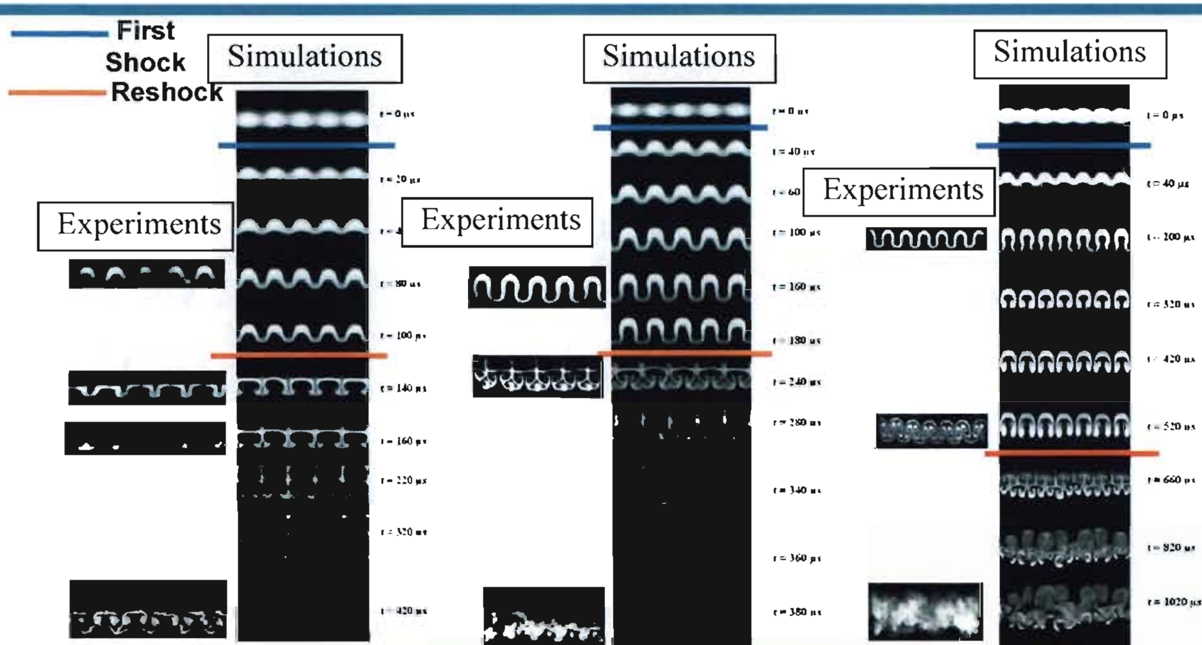

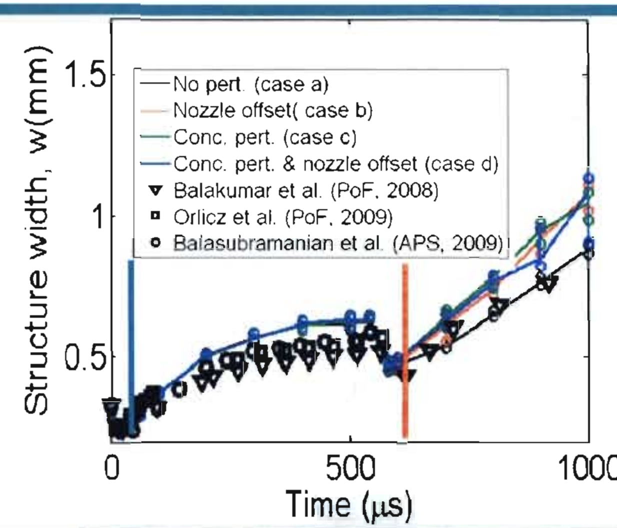

Post-reshock growth suggests issues for LES

very good agreement with lab. flow patterns and growth rates before reshock
(insensitive to ICs); late-time results fairly sensitive to ICs **after reshock !**
over-predicted early growth reflects lower effective Atwood number in expts.
(uncharacterized acetone used with *PLIF* – mixed with SF_6)

Gowardhan & Grinstein, JoT (2011), under review

NNSA

ILES RAGE of Shocked SF_6 Gas Curtain

Multi-mode IC Effects on Mixing & Transition

Gowardhan & Grinstein, JoT (2011), under review

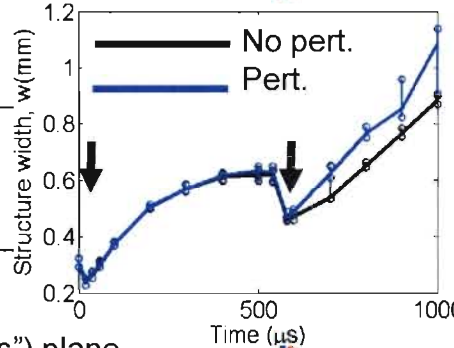

non-perturbed GC

"ballistic" growth dominates

multi-mode perturbed GC

mode-coupling promoted

visualizations at horizontal ("measurements") plane

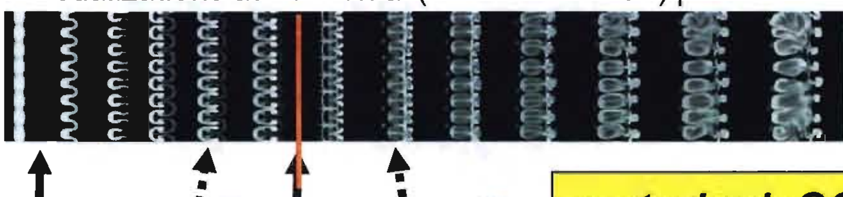

reshocked

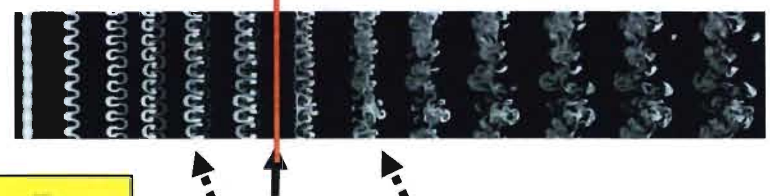

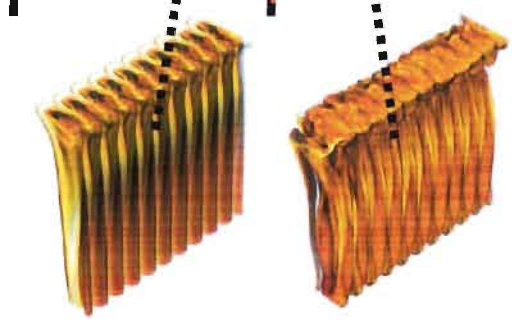

***perturbed* GC "transitions" after reshock**

- **enhanced mixing**
- **more isotropic (late times)**
- **self-similar decay spectra**

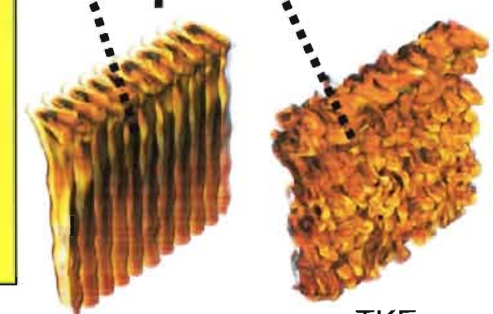

velocity variances @ t=1000μs

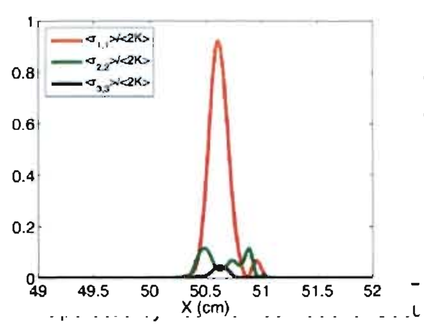

TKE spectra

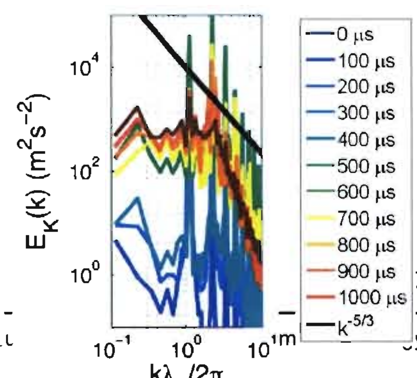

velocity variances @ t=1000μs

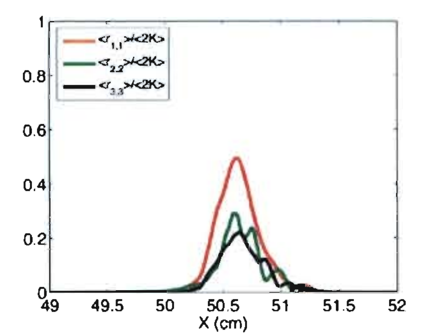

TKE spectra

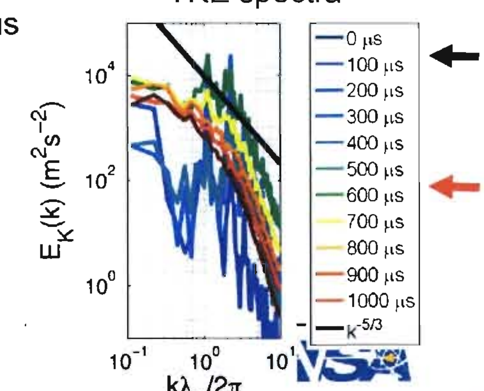

Unclassified

Bipolar RM behavior also demonstrated in terms of single IC parameter η_0 for shocked GCs

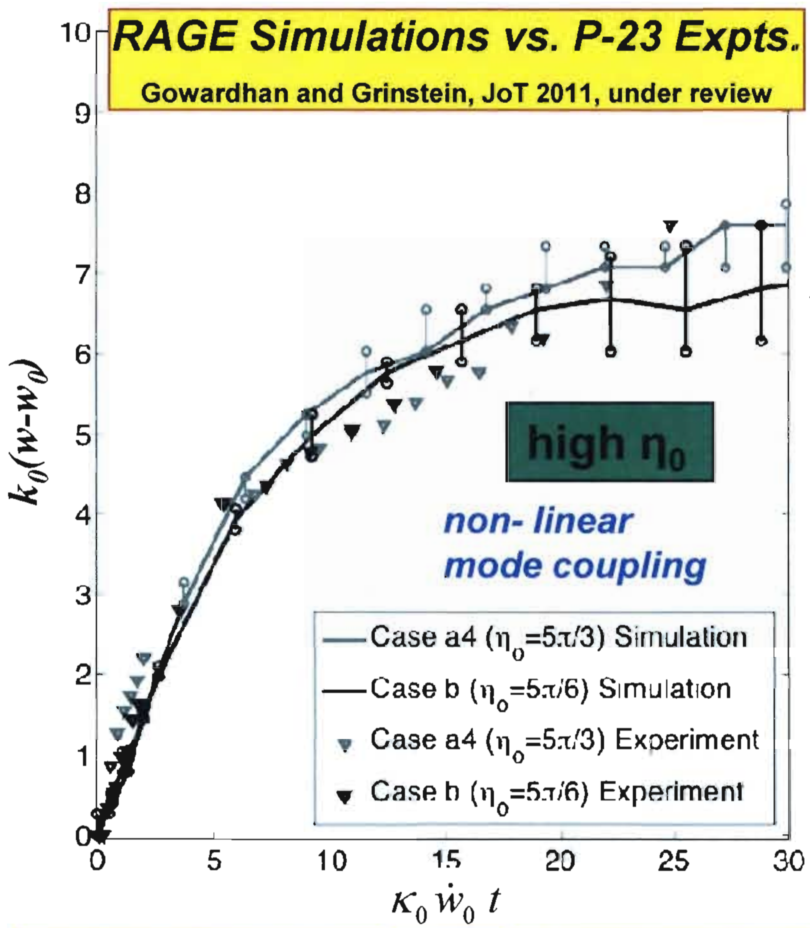

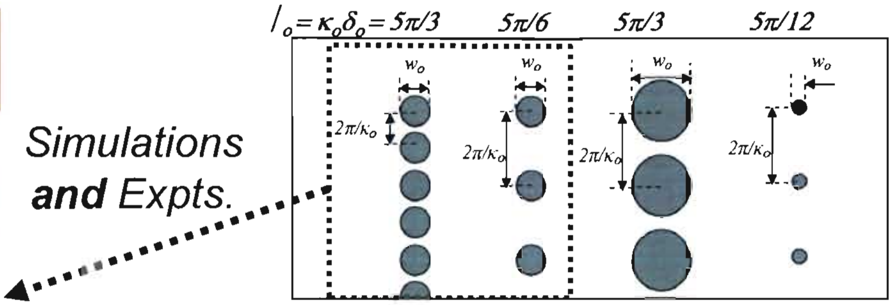

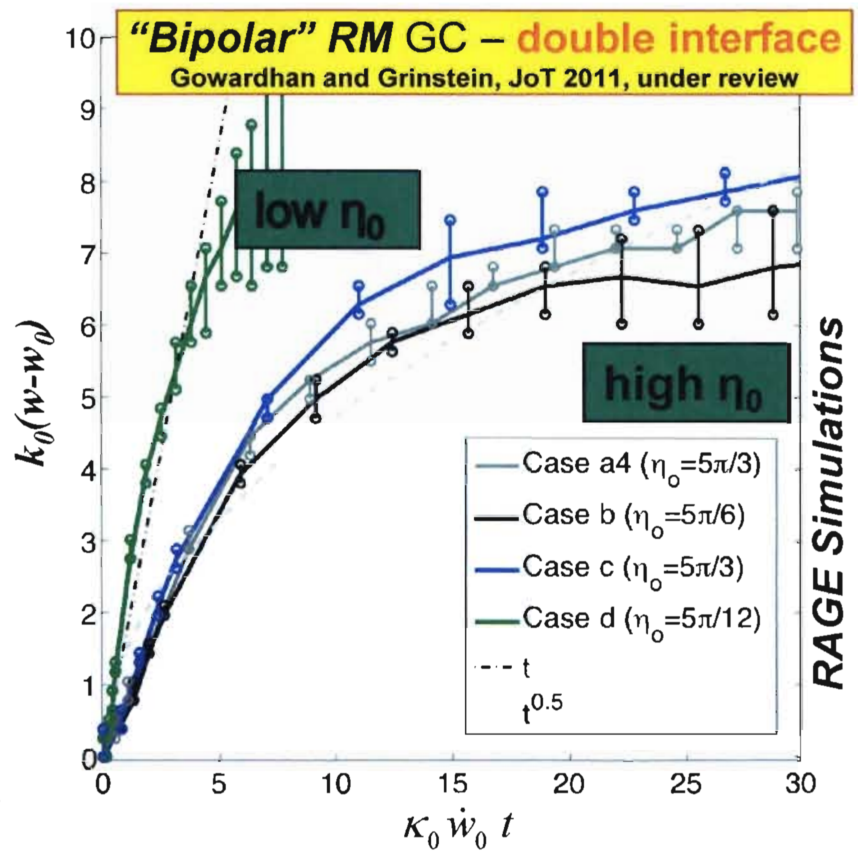

- **Modeler's Initial Condition Challenge:** two different instabilities, growth trends, and late-time characteristics
- **Instability behavior switches for $\eta_0 \sim 1$**

Bipolar RM behavior also demonstrated in terms of single IC parameter η_0 for shocked GCs

"Bipolar" RM – single interface
Gowardhan, Ristorcelli, Grinstein, PoF Letters 2011

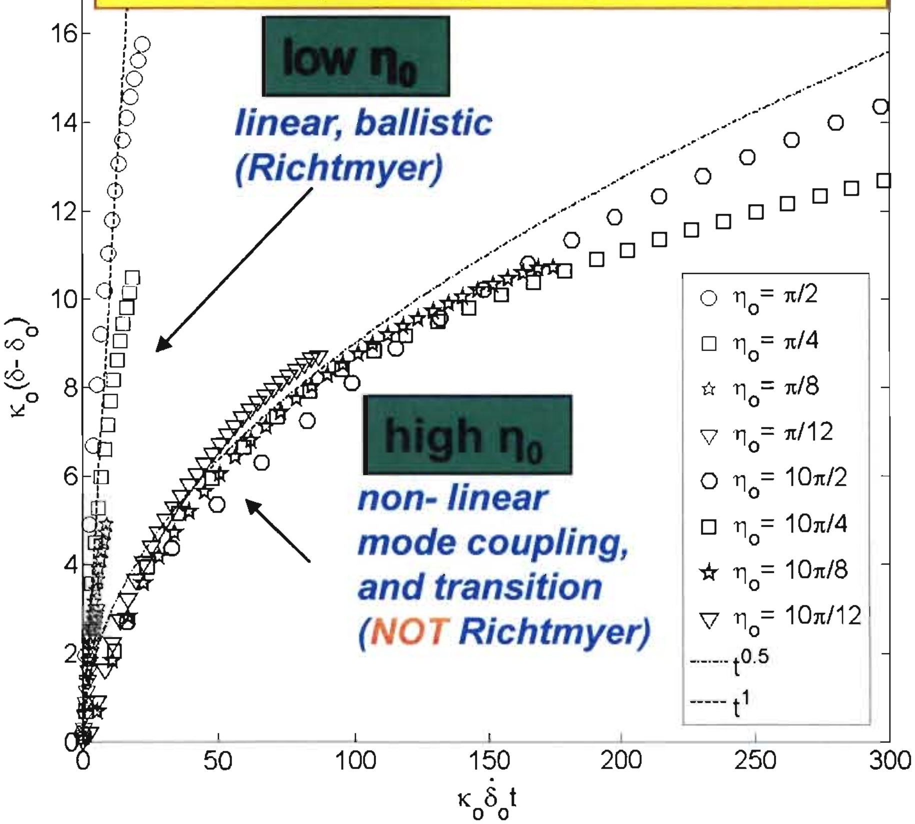

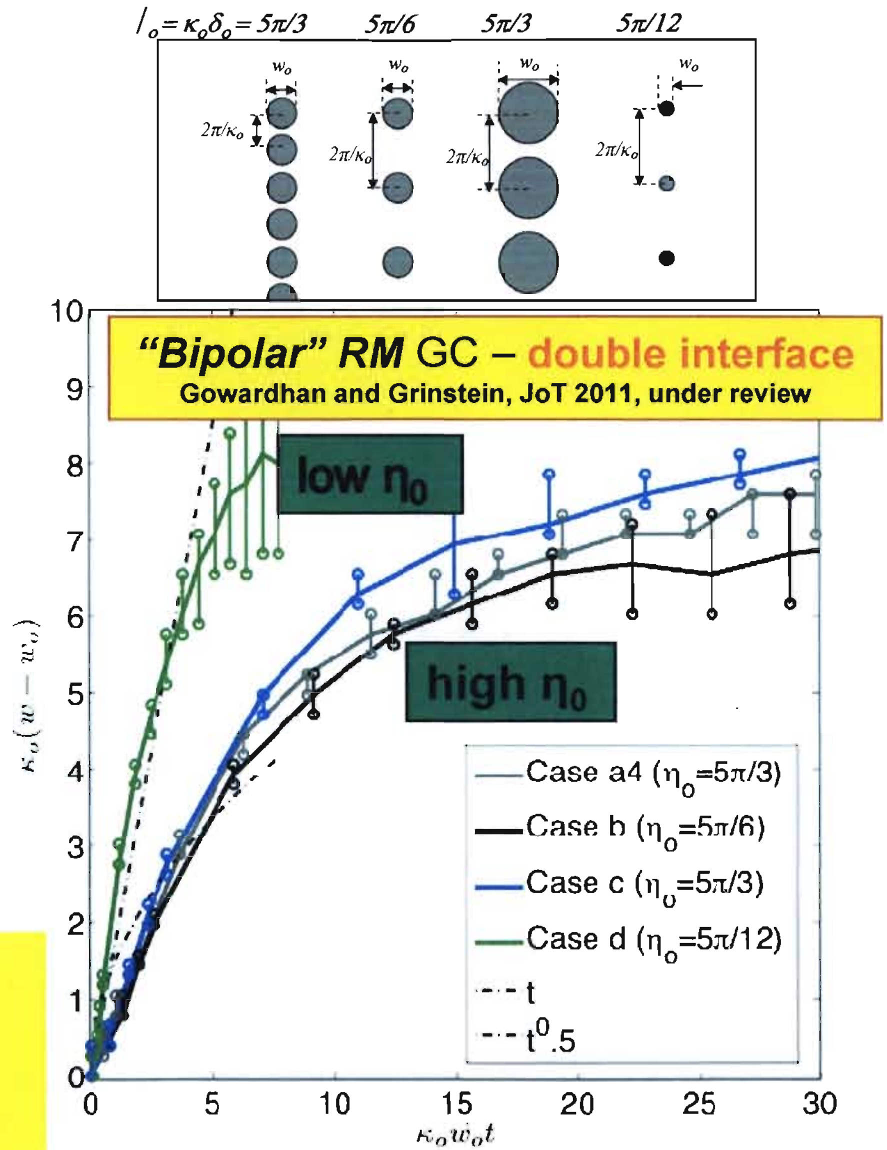

- **Modeler's Initial Condition Challenge:** two different instabilities, growth trends, and late-time characteristics
- **Instability behavior switches for η_0 ~ 1**

DNS for Initial conditions dependence in Rayleigh-Taylor

Daniel Livescu and Tie Wei (CCS-2)

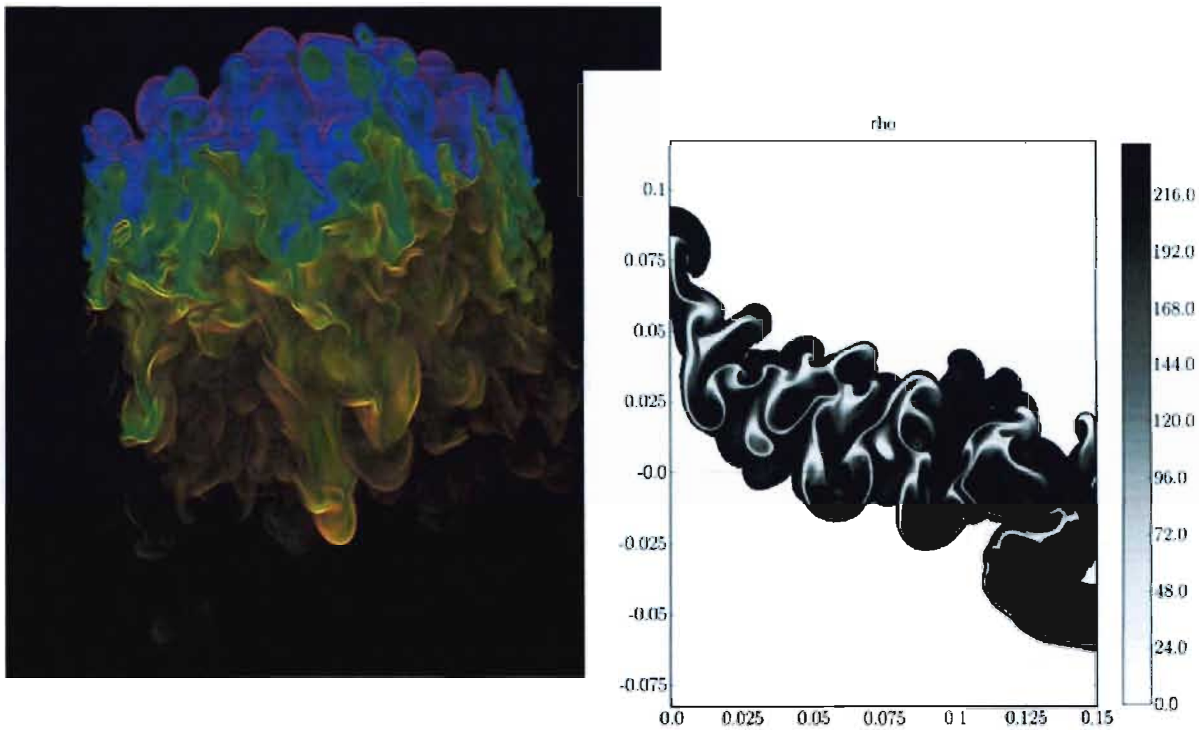

- Code used: CFDNS (Livescu et al LA-CC-09-100).
- 2-D simulations (up to $16{,}384^2$) performed at LANL and on Jaguar, ORNL.
- 3-D simulations (up to $4096^2 \times 4032$ RT) performed on Dawn, LLNL; Jaguar, ORNL; and LANL.

Two-Mode "Leaning" RT Experiments Using the New Computer Controlled Flapper (TAMU + LANL)

$$A(x) = A_1 \sin\left(\frac{2\pi x}{\lambda_1}\right) + A_2 \sin\left(\frac{2\pi x}{\lambda_2} + \delta\right)$$

$A_1 = 4mm$	$A_2 = 2mm$
$\lambda_1 = 4cm$	$\lambda_2 = 2cm$
$\rho_1 = 997.7 kg/m^3$	$\rho_2 = 99657 kg/m^3$

Phase shift : δ=0, π/2

The flapper motion imposes an initial vertical velocity given by:

$$v = \frac{dA}{dt} = \frac{dx}{dt}\frac{dA}{dx} = U_0\left(A_1 k_1 \cos(k_1 x) + A_2 k_2 \cos(k_2 x + \delta)\right)$$

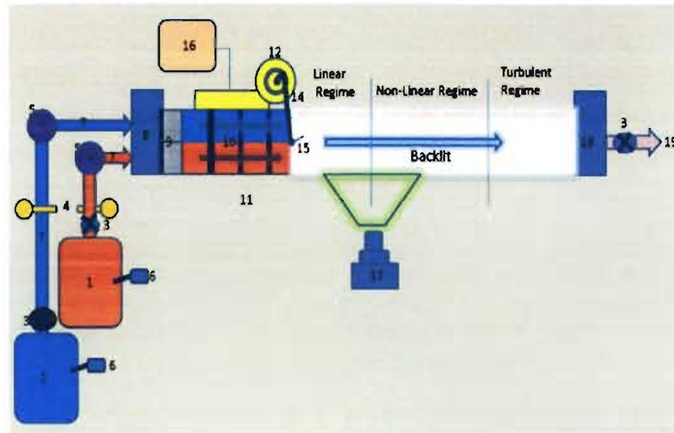

Computer controlled flapper system – up to 16 modes

Binary initial perturbation with δ ~ 0

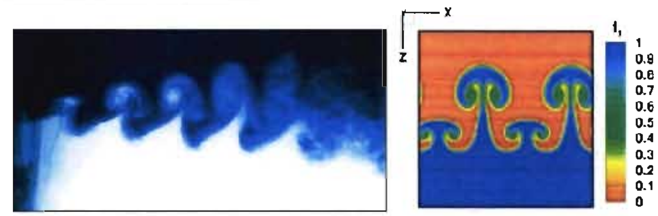

Binary initial perturbation with δ ~ π/2

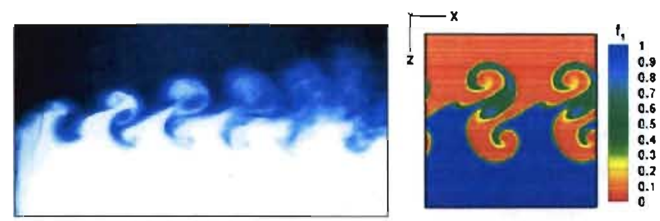

The "leaning" of the growing perturbation with an angle of π/4 observed in the experiment and the simulation is due to mode dynamics, and not mode coupling.

Single-mode RTI: growth stages and initial conditions dependence (A=0.04)

- C-A: change initial diffusion thickness
- B-A: change initial amplitude

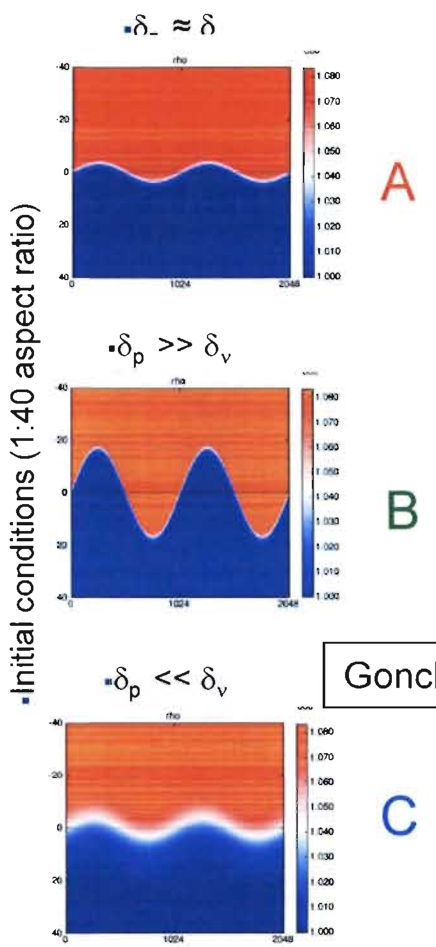

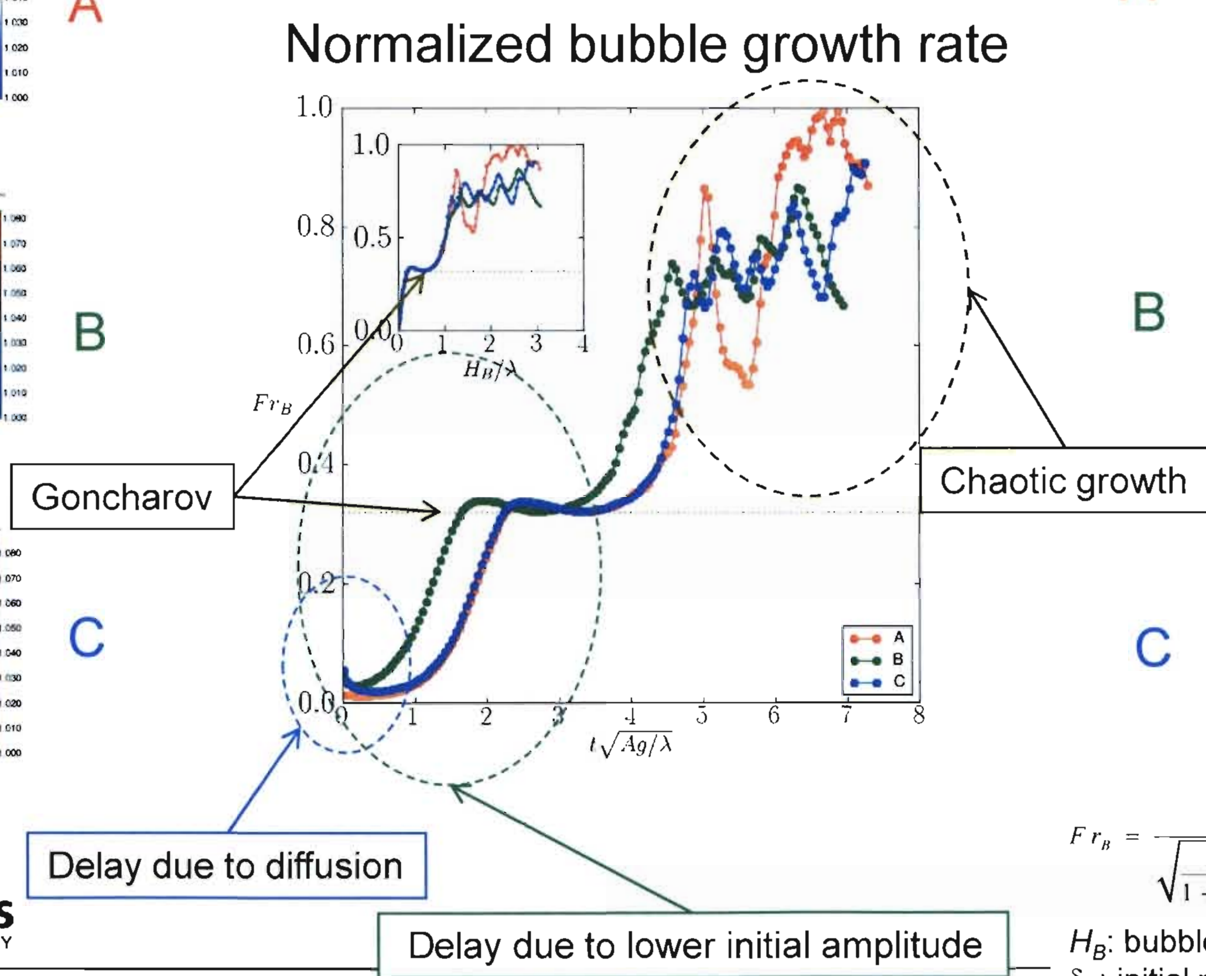

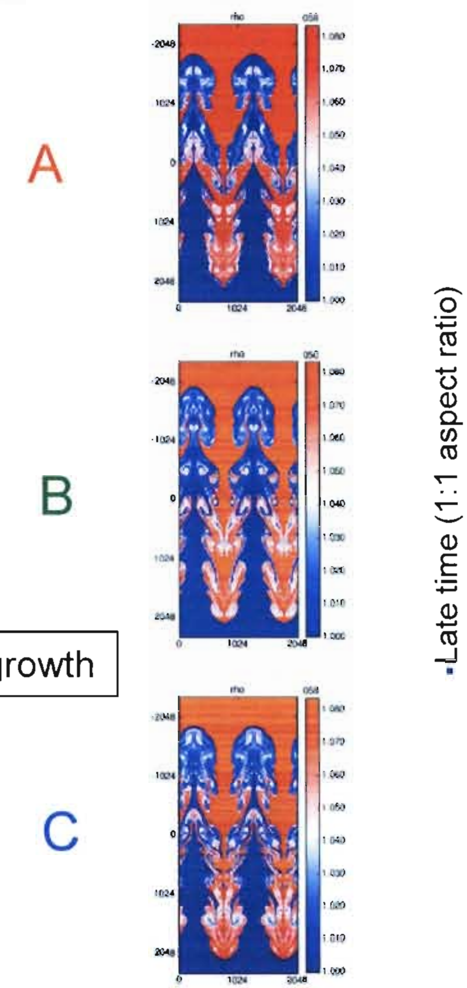

$$Fr_B = \frac{\dot{H}_B}{\sqrt{\frac{A}{1+A} g\lambda}}; \quad A = \frac{\rho_H - \rho_L}{\rho_H + \rho_L}$$

H_B: bubble height
δ_P: initial perturbation amplitude
δ_v: initial diffusion layer thickness

Single-mode RTI: Reynolds number dependence ($Re_p = \frac{\lambda\sqrt{\frac{A}{A+1}\lambda g}}{\nu}$)

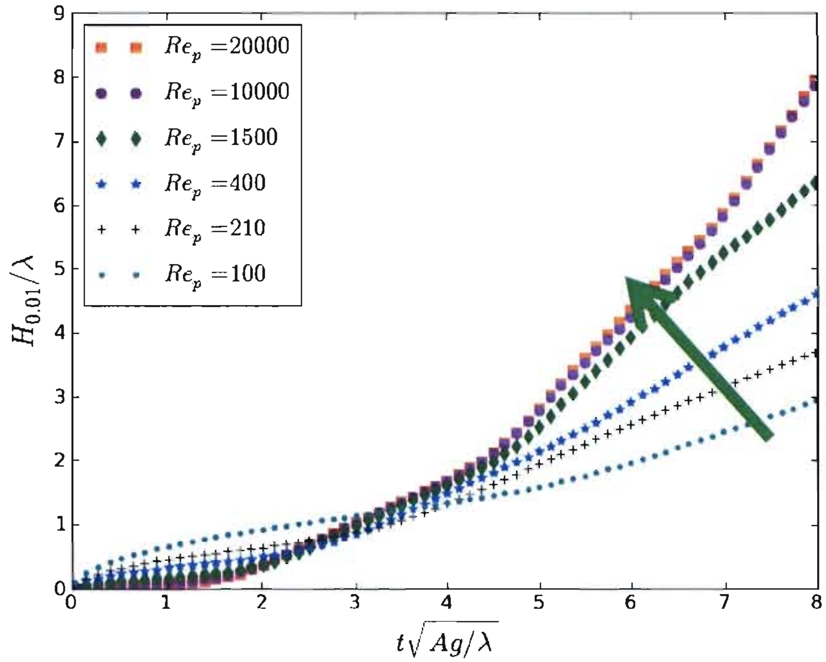

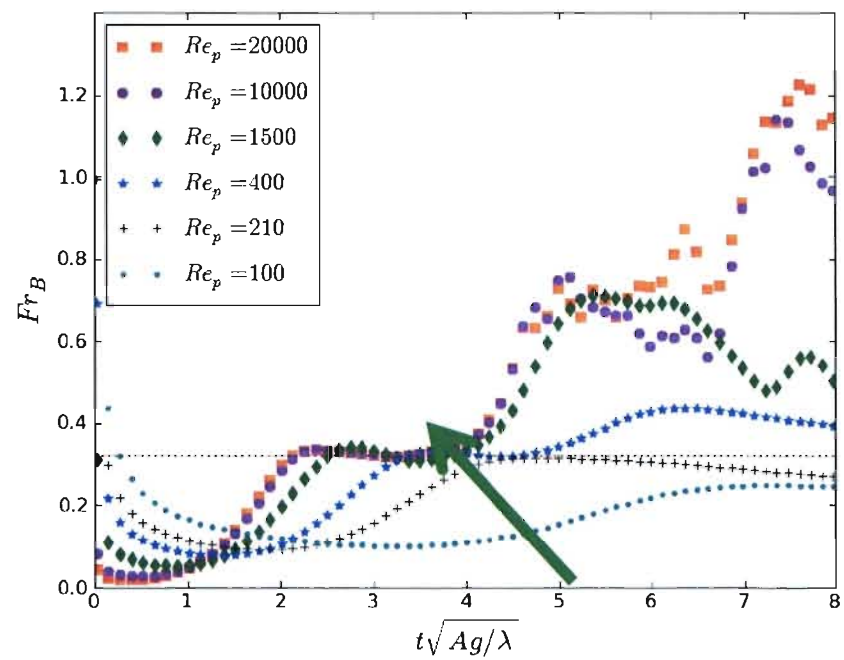

Single-mode RTI: Summary of findings

- Single-mode RTI development is strongly dependent on the perturbation Reynolds number and undergoes different growth stages at high and low Re_p.

- A new stage, chaotic development, was found at high Re_p after the re-acceleration stage.

- At high Re_p, the initial perturbation shape has a strong influence at early and late times, in the chaotic stage, but minimal during the potential flow evolution, such that the Goncharov result remains robust during this time.

- As Re_p is decreased to small values, the later instability stages are successively no longer reached; alternately, as Re_p is increased, the flows undergoes a series of mixing transitions towards the CD stage.

- **There is a minimum numerical resolution necessary to reach all stages of single-mode RTI development : coarse mesh calculations (e. g. ILES or low Re DNS) can not capture all these stages.**

Two-Mode RTI: Layer growth for different mode combinations (A=0.04)

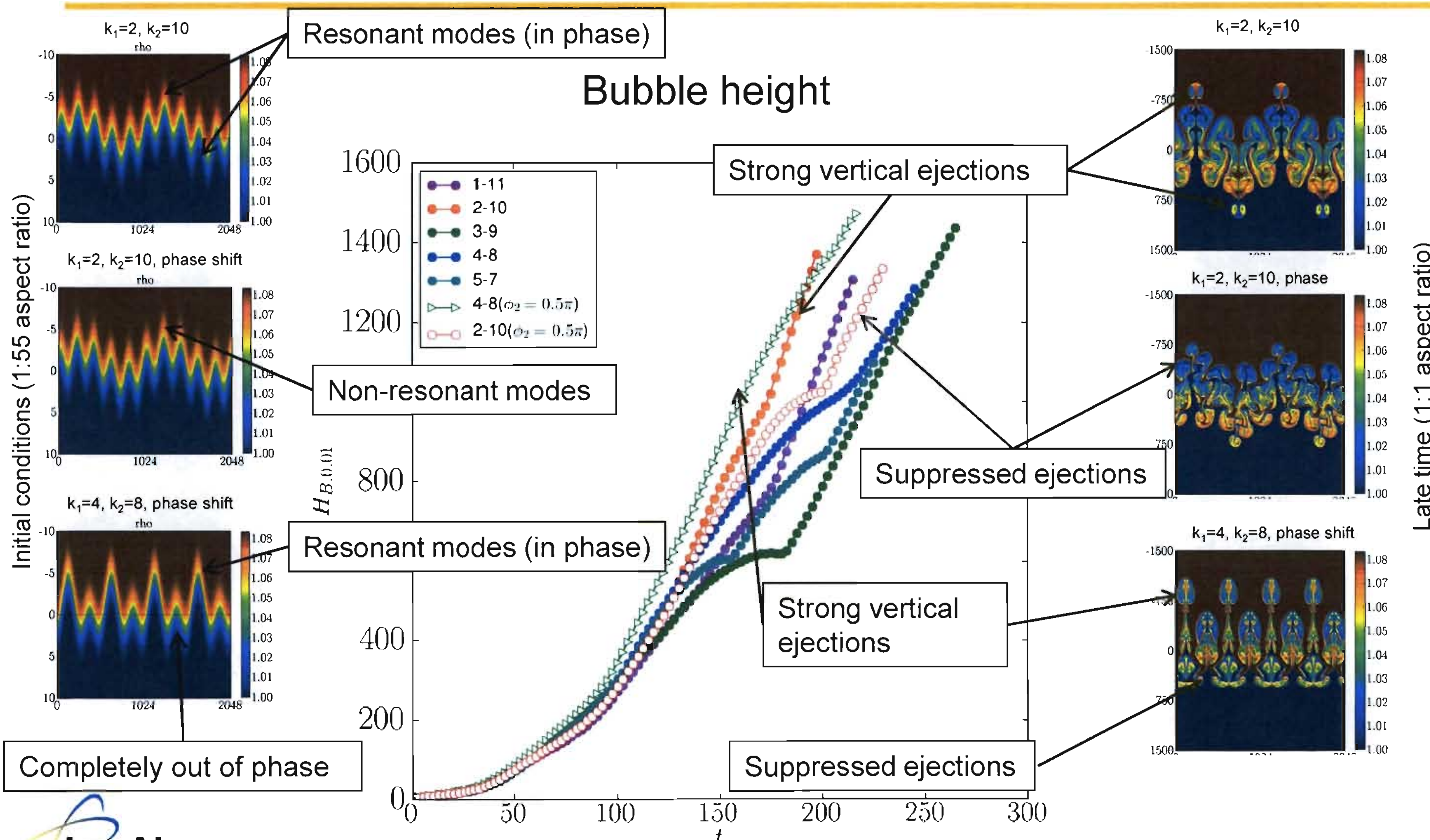

Two-mode RTI: Summary of findings

- **Two-mode RTI development is strongly dependent on the combination of mode numbers and phase shift:**

1. Modes are in phase → The resulting vortex pairs lead to strong ejections in the vertical direction which maximize the instability growth rate.
2. Modes are out of phase → The induced velocity due to the vortex pairs opposes the layer growth and minimizes the instability growth rate.
3. Unrelated phases → Ejections (which are more likely to be complete) are inclined ("leaning") and contribute only partially to the instability growth.

4. The two sides of the layer can be asymmetric at any A with the modes on each side independently in or out of phase or of unrelated phases.

5. Any symmetry in the initial conditions will be maintained if allowed by the BC. The resulting patterns can maximize or minimize the growth rate. Such patterns can also form in the multi-mode case.
   - ❑ Periodic BC allow patterns with translational and/or reflectional symmetries.
   - ❑ Wall BC only allow reflection symmetric patterns.

Single-mode RTI (again): There is a pattern with reflectional symmetry and (efficient) balanced vortical motions. Single-mode RTI grows faster than the corresponding two-mode RTI with the same k.

Problem description: New Archival Suite of Direct Numerical Simulations of Rayleigh-Taylor instability

- Suite of $1024^2 \times 4608$ simulations at A=0.04, 0.5, 0.75, 0.9:
  - Base simulations with initial perturbation peaked around the most unstable mode of the linear problem.
  - After the layer width had developed substantially, the simulations were branched into reversed (g -> -g) and zero (g -> 0) gravity simulations.
  - Different initial perturbation spectra, viscosity and diffusion coefficients to study the effects of various parameters.

- $4096^2 \times Nz$ simulation at A=0.75 (NZ_{max}=4032).

- These have reached Reynolds numbers of:

$$Re_b = h\dot{h}/\nu > 40{,}000$$

$$Re_T = \widetilde{k}^2/\nu\varepsilon > 5500$$

Multi-mode Rayleigh-Taylor instability: A=0.75, grid size 4096^2 x4032

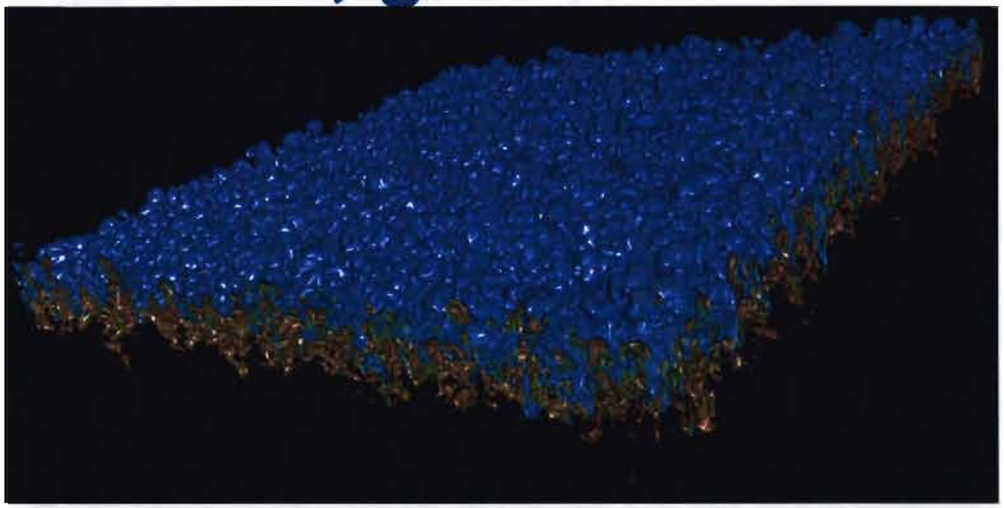

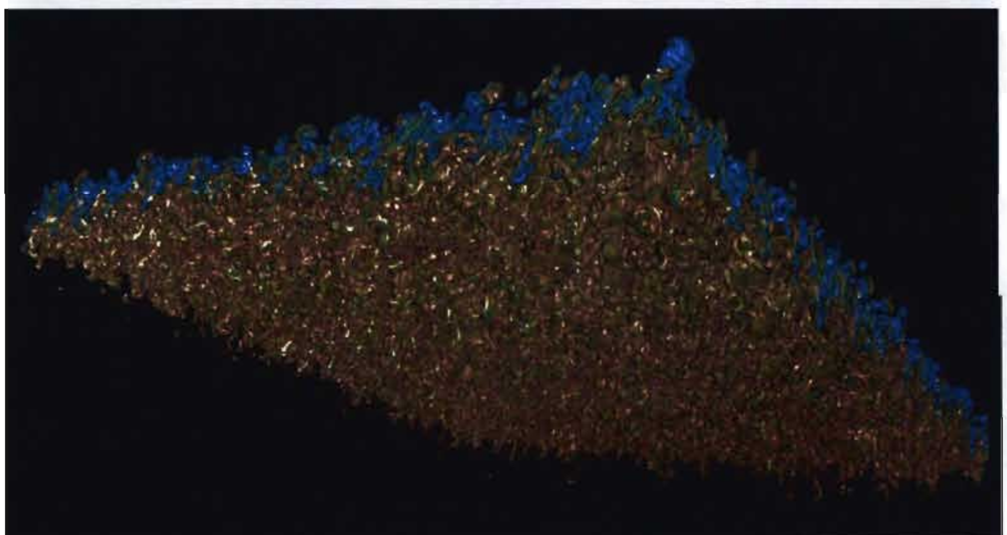

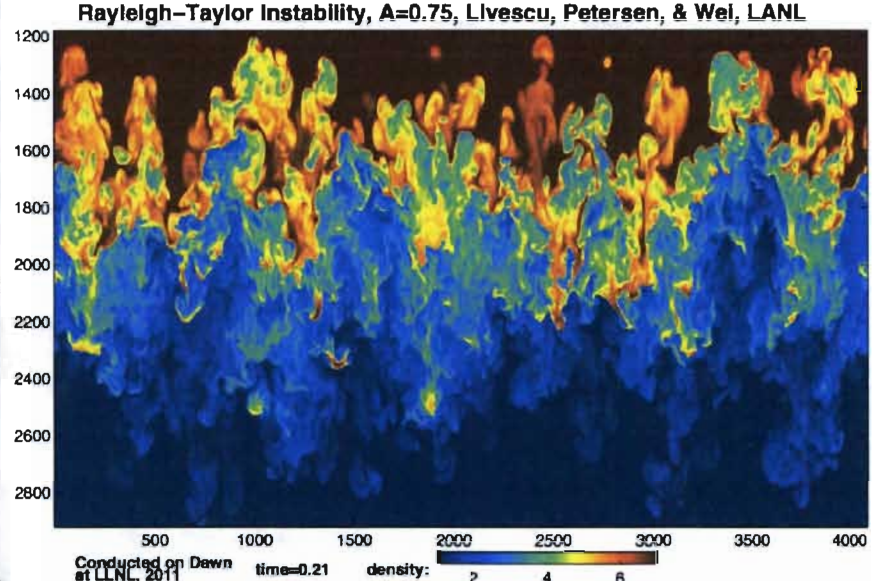

Global measures: mixing layer growth

- Ristorcelli & Clark, (2004) and Cook et al. (2004) showed that self-similarity of the layer width leads to the solution

$$h(t) = \alpha A g t^2 + 2(\alpha A g h_0)^{1/2} t + h_0$$

- Cabot and Cook (2006) measure $\alpha = \dot{h}^2 / 4Agh$
- We introduce a smoother variation that avoids derivatives (left).
- David Youngs uses an integral mix measure, h_{DY} , to define α_{DY} (right).

$$\alpha = \frac{\left(\sqrt{h_{0.01}(t)} - \sqrt{h_{0.01}(t_0)}\right)^2}{Ag(t-t_0)^2} \qquad \alpha_{DY} = \frac{\dot{h}_{DY}^{\,2}}{4Agh_{DY}}$$

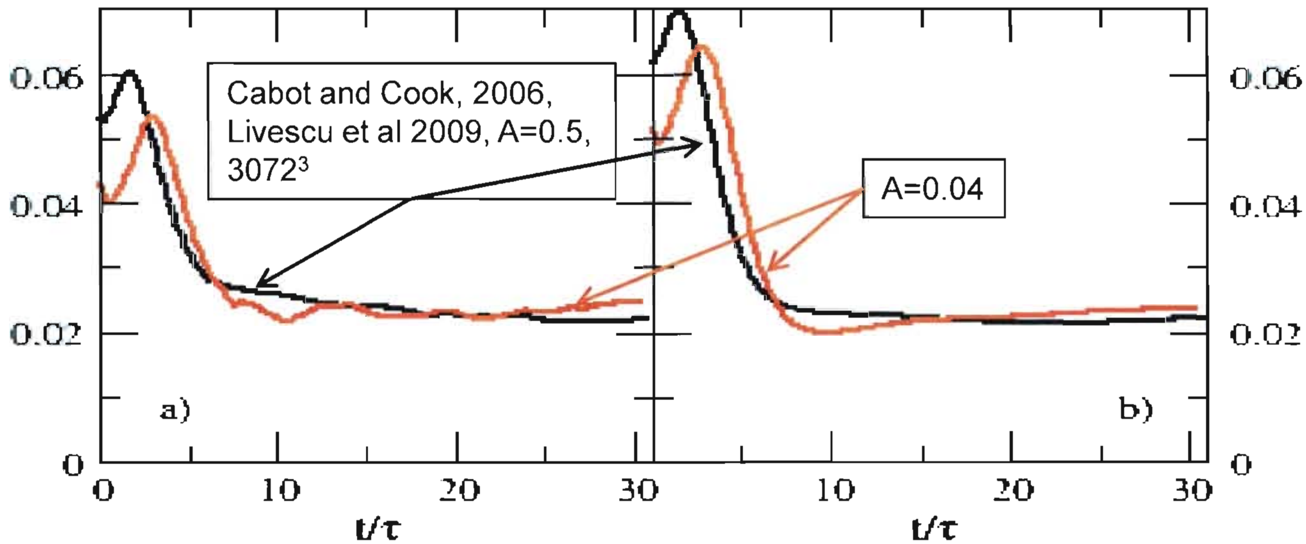

$\tau = \sqrt{L_0 / (Ag)}$

L_0= characteristic lengthscale of the initial perturbation

Global measures: mixing layer growth for different perturbation spectra

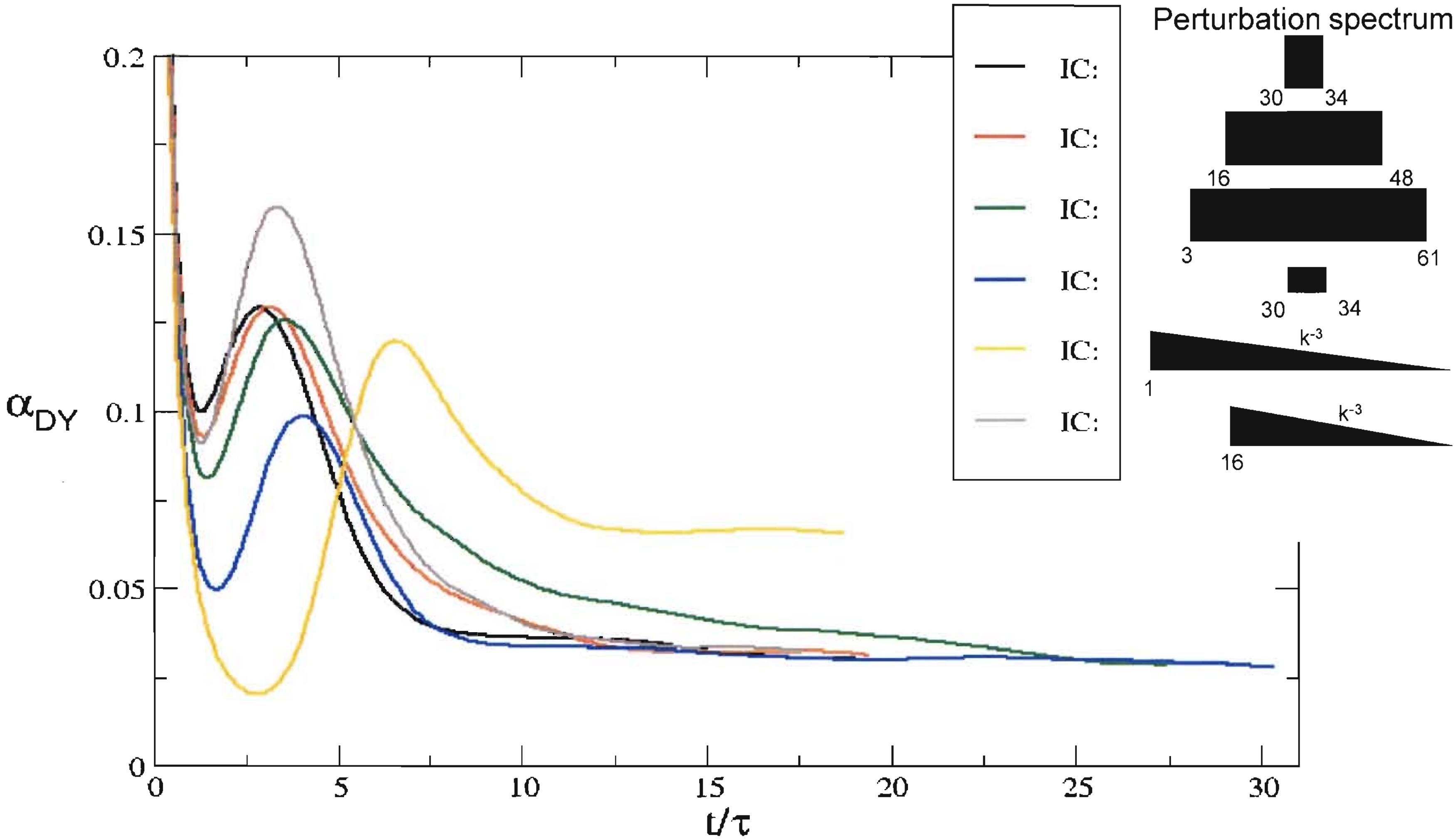

Multi-mode RTI growth: Summary of findings

• **DNS with specific perturbation spectra reproduce the higher alpha seen in many experiments. These high values appear to be due either or both of** (this is also supported by the experiments of Carles et al 2006; Olson and Jacobs 2009):

- too short an experimental time or
- significant low wave number content in the IC.

Since the early time and the confined RTI behavior are not general, this imposes serious obstacles for modeling most RTI experiments.

Considerations on the confined RTI problem:

• RTI is relatively inefficient at converting potential energy into vertical kinetic energy; the growth rate coefficient, alpha, is much lower than that corresponding to free fall.

• Vertical ejections, which are associated to induced vortical velocities, can convert back horizontal kinetic energy into vertical kinetic energy and increase the value of alpha.

• Confined RTI, especially with a perturbation spectrum of the type k^{-3}, is just "single-mode RTI with noise." Enhanced vertical ejections activity is expected, along with higher growth rates.

Considerations on the transition to turbulence and the time when a turbulence model can be used for multi-mode RTI

Definition: The flow is fully turbulent when the modeling assumptions (if these are well posed) become valid.

Examples in BHR, mass flux equation:

- **Gradient diffusion hypothesis for turbulent transport is valid when:**
- **Destruction term model is valid when:**

$$<\rho u_z u_z> = C_a (S\sqrt{K} \quad or \quad \tilde{k}^2/\tilde{\varepsilon})\bar{\rho}\,\partial a_z/\partial z$$

$$<v p_{,z}> = -C_{a1} a_z (\sqrt{K}/S \quad or \quad \tilde{\varepsilon}/\tilde{k})$$

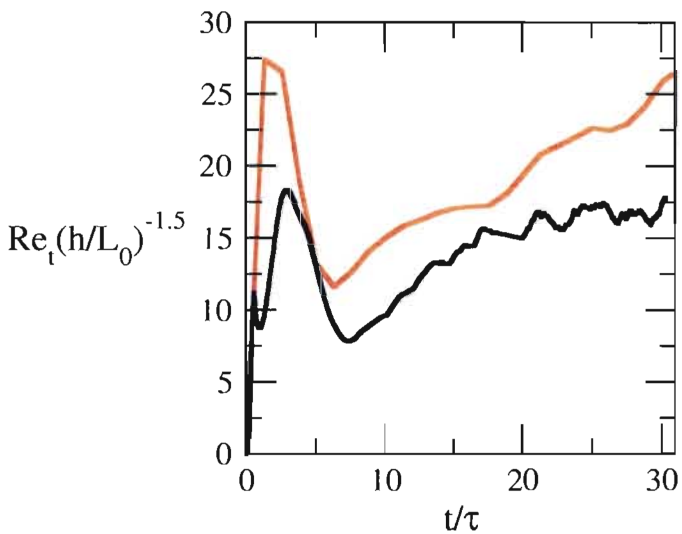

- Although the layer width becomes self-similar relatively fast, derived quantities, such as the turbulent Reynolds number, in general, require longer time to reach self-similarity.
- Since Re_t is proportional to the eddy viscosity in the usual gradient transport model, this suggests such a model becomes applicable later than the onset time for layer self-similarity.

A Modal Model for Rayleigh-Taylor Instability

Bertrand Rollin (CCs-2),

Malcolm J. Andrews (XCP-4)

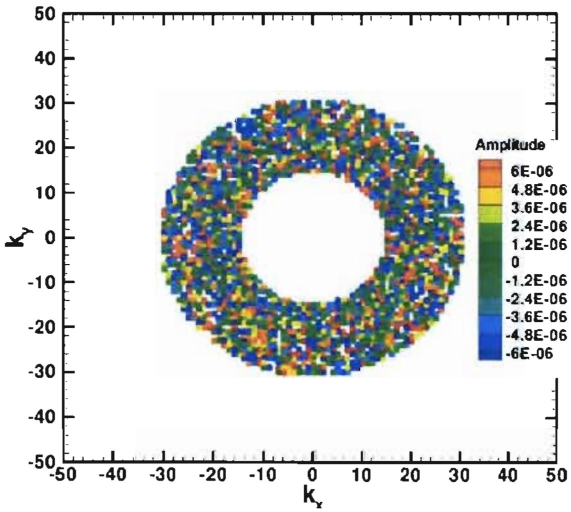

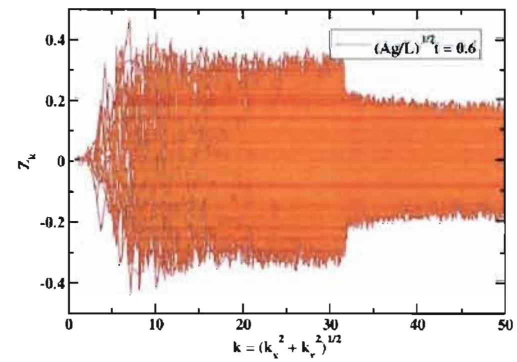

$$\ddot{Z}_k = \frac{4(k-8\eta_2)}{k^2-4A_Tk\eta_2-32A_T\eta_2^2}\left(-\dot{Z}_k^2k^2\frac{(5A_T-4)k^2+16(2A_T-3)k\eta_2+64A_T\eta_2^2}{8(k-8\eta_2)^2}-A_Tg\eta_2\right)$$

Why a Modal Model?

A Rayleigh-Taylor Multi-Mode Study with Banded Spectra and Their Effect on Late-Time Mix Growth (Banerjee & Andrews, 2009)

Initial Spectrum

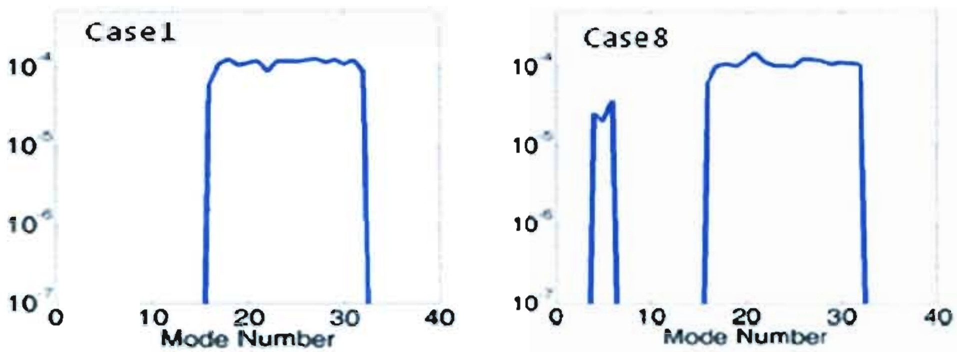

$$\frac{\overline{h_0'^2}}{2} = \int_{k_{\min}}^{k_{\max}} E_{h0}(k)dk = \int_{k_{\min}}^{k_1} E_{h1}(k)dk + \int_{k_2}^{k_{\max}} E_{h2}(k)dk = \frac{\overline{h_1'^2}}{2} + \frac{\overline{h_2'^2}}{2}$$

$$\Lambda = \overline{h_2'^2} \Big/ \overline{h_1'^2}$$

3-D ILES Simulations

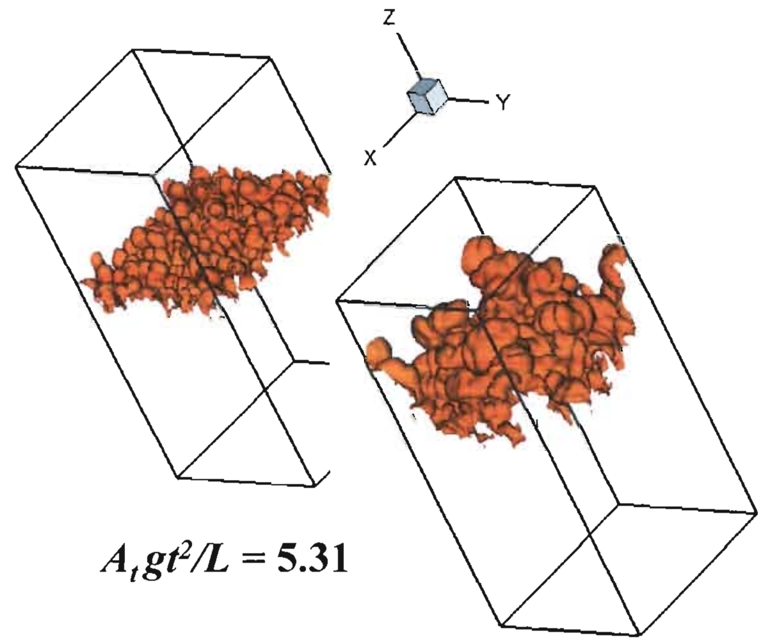

$A_t g t^2/L = 5.31$

$A_t g t^2/L = 19.62$

Why a Modal Model?

3-D ILES Simulations of Banded Spectra and Late-Time Appearance of Long Wavelengths (Banerjee & Andrews 2009)

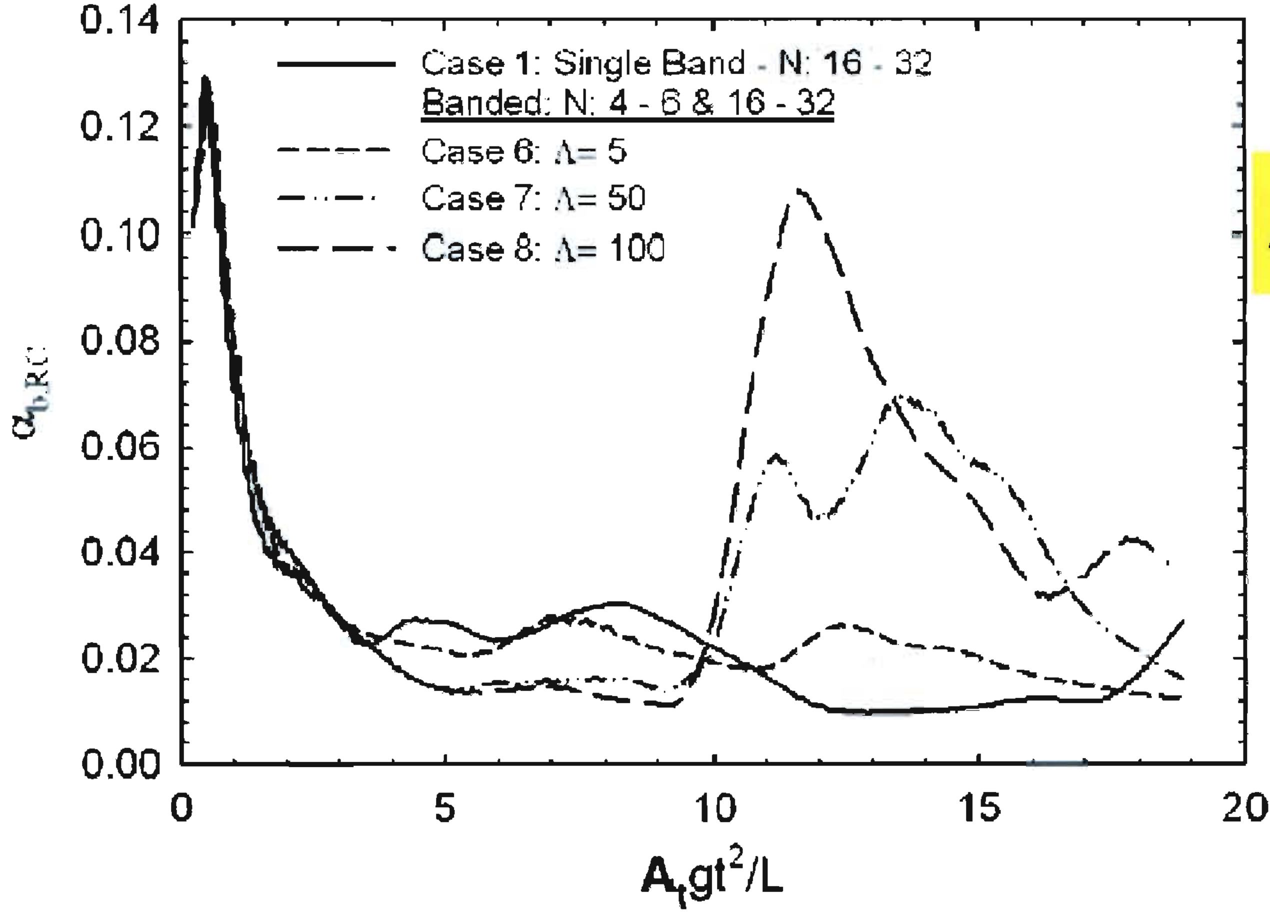

$$h_b = \alpha A_t g t^2$$

$$\alpha_b = \frac{\dot{h}_b^{\,2}}{4 A_t g h_b}$$

A Potential Flow Model for Single Mode Perturbation

Goncharov model:

$$\Delta\phi^{h/l} = 0$$

$$\phi^h = a(t)J_0(kr)e^{-k(z-\eta_0)}$$

$$\phi^l = b_1(t)J_0(kr)e^{k(z-\eta_0)} + b_2(t)z$$

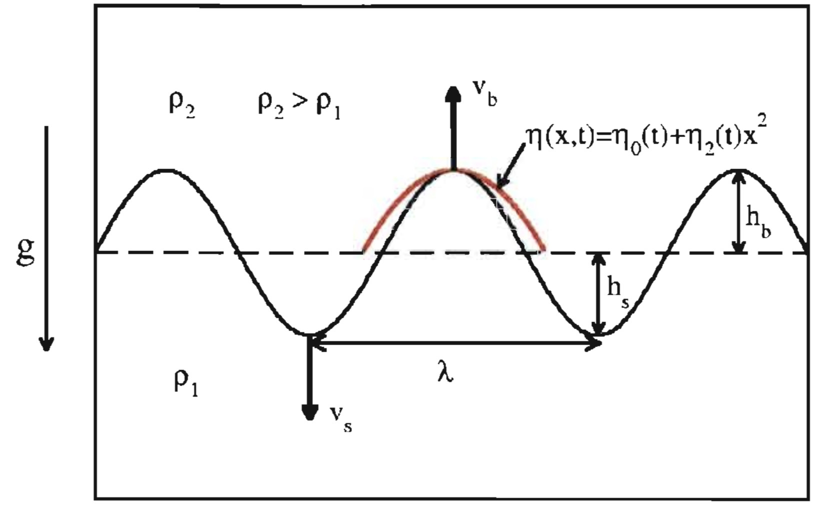

$$\partial_t\eta + v_r^{h/l}\partial_r\eta = v_z^{h/l} \qquad [v_z - v_r\partial_r\eta] = 0 \qquad [Q] = Q^h - Q^l$$

$$\left[\rho\left(\partial_t\phi + \frac{1}{2}v^2 + g\eta\right)\right] = P$$

The velocity potential are expended to 2nd order and plugged in the interfacial conditions

Single Mode Model Results

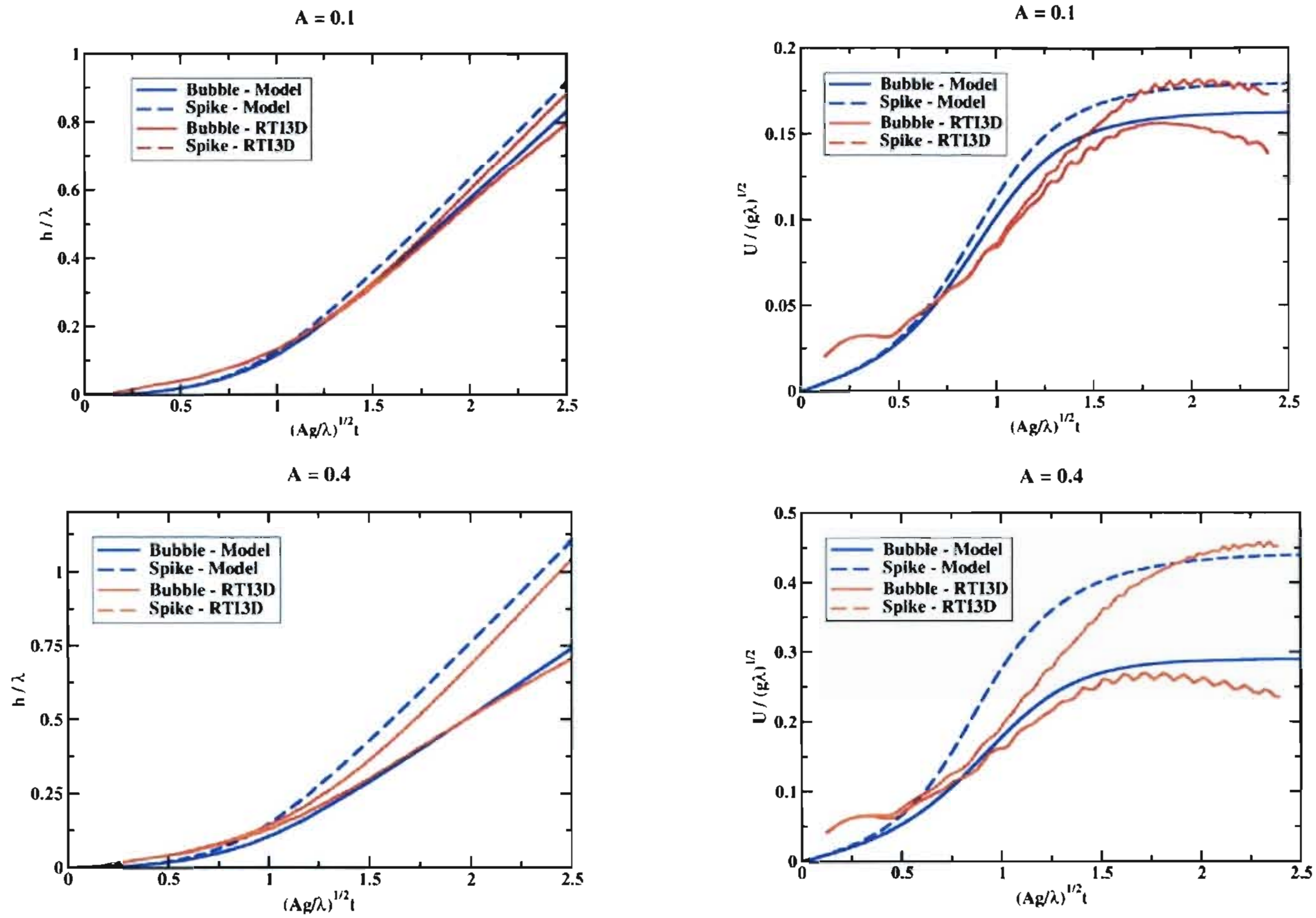

The Goncharov model performs well for low Atwood numbers

Single Mode Model Summary

- Nonlinear model
- Valid on a large range of A_T ($0 \leq A_T \leq 0.4$)
- Good prediction for bubble

- Spike inaccurate for high A_T

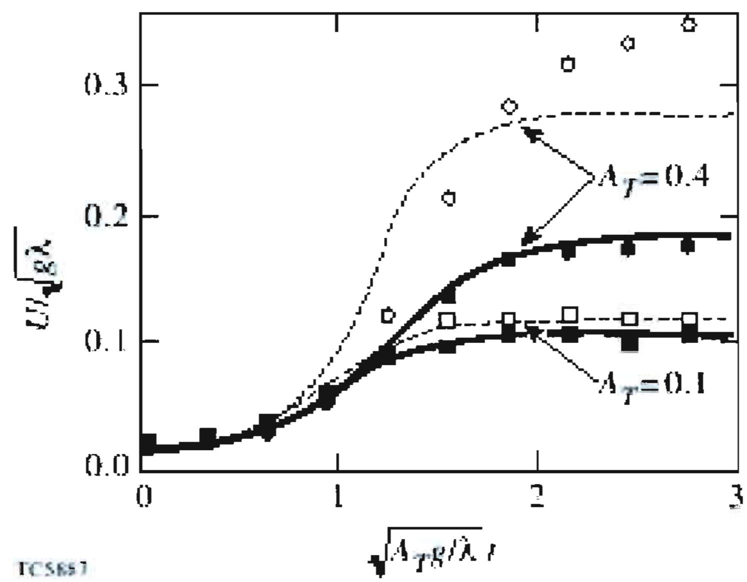

Goncharov, PRL, **88**, 2002

Multi-mode Study Using ODE's to Predict the Envelope of the Bubble Mix Region (Andrews+Rollin)

ILES or DNS

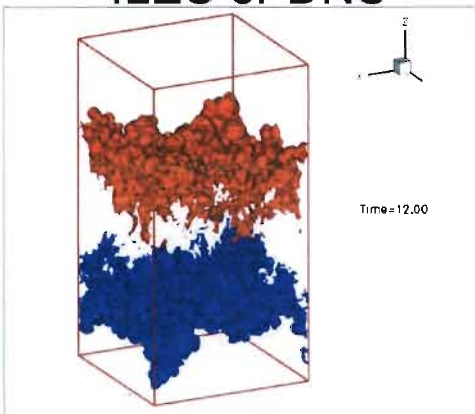

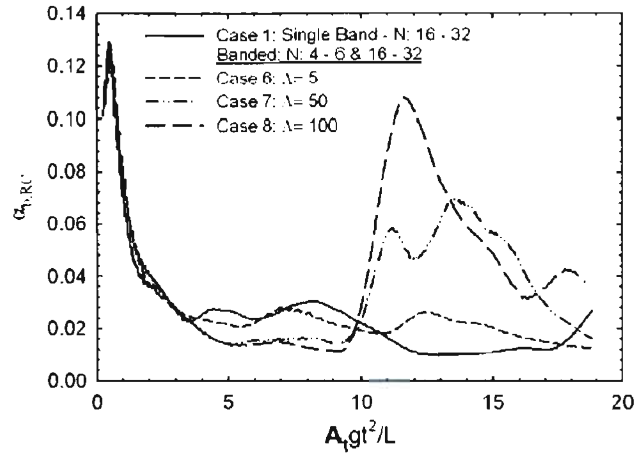

ODE Model

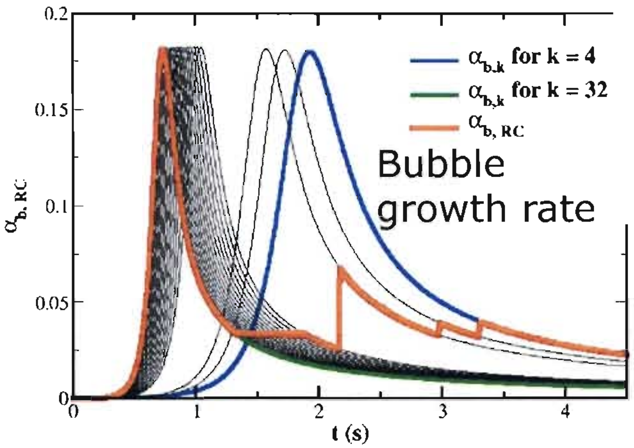

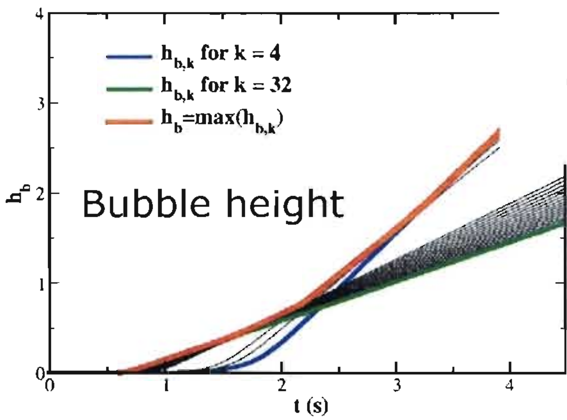

- At late time, h_b is governed by the longest wavelength evolution
- Each band of the initial spectrum is 'seen' in the growth rate

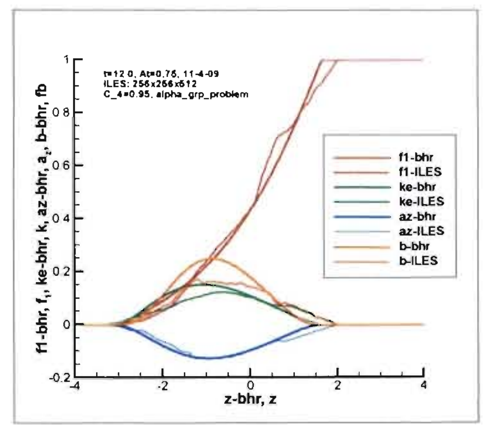

Weakly Nonlinear Model Summary

- Nonlinear model
- Valid for all Atwood number
- Multimode model, i.e., handle mode coupling

- Valid until early transition to nonlinear behavior, so here is what we do:

For all k,

$$\begin{cases} \ddot{Z}_k = G(k) + A_T k \sum_{\vec{m}} \left\{ \ddot{Z}_m Z_n \left(1 - \hat{m}\cdot\hat{k}\right) + \dot{Z}_m \dot{Z}_n \left(\frac{1}{2} - \hat{m}\cdot\hat{k} - \frac{1}{2}\hat{m}\cdot\hat{n}\right)\right\} & \text{Before k saturates} \\ \ddot{Z}_k = A_T k \sum_{\vec{m}} \left\{ \ddot{Z}_m Z_n \left(1 - \hat{m}\cdot\hat{k}\right) + \dot{Z}_m \dot{Z}_n \left(\frac{1}{2} - \hat{m}\cdot\hat{k} - \frac{1}{2}\hat{m}\cdot\hat{n}\right)\right\} & \text{After k has saturated } |m|,|n| < |k| \end{cases}$$

Banded Spectrum Case

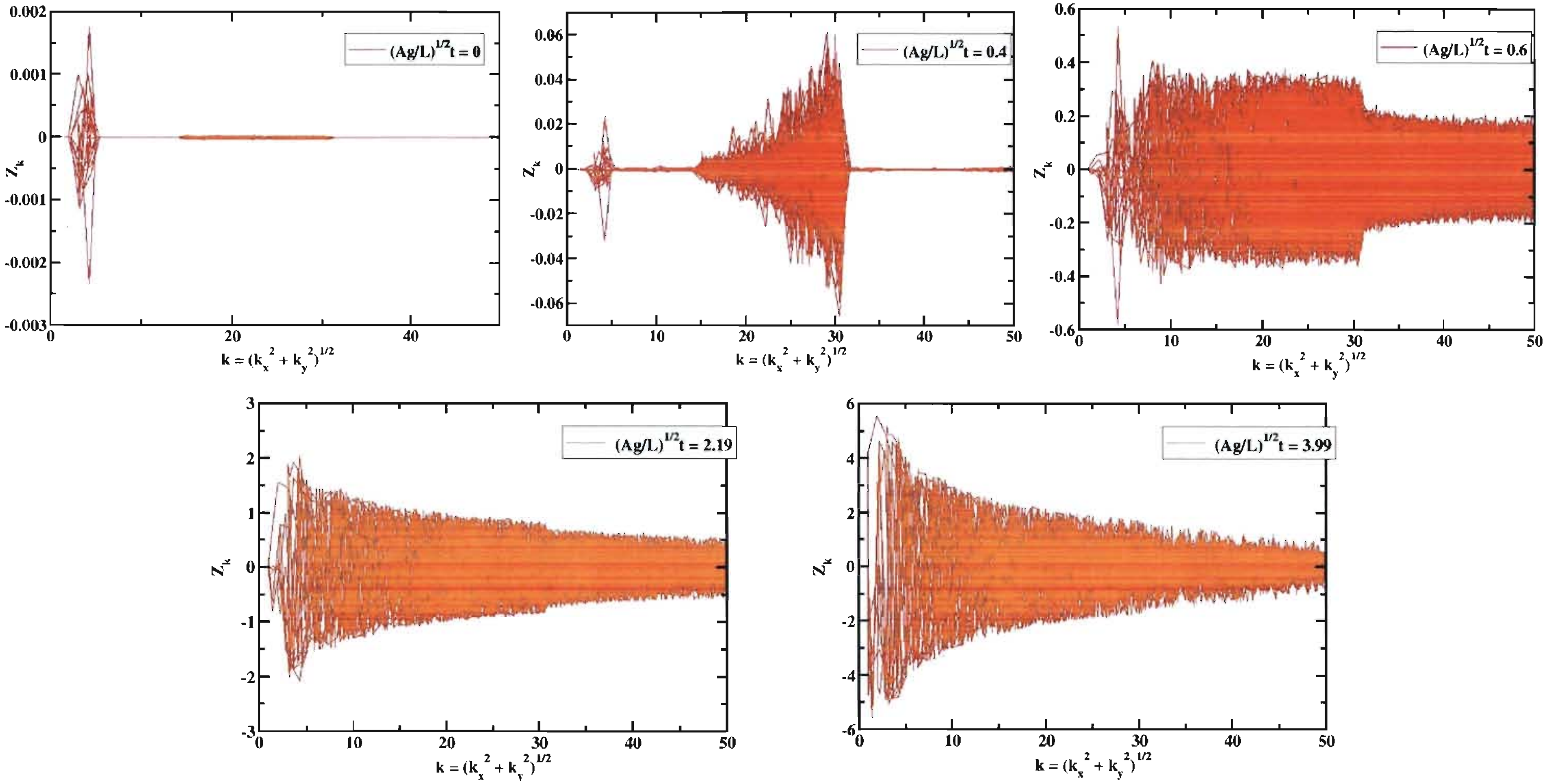

Existing long wavelength in the initial spectrum is not washed out by mode coupling

Banded Spectrum Case

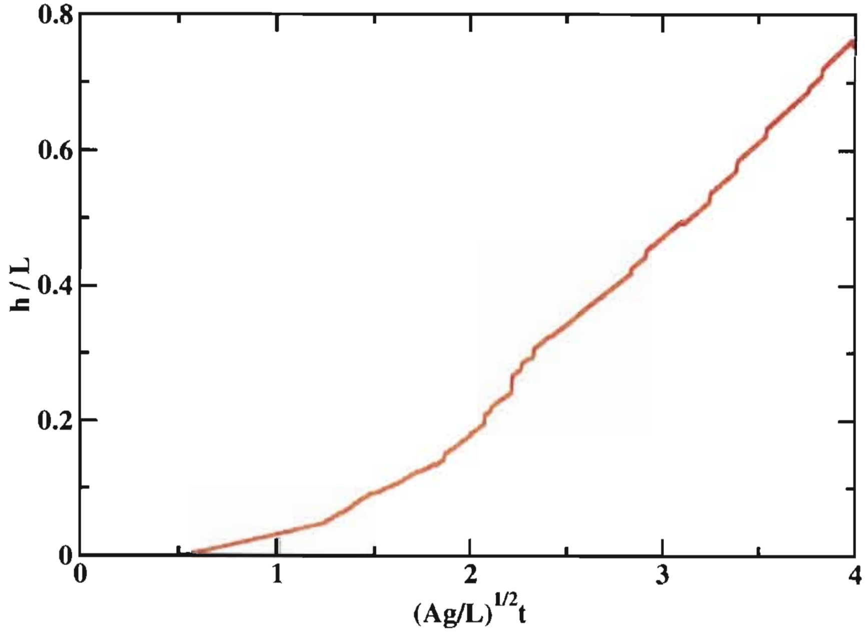

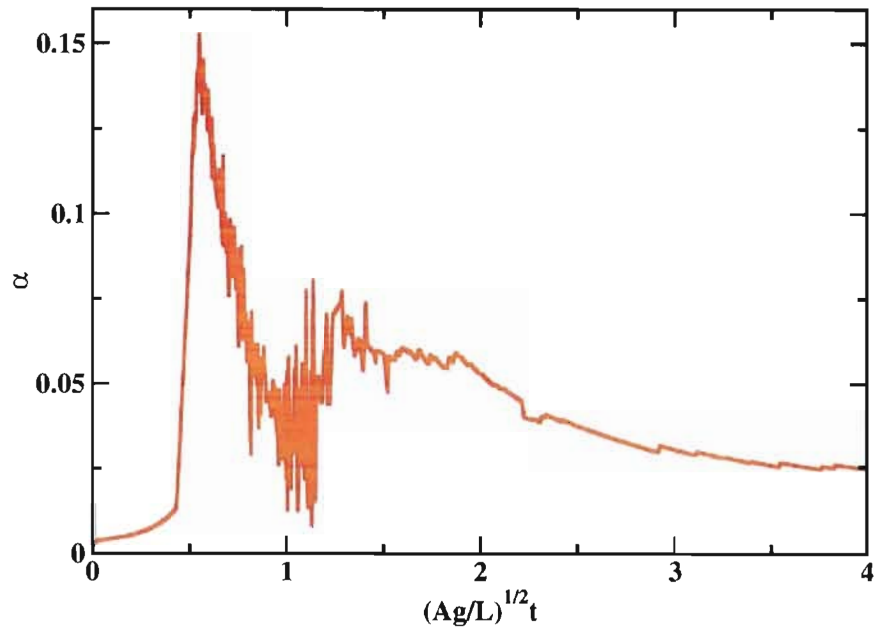

The mixing layer expansion experience an "extra kick" when the long wavelengths of the initial pertubation become the dominant modes

BHR Turbulence Model for RT Instability

Selected Besnard-Harlow-Rauenzhan (BHR) turbulence model, but could use others just as well:

- Single-point turbulent transport model
- Designed for variable density turbulence

D. Besnard, F. H. Harlow, R. Rauenzhan, LA-10911-MS (1987)

Model Variables:

$$k = \frac{1}{2}\overline{u_i' u_i'} \qquad a_i = \frac{\overline{\rho' u_i'}}{\overline{\rho}} \qquad b = -\overline{\rho' v'} \qquad S = \frac{k^{3/2}}{\varepsilon} \qquad \nu_t = C_\mu k^{1/2} S$$

Governing equation for the variable S:

$$\partial_t S = \left(\frac{3}{2} - C_4\right) a_z g \frac{S}{k} + \frac{1}{\rho}\partial_z\left(\rho \frac{\nu_t}{\sigma_S}\partial_z S\right) - \left(\frac{3}{2} - C_2\right) k^{1/2}$$

BHR initiated with:

- **Profiles for:** $k \quad a_i \quad b \quad S$
- **Values for:** $C_4 \quad C_2 \quad C_\mu \quad \sigma_S \quad \ldots$

C_4 .. Controls RT mix width

Self-Similar Solution for "Dynamic" C_4 Derivation

Self-similar soln. into BHR ➡

$$k = \alpha_k A_T^2 g^2 t^2 \quad a_z = \alpha_a A_T g t \quad S = \alpha_S A_T g t^2$$

$$\partial_t S = \left(\frac{3}{2} - C_4\right) a_z g \frac{S}{k} + \frac{1}{\rho}\partial_z\left(\rho \frac{\nu_t}{\sigma_S}\partial_z S\right) - \left(\frac{3}{2} - C_2\right) k^{1/2}$$

Obtain algebraic eqn. for α's ➡

$$2\alpha_S = \left(\frac{3}{2} - C_4\right)\frac{\alpha_a \alpha_S}{\alpha_k A} - \left(\frac{3}{2} - C_2\right)\alpha_k^{1/2}$$

Solve for BHR coefficient ➡

$$\boxed{C_4 = f(\alpha_k, \alpha_S, \alpha_{a_z}, C_2)}$$

Ballistic mode metrics ➡

$$\alpha_k = \frac{\frac{d^2 k}{dt^2}}{2 A_T^2 g^2}, \alpha_a = \frac{\frac{da}{dt}}{A_T g}, \alpha_s = \frac{\frac{d^2 S}{dt^2}}{2 A_T g}$$

Bubble Growth Rate Prediction with a Dynamic C_4

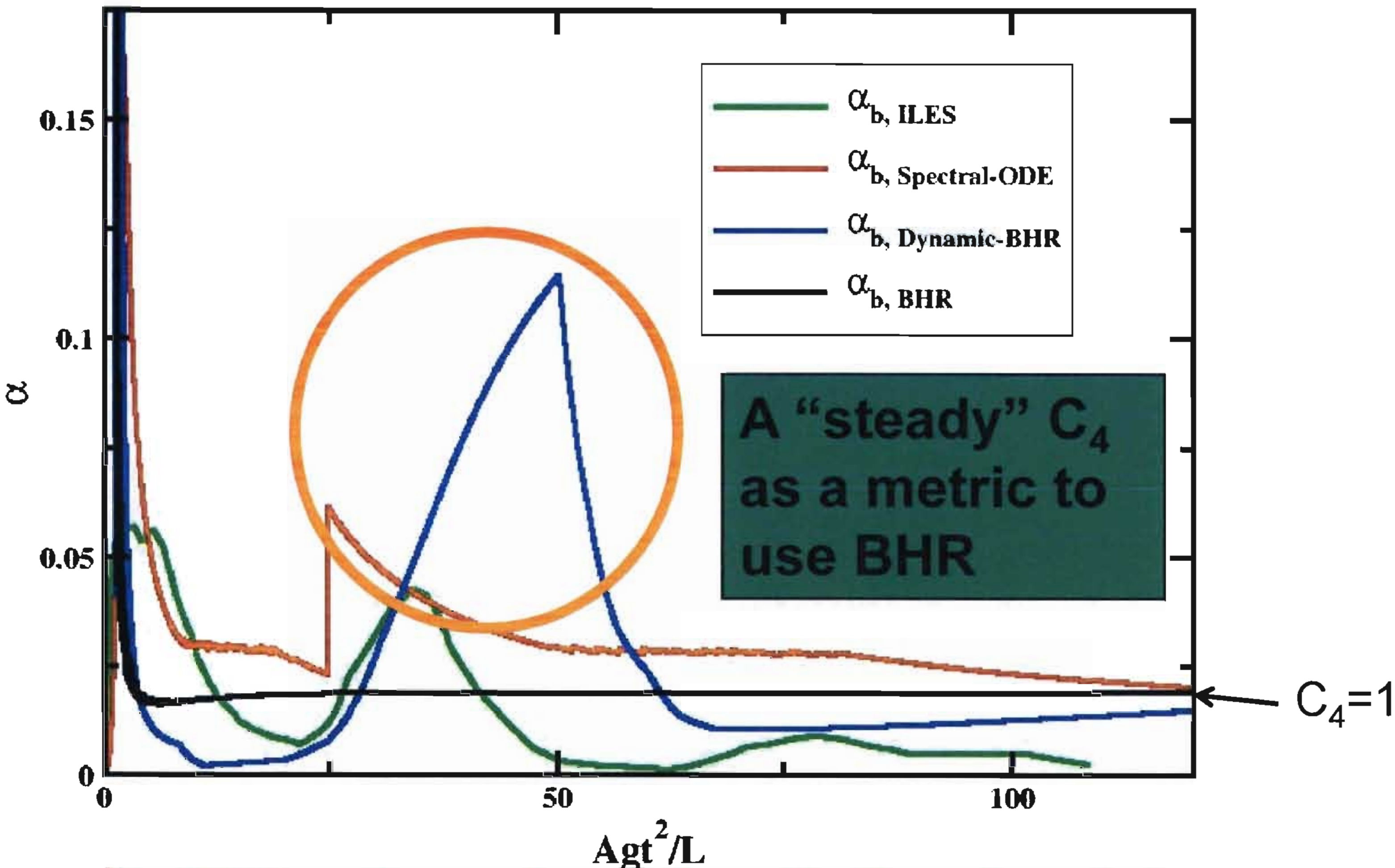

➢ **BHR captures dynamics of α for a banded spectrum with "dynamically" prescribed C_4**

Two-Fluid Initial Profiles for BHR Variables

$$\overline{\rho} = f_l \rho_l + f_h \rho_h \qquad \overline{\mathbf{u}} = f_l \mathbf{u}_l + f_h \mathbf{u}_h$$

$$k = C_k \frac{3}{2} \left(\overrightarrow{v_b} - \overrightarrow{v_s} \right)^2 \frac{f_h f_l \rho_h \rho_l}{\left(f_h \rho_h + f_l \rho_l \right)^2}$$

Isotropy hypothesis

$$a_z = C_{a_z} \frac{f_h f_l}{f_h \rho_h + f_l \rho_l} \left(\rho_h - \rho_l \right) \left(\overrightarrow{v_s} - \overrightarrow{v_b} \right)$$

$$b = C_b \frac{f_h f_l \left(\rho_h - \rho_l \right)^2}{\rho_h \rho_l}$$

Self-similarity hypothesis

Derived for low Atwood number

$$C_k = C_S = C_b = C_{a_z} = 1$$

$$S = C_S \left(h_b + h_s \right) \left(4 f_h f_l \right)^{1/2}$$

Profiles of f, and values for v_b, v_s, h_b and h_s come from the ballistic model

Two fluid model predictions

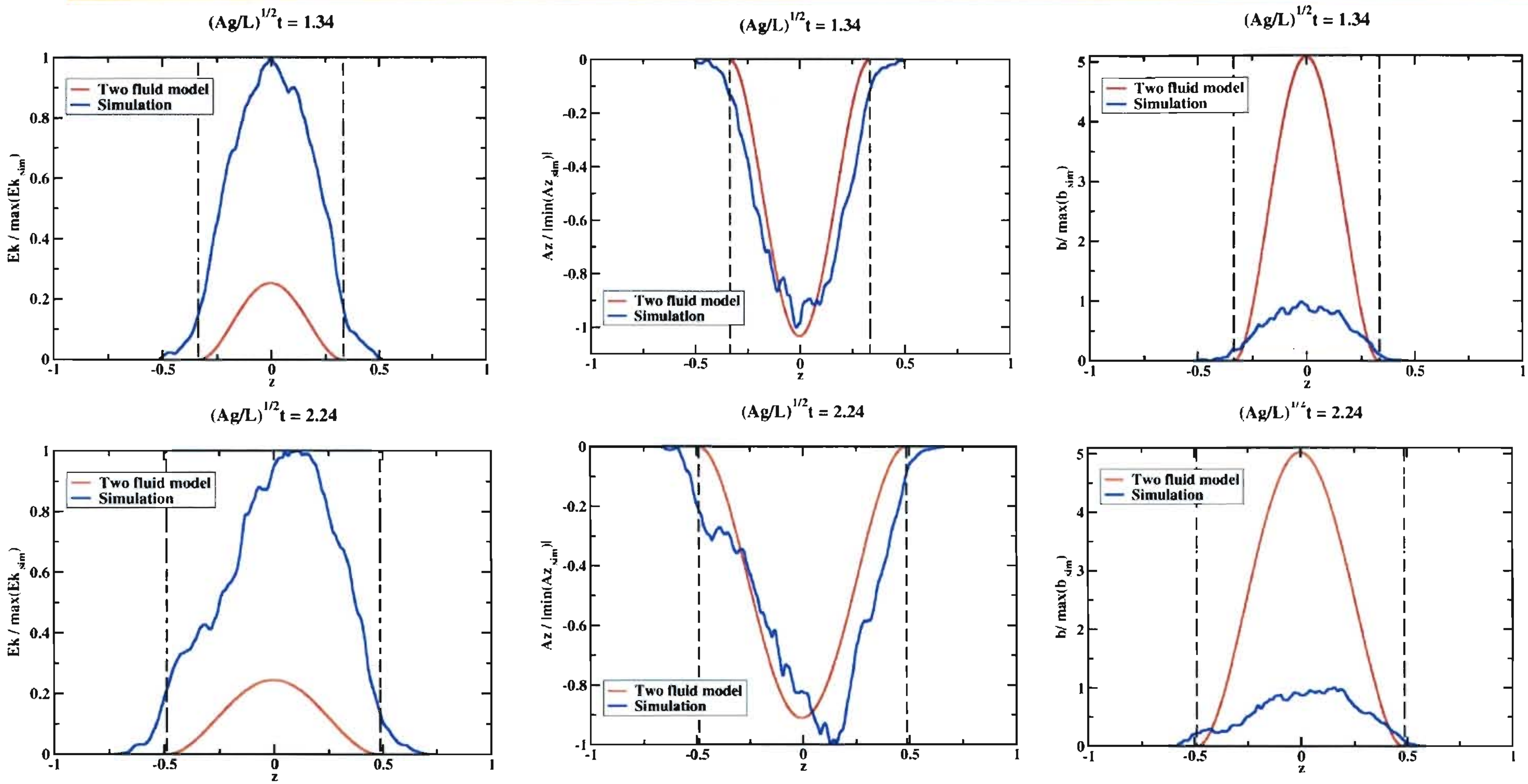

Two-fluid formulation produces reasonable profiles that need to be adjusted correction coefficients

Application to RM instability

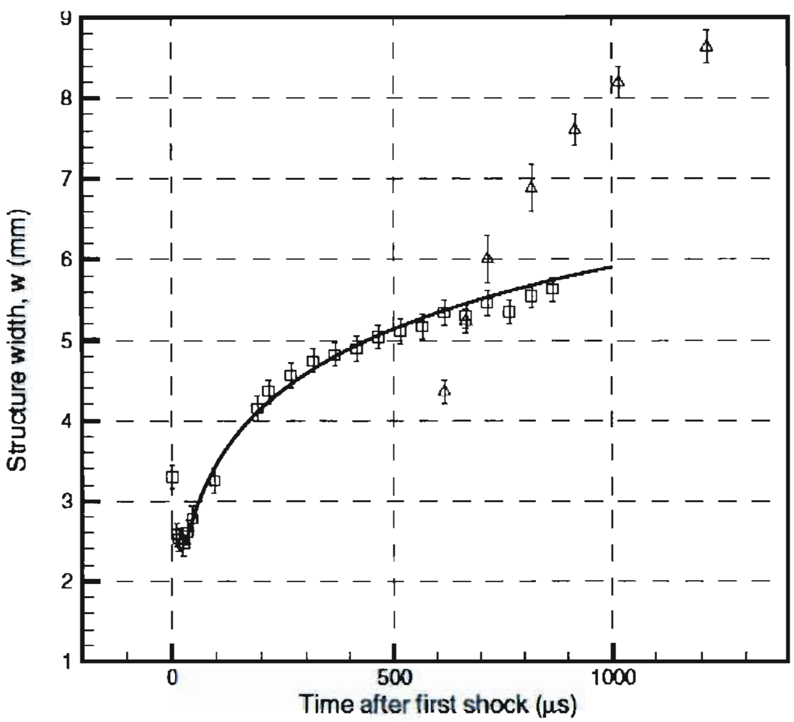

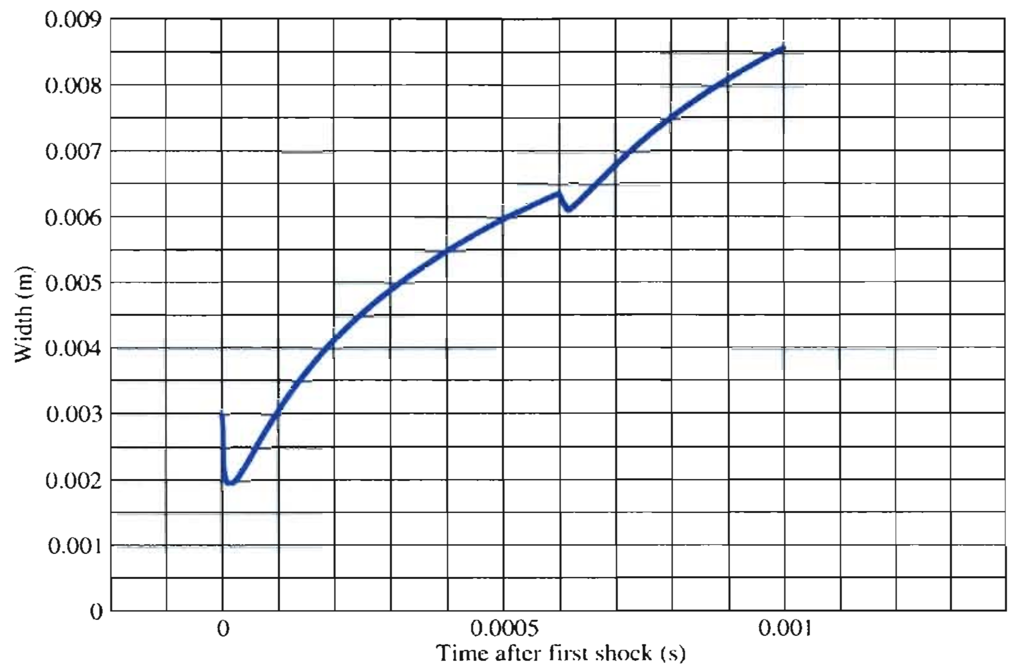

The Goncharov model applied to the gas curtain experiment produces a very close result

A Useful Integrated DR?

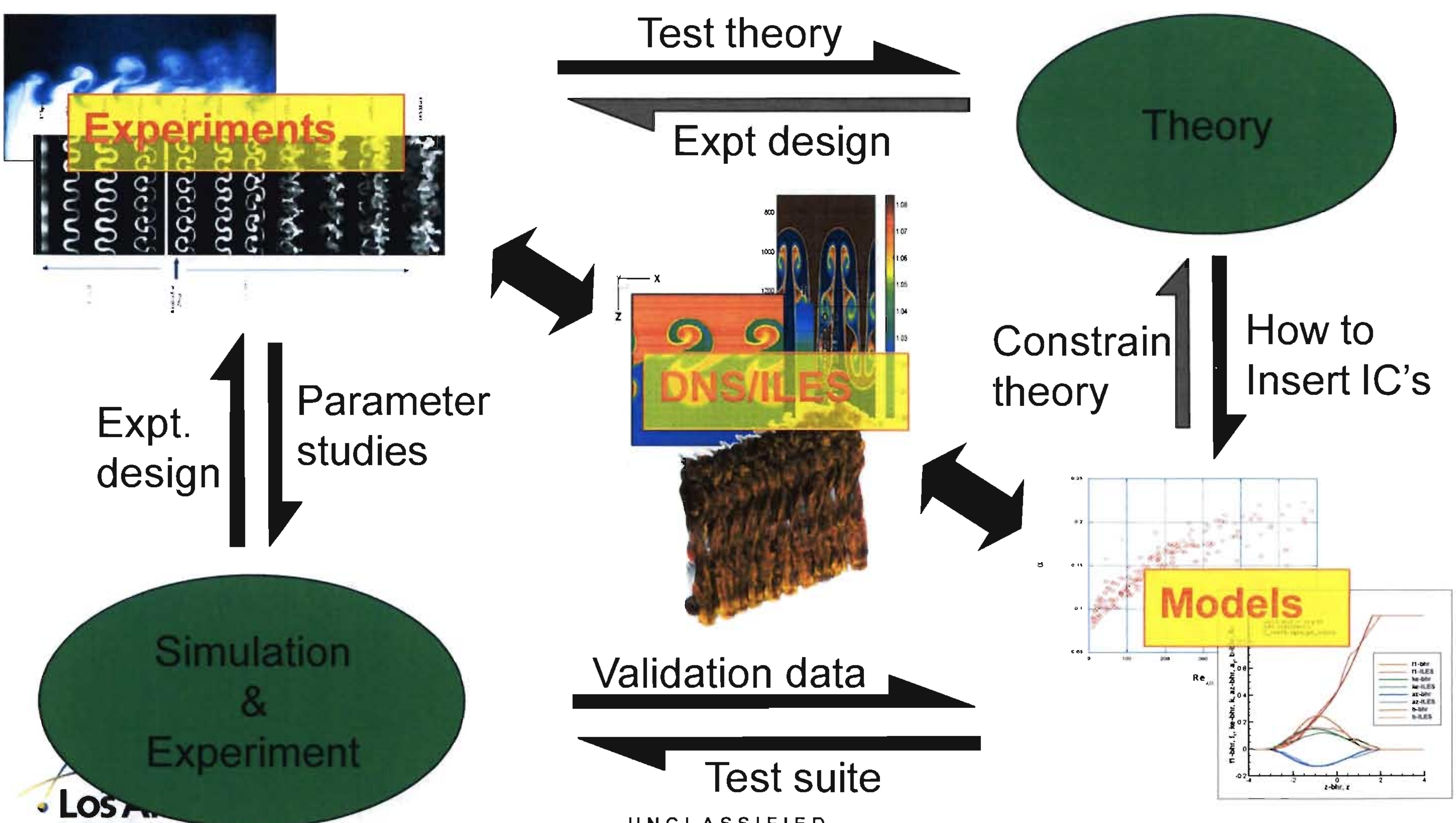

Did we validate the Hypothesis?

Initially seeded small amplitude, long wavelength, perturbations can develop at late-time and be used to control turbulent transport and mixing effectiveness.

- **Prestridge et al. RM experiments clearly show $\eta = \kappa\delta$ effect of IC's, and in the bi-polar discovery of Grinstein**
- **Grinstein/Gowardhan identified the $\eta \sim 1$ transition, a new design criteria**
- **Livescu/Wei quantified a variety of initial condition phenomena, including strong asymmetry associated with bi-modal IC's and phase shifts**
- **Livescu/Wei demonstrated RT 3-D DNS simulations with different initial spectra that have different late-time(?) characteristics**
- **Andrews/Rollin constructed a ballistic model that facilitates evaluation of the development of complex initial spectra for RT, and shown how it connects to turbulence model initialization**

Where next?

- Transition IC specifications to models via implementation and testing
- Transition "metrics" (κδ, ballistic model, C_4)
- "Bipolar" discovery
- Experimental ("b", spectra. IC conditions for GC), DNS data into a repository
- Definition of test problem suite (Gas Curtain for J32Mix)
- Other turbulence problems IC specifications – At and Ma effects on κδ (look to RM formulas) – miscible – shear.

SPARES

Overview of the Proposed Research

- **Overall goal: To describe birth to full development of turbulent mixing (Rayleigh-Taylor & Richtmyer-Meshkov) – so enabling prediction and design.**
- **Research Direction: Theory "leads the way", with experiment and simulation providing data and discovery, and V&V.**
- **An Integrated Team: We have a world-class, closely integrated team, of fluid experts that cover theory, experiment and simulation.**
- **Primary Deliverable: A predictive/design capability for turbulent mixing (e.g. advanced turbulence models, BHR)**
- **Research spin-offs: We expect discoveries associated with the physics of fluid "transition", numerical representation of turbulence, and new theory/models for broad usage.**

Power spectra of the late-time mixing, as well as the density-specific volume covariance, help us to quantify mixing differences

t_{RS}

90μs

170μs

280μs

385μs

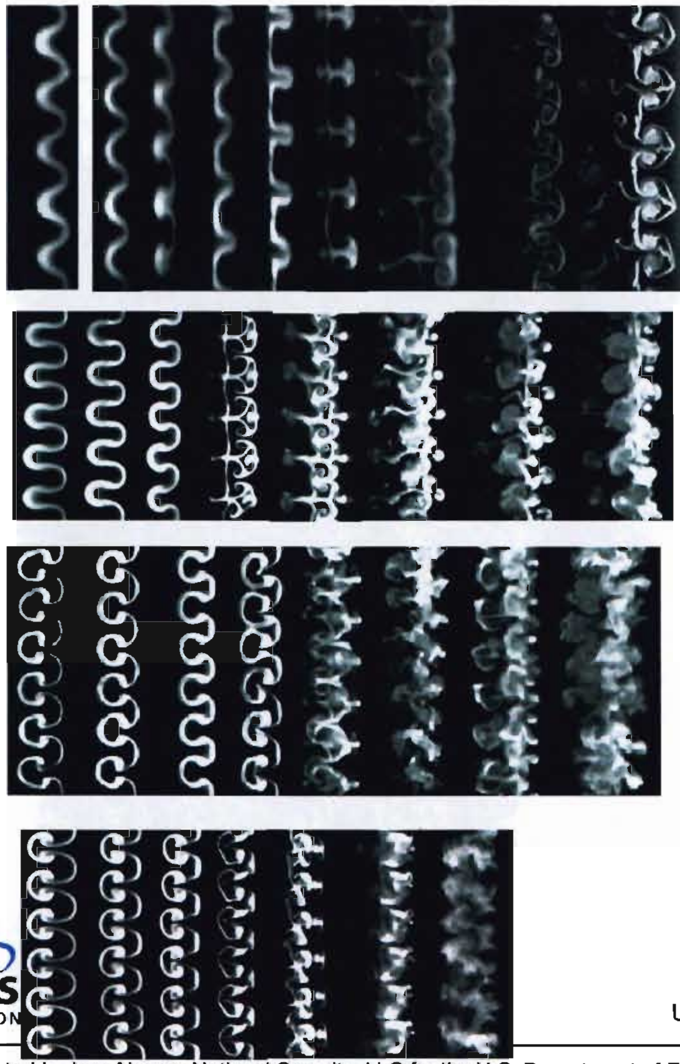

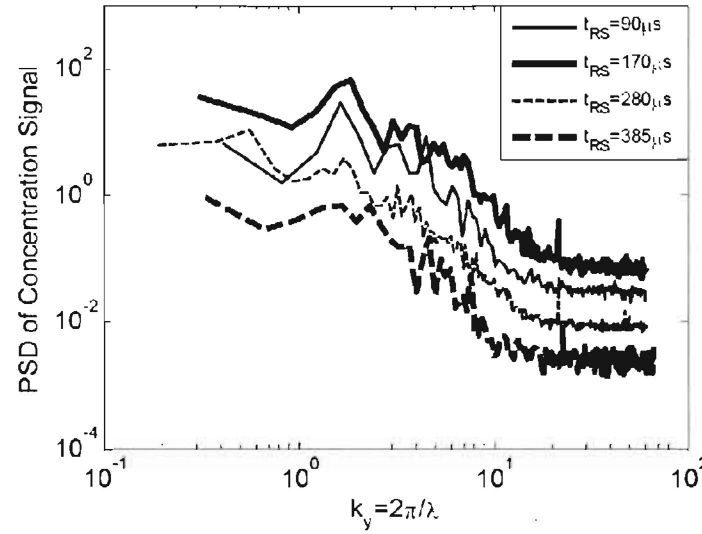

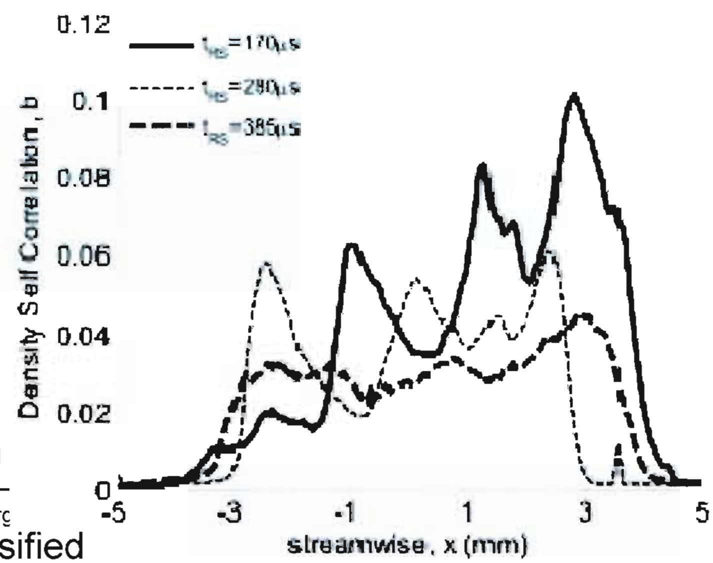

$$b(x) = -\frac{\sum_{i=1}^{N} \rho_i'(x,y)\left(\frac{1}{\rho}\right)'(x,y)}{N}$$

High value of b indicates less mixing.

Differences in TKE are observed for different $\kappa\delta$ initial conditions

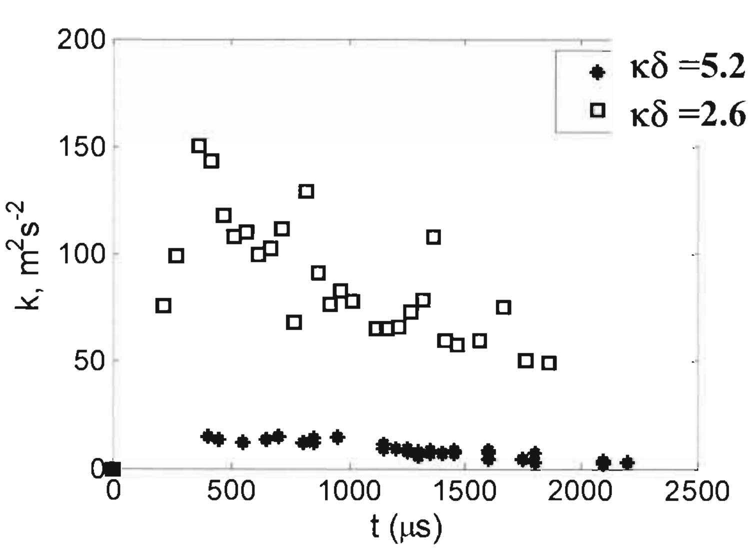

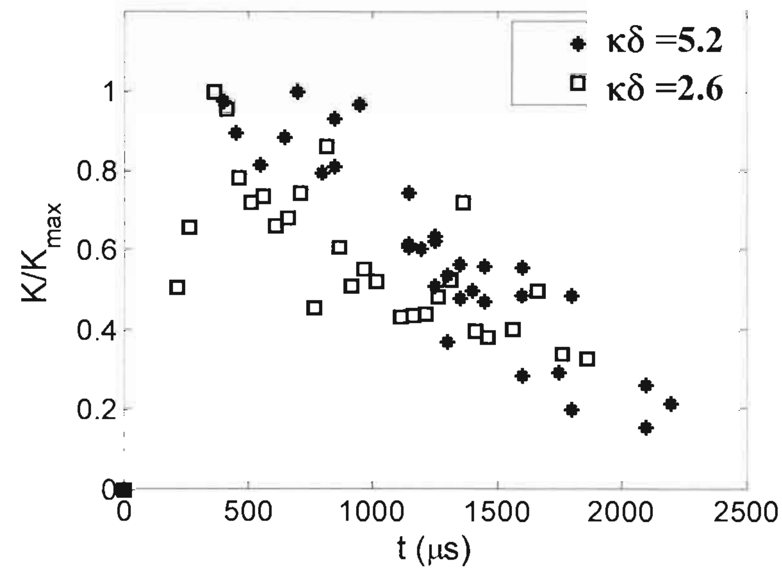

2-D Turbulent Kinetic Energy

$$K = 0.5*(\overline{u'^2} + \overline{v'^2})$$

Turbulent Reynolds Number

$$Re_K = \frac{\sqrt{k}\delta}{\nu}$$

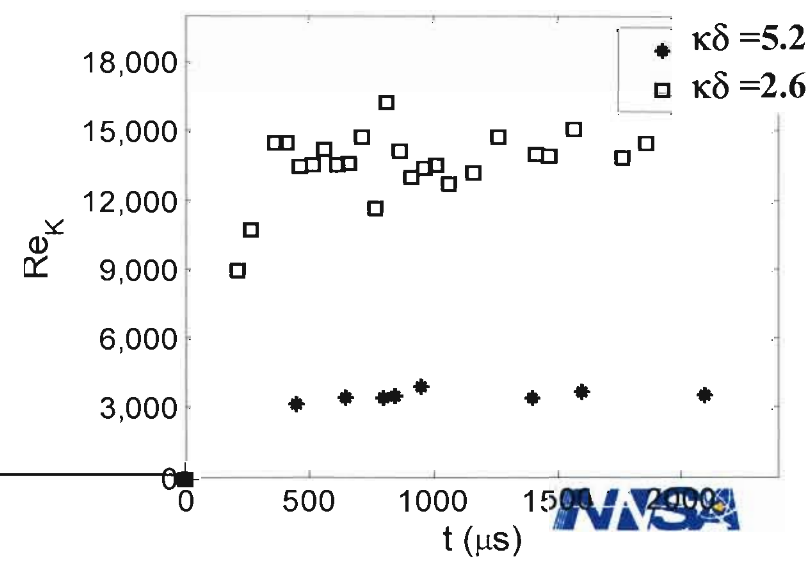

Two-Mode RTI: Resonance, leaning, symmetries, and pattern formation (k1=16, k2=80)

Resonant modes (strong vertical ejections): fastest growth

No phase shift

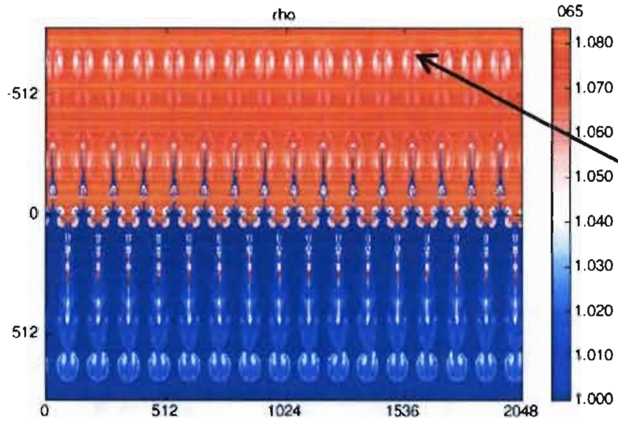

Non-resonant modes (inclined ejections or "leaning"): reduced growth

Phase shift: 0.01π

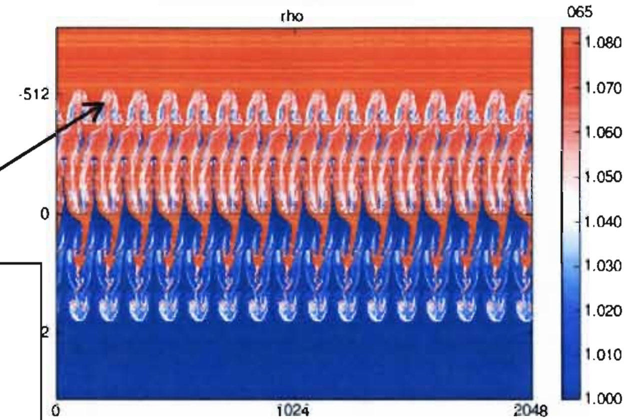

Translation symmetric patterns allowed by the periodic BC

Completely out of phase modes: slowest growth

Phase shift: π

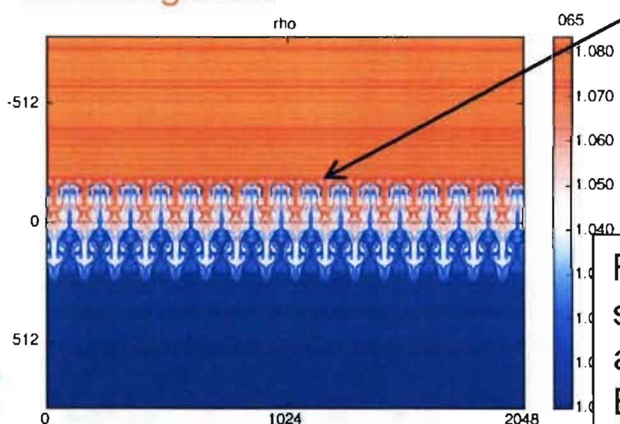

Balanced vortical motions due to the walls

No phase shift

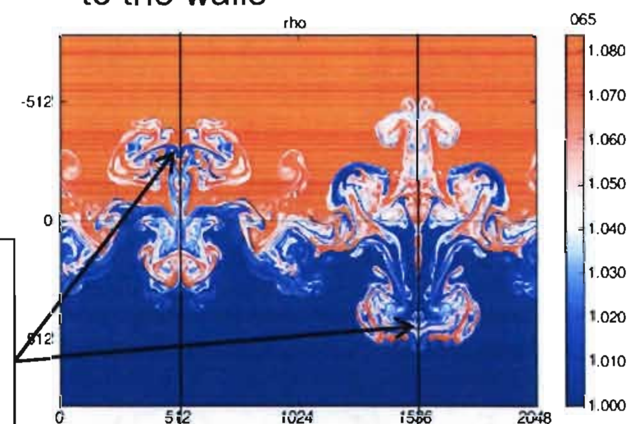

Reflection symmetric patterns allowed by the walls BC (the wall acts as a mirror)

Slip-walls

Two-Mode RTI: pattern formation and balanced and unbalanced vortical motions (k1=16, k2=81)

Unbalanced vortices: complete ejections more likely, but ejections do not occur in the vertical direction.

No phase shift

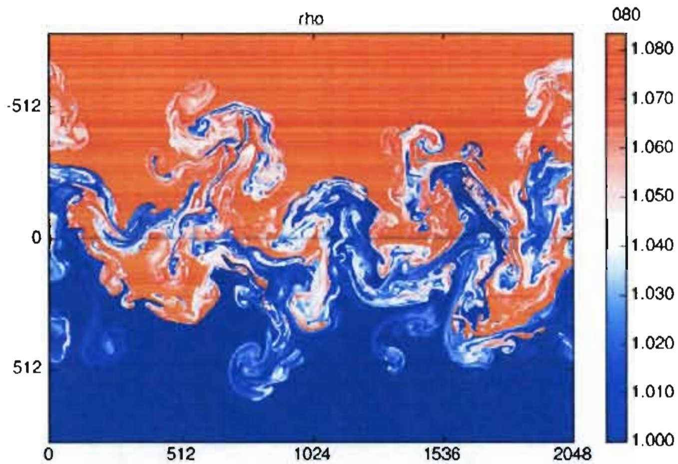

Resonant and out of phase modes: faster growth in the light fluid (in phase), slower growth in the heavy fluid (out of phase)

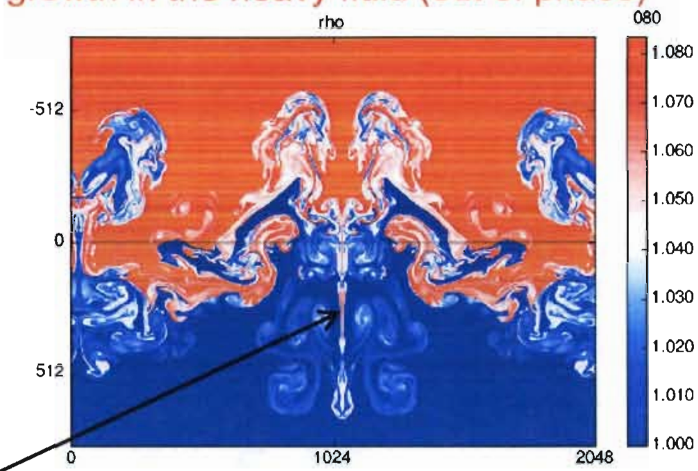

Phase shift: 0.03π

Balanced vortical motions due to the walls

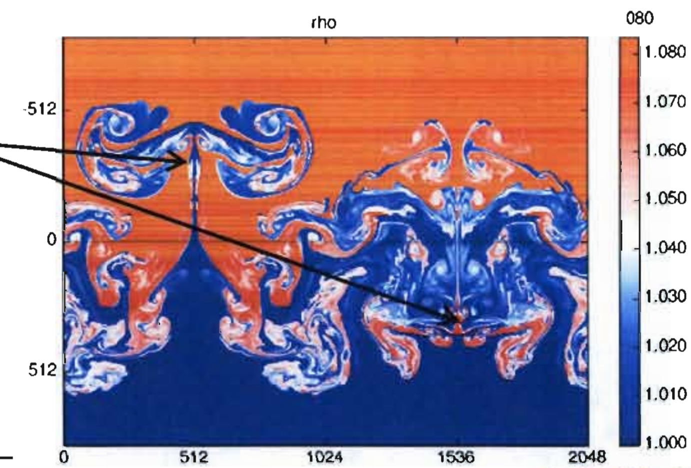

No phase shift

Reflection symmetric patterns allowed by the walls BC or generated by the IC

Two-Mode RTI: Resonance, leaning, symmetries, and pattern formation (k1=16, k2=80)

No phase shift

Resonant modes (strong vertical ejections): fastest growth

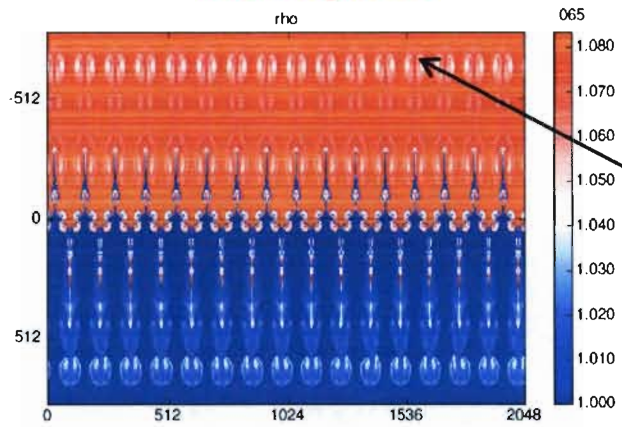

Non-resonant modes (inclined ejections or “leaning”): reduced growth

Phase shift: 0.01π

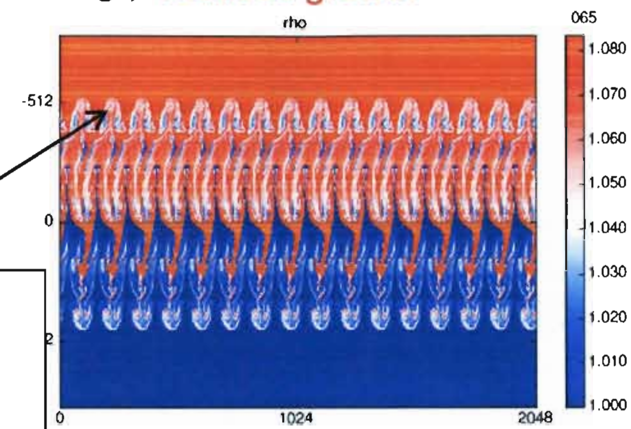

Translation symmetric patterns allowed by the periodic BC

Phase shift: π

Completely out of phase modes: slowest growth

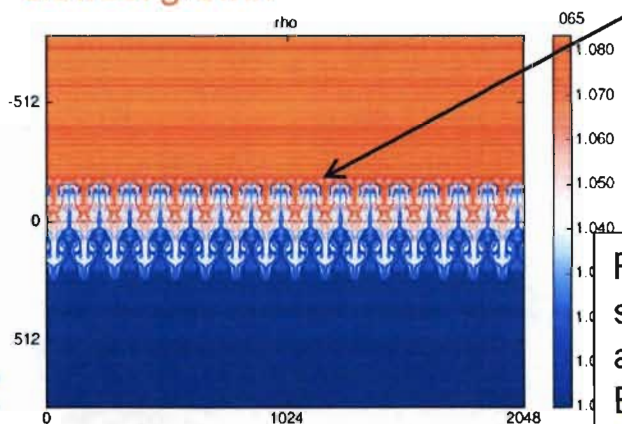

Balanced vortical motions due to the walls

No phase shift

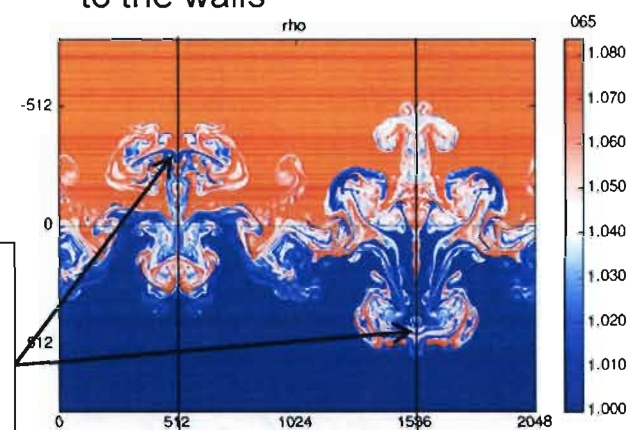

Reflection symmetric patterns allowed by the walls BC (the wall acts as a mirror)

Slip-walls

Two-Mode RTI: pattern formation and balanced and unbalanced vortical motions (k1=16, k2=81)

Unbalanced vortices: complete ejections more likely, but ejections do not occur in the vertical direction.

No phase shift

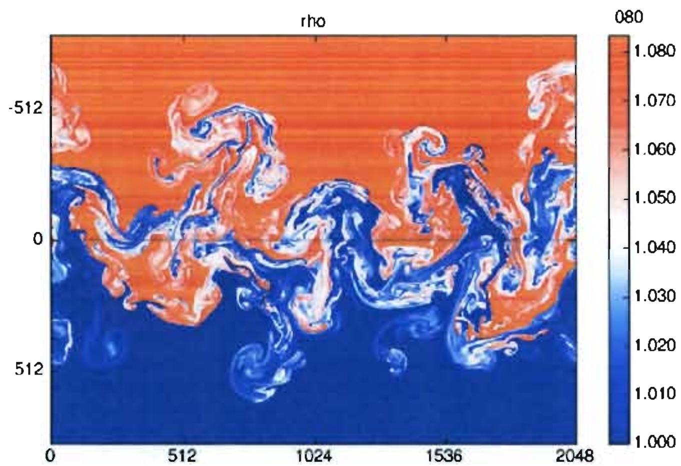

Resonant and out of phase modes: faster growth in the light fluid (in phase), slower growth in the heavy fluid (out of phase)

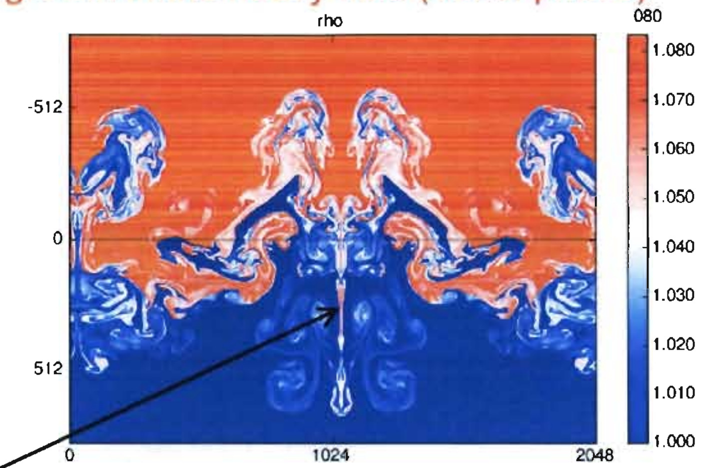

Phase shift: 0.03π

Balanced vortical motions due to the walls

Reflection symmetric patterns allowed by the walls BC or generated by the IC

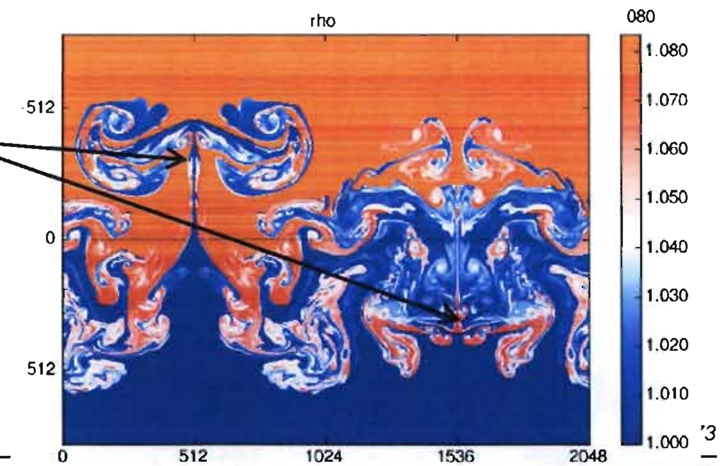

No phase shift

Progress Toward an ODE model with Mode Coupling for Non-Linear Evolution of Multi-Mode IC's

Driving idea:

- **A source term to the Goncharov nonlinear ODE for single mode evolution that expresses the contribution by coupling of the wavenumber of interest with a direct neighbor**

$$\ddot{h}_{b,k} = G(k, A, g, etc...) + A \times k \times F(k, k+1) \times \left(\ddot{h}_{b,k+1} h_{b,k+1} + \dot{h}_{b,k+1}^{2}\right)$$

- $G(k, A, g, etc...)$ **is given by Goncharov's model for a single mode perturbation**
- $F(k, k+1)$ **is a coupling factor of order 1**
- **The ODE are solved for all modes and the dominant mode gives the height of the mixing layer**

$$h_b(t) = \max_k (h_{b,k}(t))$$

ODE model with Mode Coupling for Non-Linear Evolution of Multi-Mode IC's

Bubble growth rate

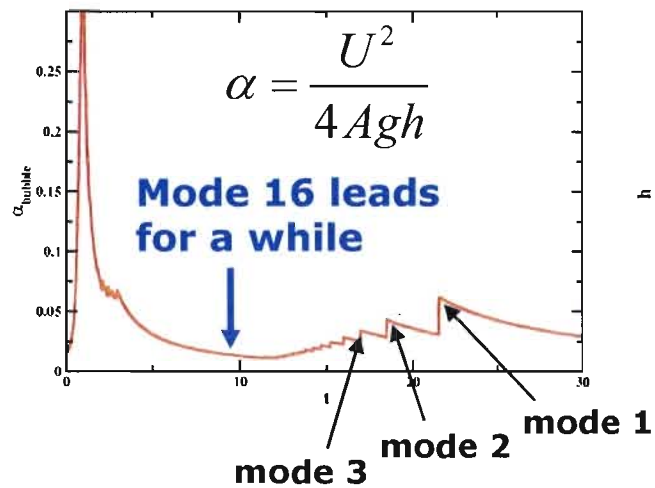

Height evolution for each mode

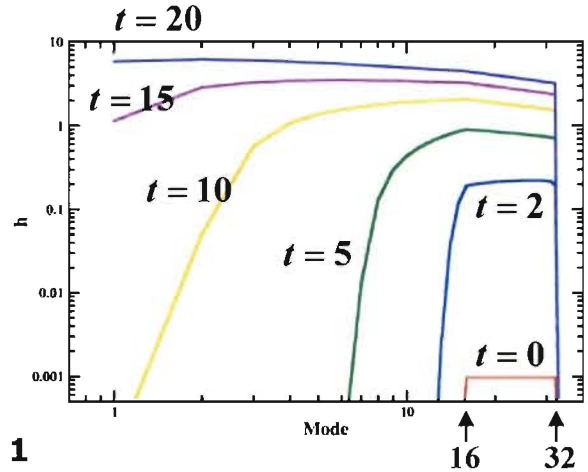

Bubble velocity

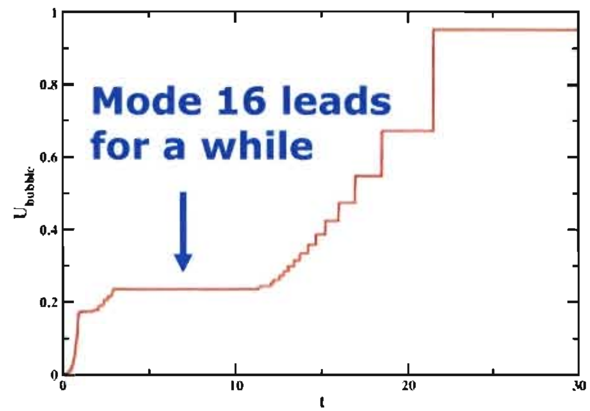

- The model generates modes toward lower wavenumbers
- Work is needed for the coupling factor as the seeded modes have a much too low generated amplitude.

ODE model with Mode Coupling for Non-Linear Evolution of Multi-Mode IC's

Bubble growth rate

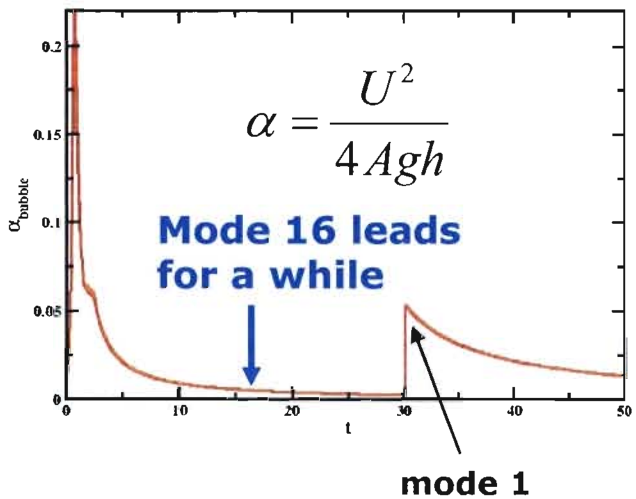

Height evolution for each mode

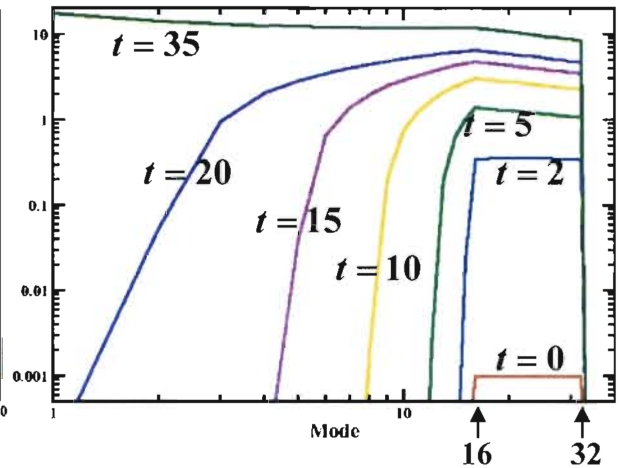

Bubble velocity

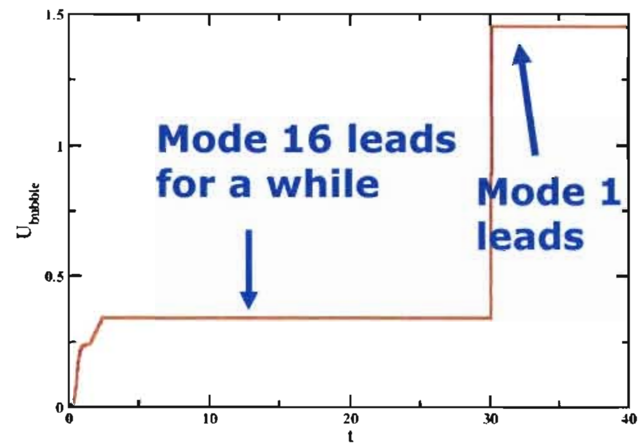

- The model generates modes toward lower wavenumbers

- Improvement is needed for the coupling factor as the seeded modes have a much too low generated amplitude.

Post-saturation treatment

Ofer *et al.*, Phys. Plasmas, **3** (1996)

Evolution of a two mode initial perturbation, modes 2 & 3

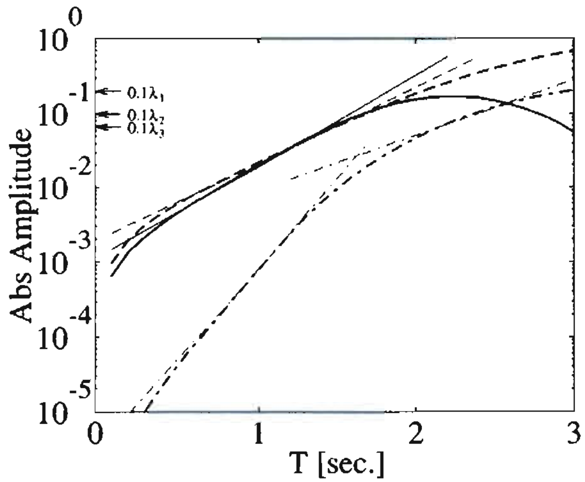

Evolution of a two mode initial perturbation, modes 1 & 2

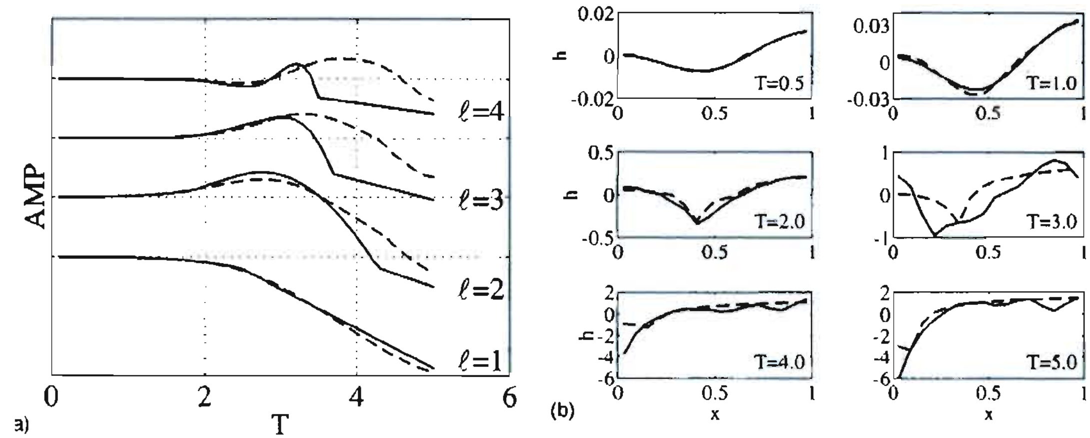

A saturated mode cease to contribute to mode coupling

A saturated mode k can only be affected by two lower-k modes. Its velocity can never exceed its saturation velocity.

Modal Model Behavior

Mode Coupling

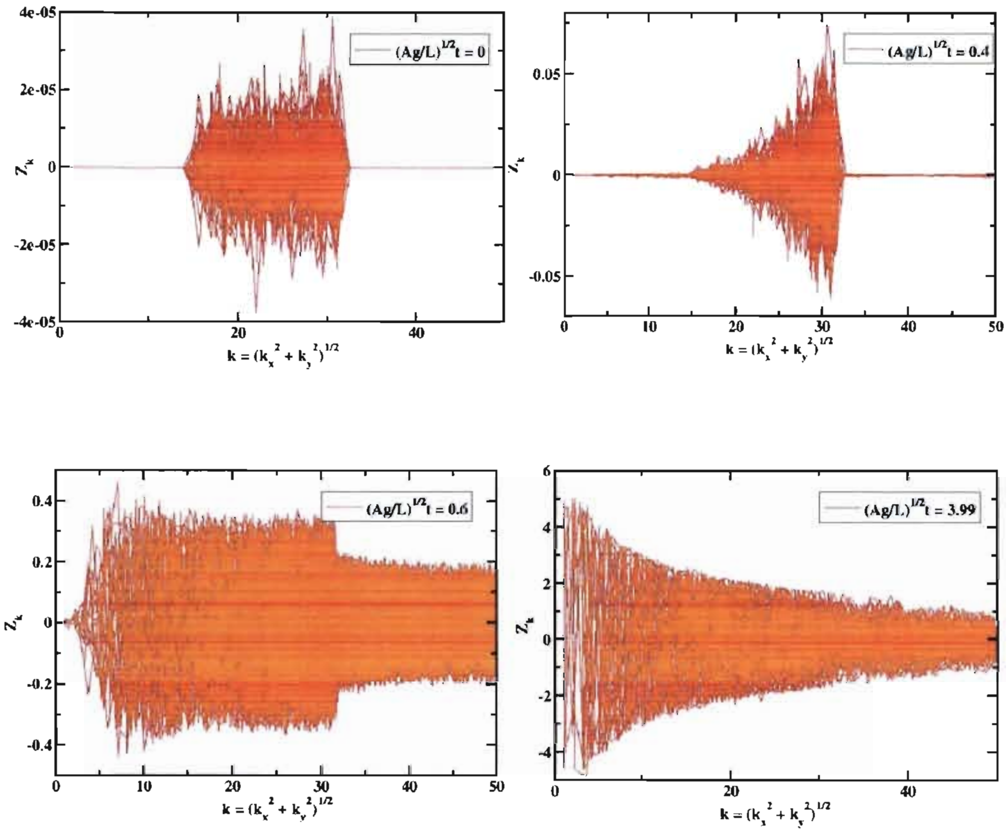

No Mode Coupling

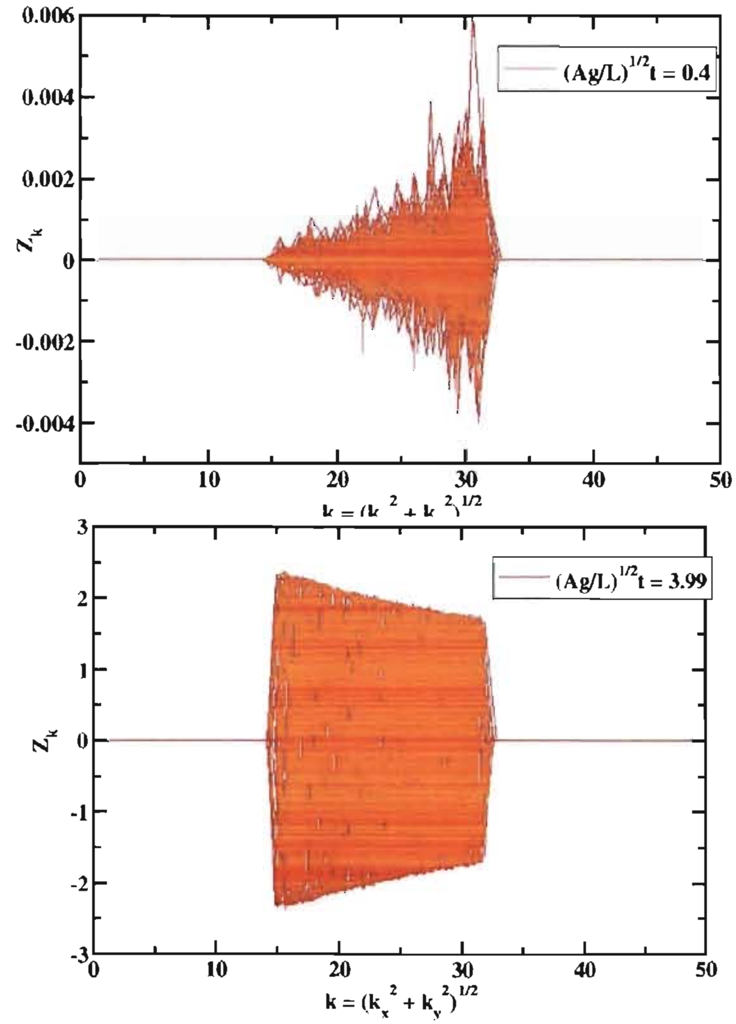

The mode coupling function will "populate" the entire spectrum

Modal Model Behavior

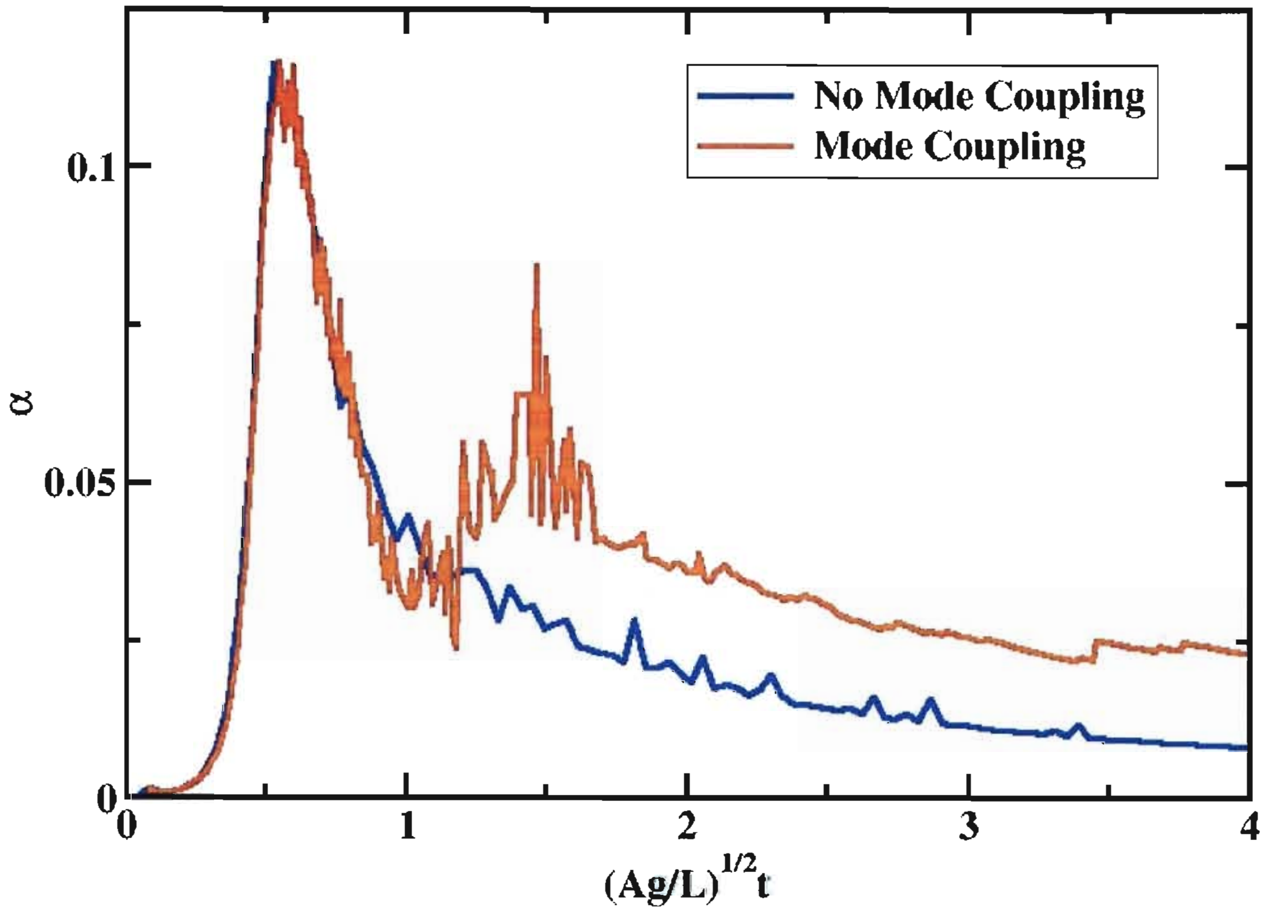

Mode coupling is at the origin of self similarity

A Modal Model for Multimode RT: Linear regime

An modal model for multimode RT built from the "fusion" between a potential flow model for single mode and a weakly nonlinear model:

For all k,

$$\ddot{Z}_k = \frac{4(k-8\eta_2)}{k^2 - 4A_T k\eta_2 - 32A_T\eta_2^2}\left(-\dot{Z}_k^2 k^2 \frac{(5A_T-4)k^2 + 16(2A_T-3)k\eta_2 + 64A_T\eta_2^2}{8(k-8\eta_2)^2} - A_T g\eta_2\right)$$
$$+ A_T k \sum_{\vec{m}} \left\{ \ddot{Z}_m Z_n \left(1 - \hat{m}\cdot\hat{k}\right) + \dot{Z}_m \dot{Z}_n \left(\frac{1}{2} - \hat{m}\cdot\hat{k} - \frac{1}{2}\hat{m}\cdot\hat{n}\right)\right\}$$

$$k = \sqrt{k_x^2 + k_y^2}$$

Initial perturbation in wave space

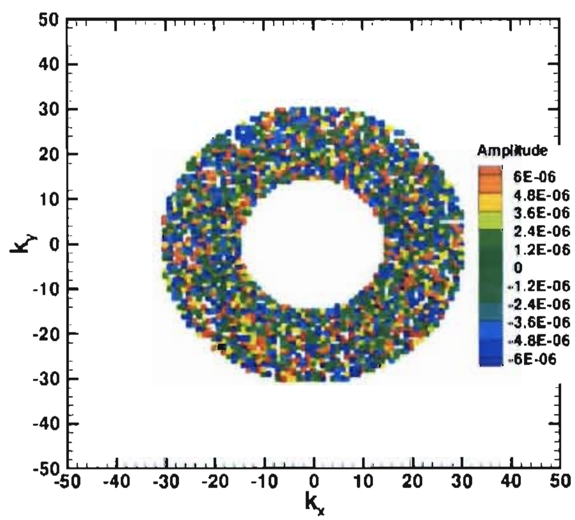

Using a two dimensional initial perturbation spectrum for the model allow a one-to-one match with ICs for 3D simulations

Approximation for Density Profile

Heavy Fluid Volume Fraction Profile

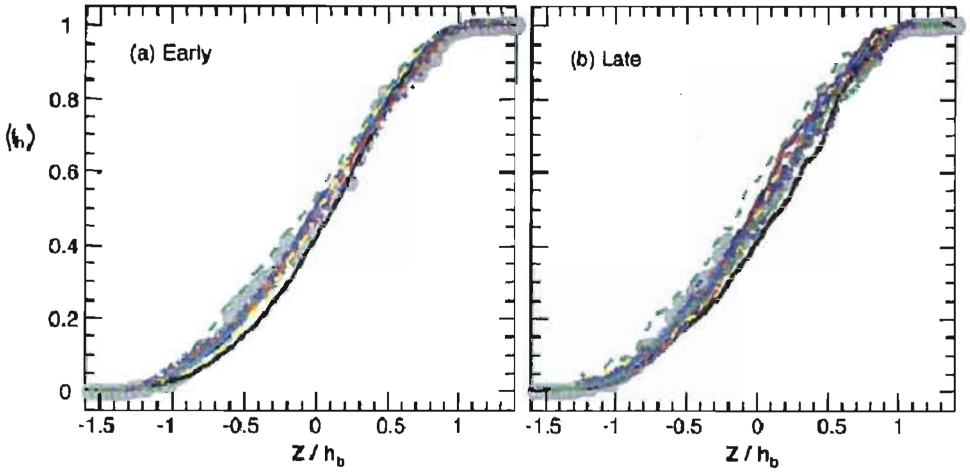

Dimonte *et al*., Phys. of Fluids, **16** (2004)

Density Profile

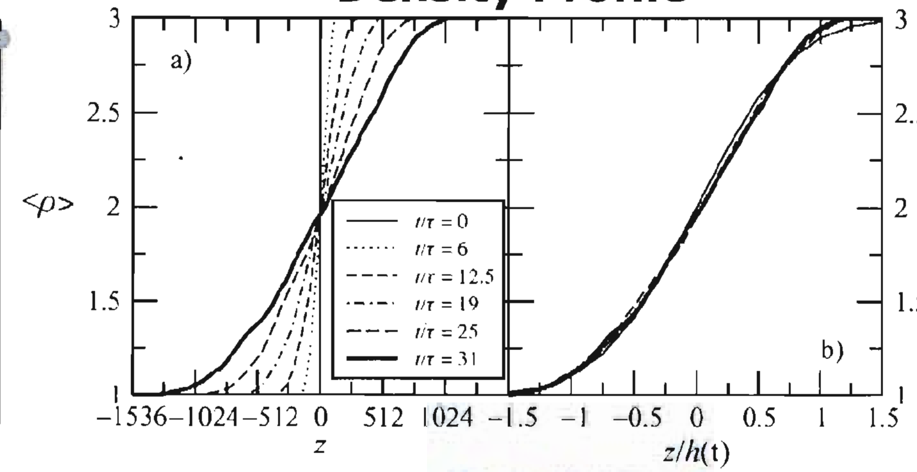

Livescu *et al*., J. Turbulence, **10** (2009)

$$\rho = f_l \rho_l + f_h \rho_h$$

$$\begin{cases} f_l = \dfrac{\rho - \rho_h}{\rho_l - \rho_h} \\ f_h = 1 - f_l \end{cases}$$

$$\begin{cases} f_h = 0 & \text{if} \quad z < -h_s \\ f_h = 0.5\dfrac{z + h_s}{h_s} & \text{if} \quad -h_s \le z < 0 \\ f_h = 0.5\dfrac{z}{h_b} + 0.5 & \text{if} \quad 0 \le z \le h_b \\ f_h = 1 & \text{if} \quad z > h_b \end{cases}$$

For a smooth mixture fraction description

$$\tilde{f}_h(z) = \int_{h_s}^{h_b} (z - h_s)^{a-1}(h_b - z)^{b-1}\,dz$$

$$f_h(z) = \frac{\tilde{f}_h(z)}{\tilde{f}_h(h_b)}$$

Establishement of a nonlinear cascade process

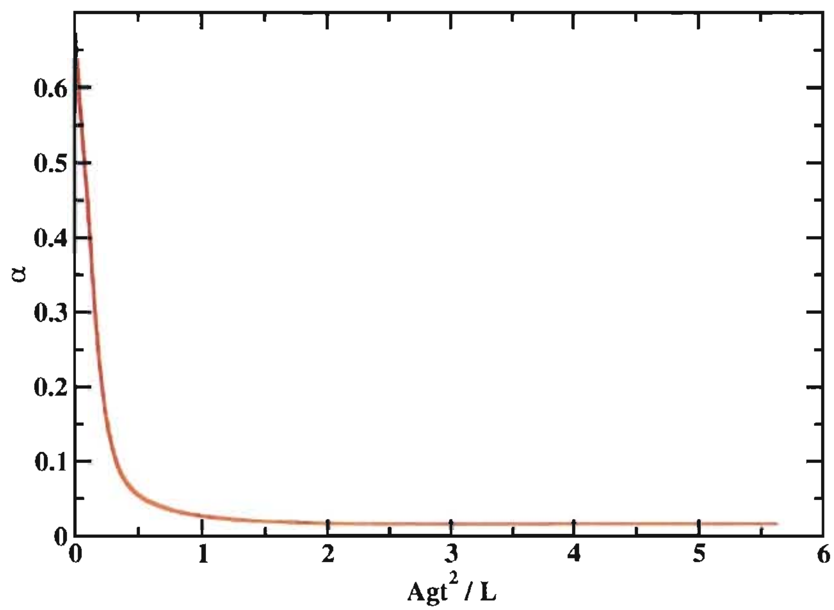

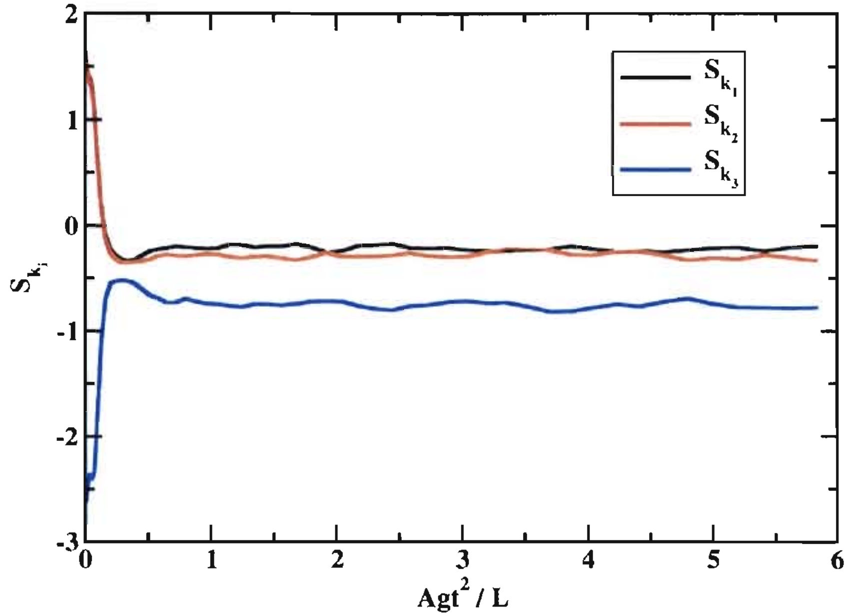

It appears that the establishment of a nonlinear cascade process occurs at about the same time as the mixing layer growth becomes self-similar

How does interfacial morphology control the evolution of RM?

A reminder about κδ; if $X_s(y,z)$ describes the material interface, the rms **slope of the interface "η_o" is:**

$$\eta_o = \kappa_o \delta_o$$

$$\sim \langle \nabla X_s \nabla X_s \rangle^{1/2}$$

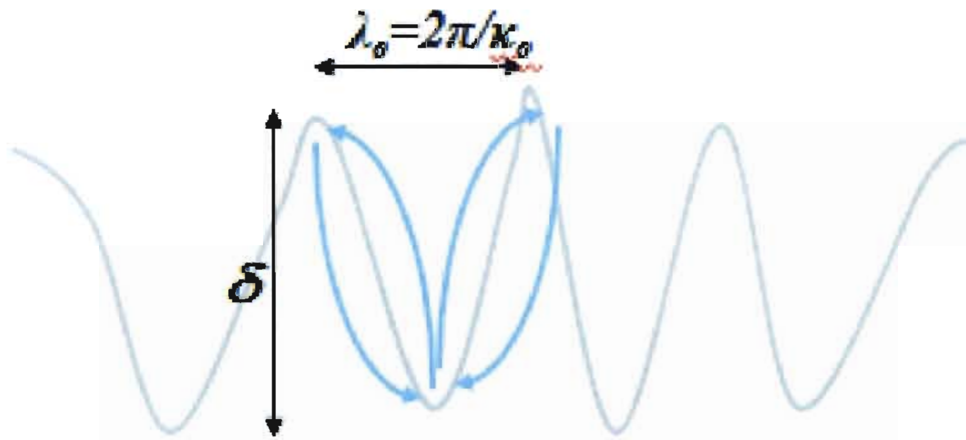

low η_0

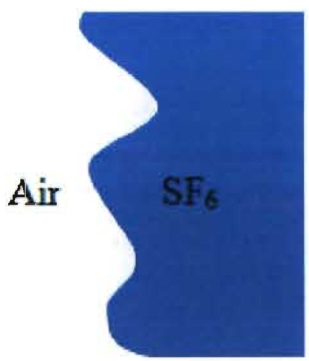

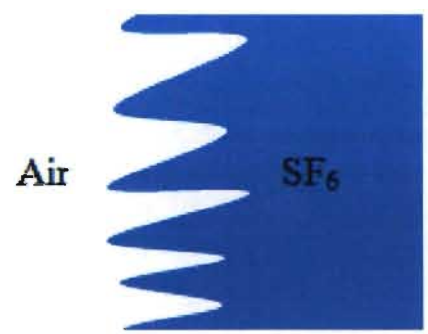

high η_0

Unclassified

ILES RAGE – Planar RM Expts.:

Spectral IC effects on material mixing

Grinstein, Gowardhan, and Wachtor, *PoF*, **23**, 3, 2011

egg crate (λ_o) $\theta = (1 - Y_{SF6}) Y_{SF6}$ + (0.4-4λ_o)

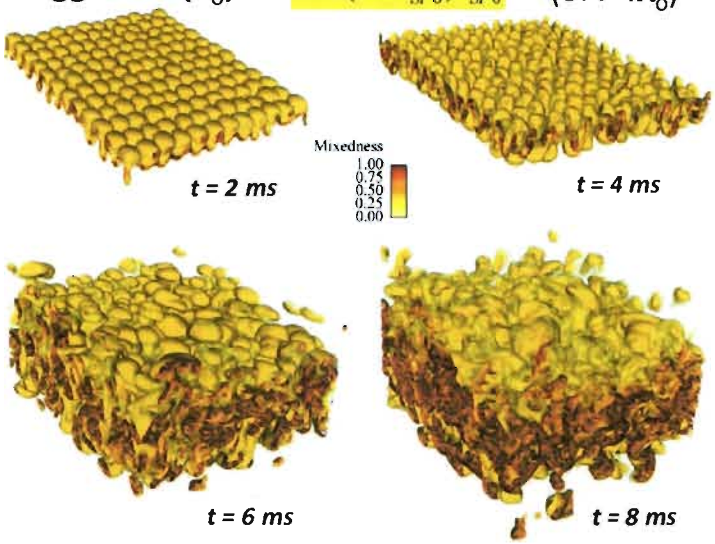

10% IC perturbation added to mode (λ_o)

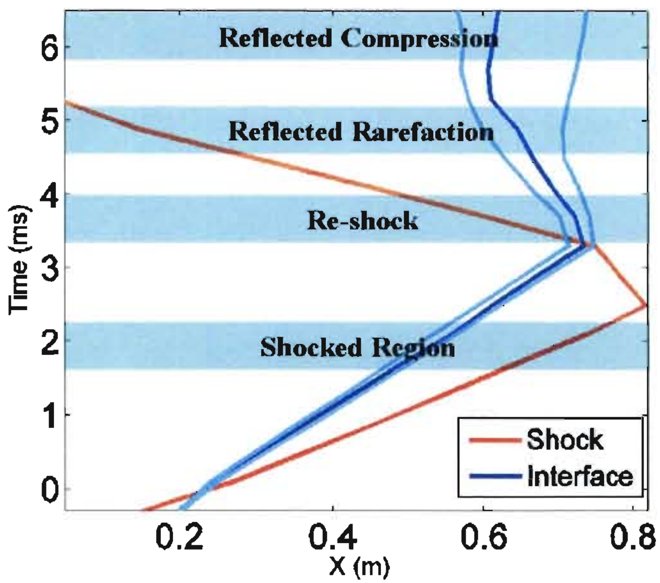

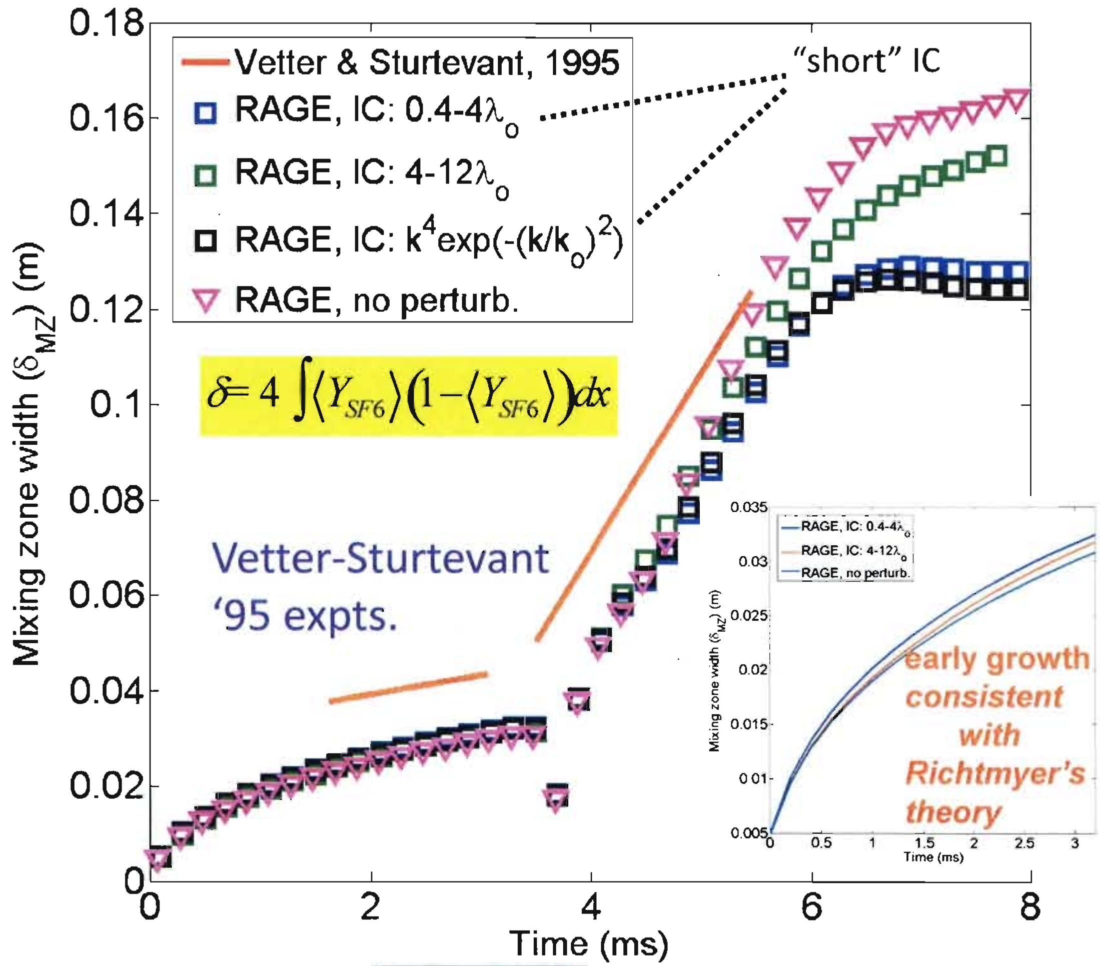

- **results for "thin" low η_0 initial material interface**
- **early-time** (t<~5ms) **growth not sensitive to ICs**
- **late-time sensitive to ICs** (more so for "longer" IC)

Turbulence Metrics

turbulent kinetic energy **enstrophy**

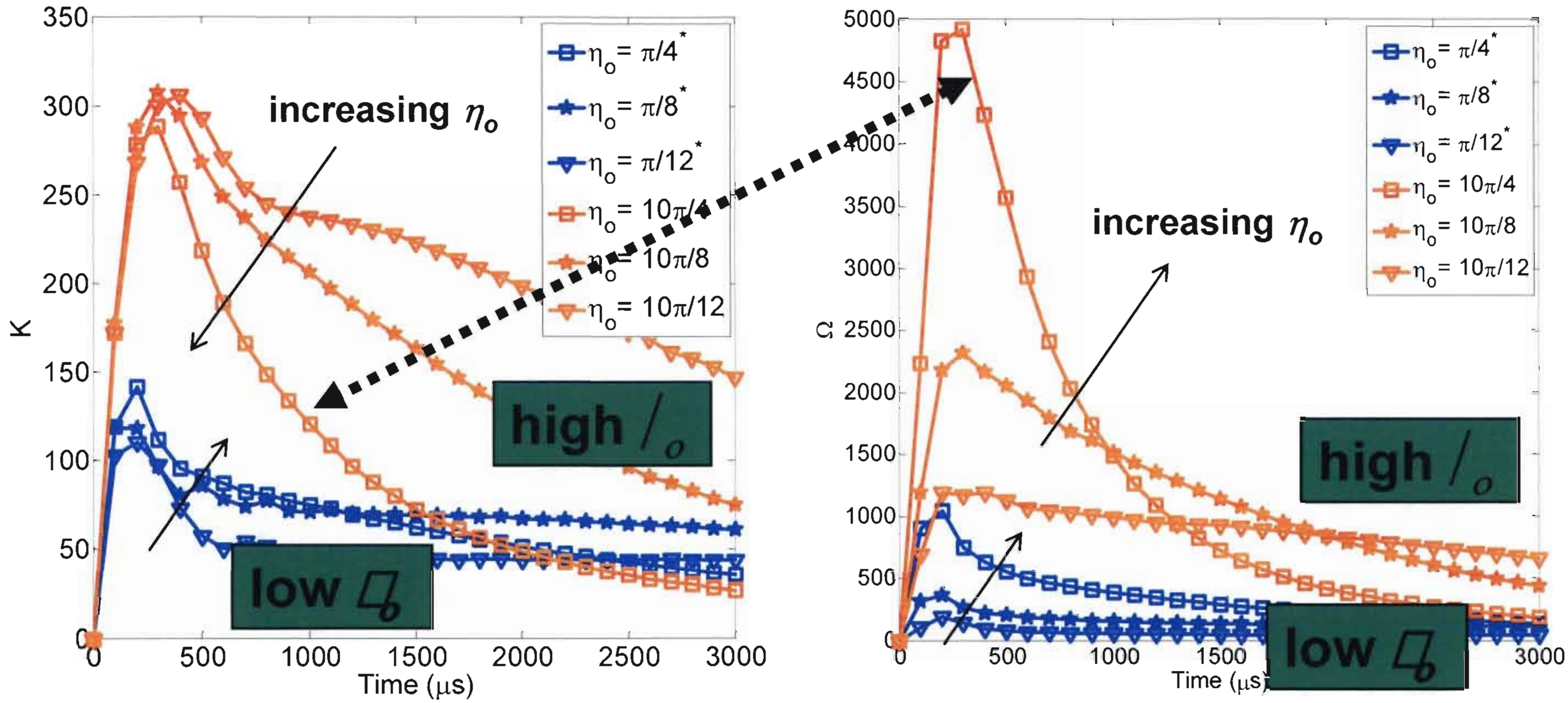

- **more enstrophy – less turbulent kinetic energy**
- **the modeler's IC challenge**: two different instabilities & growth trends

Generating Perturbed 3D initial conditions for the GC

Large scale perturbation: Achieved by slightly offsetting (randomly, <0.05R) the nozzle in the shock direction

Small scale perturbation: Achieved by adding 3D concentration perturbation (s.d. ~2%) to baseline 3D GC

a0) No perturbation (baseline) 

a1) Nozzle offset 

a2) 3D concentration perturb. 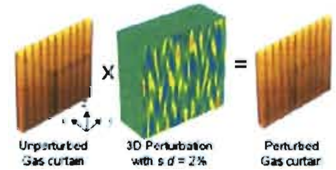

a3) Nozzle offset and 3D conc. Perturb.

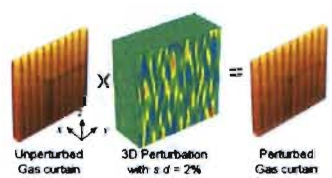

Simulations vs. ICs

(SF_6 mass-fraction visualizations)

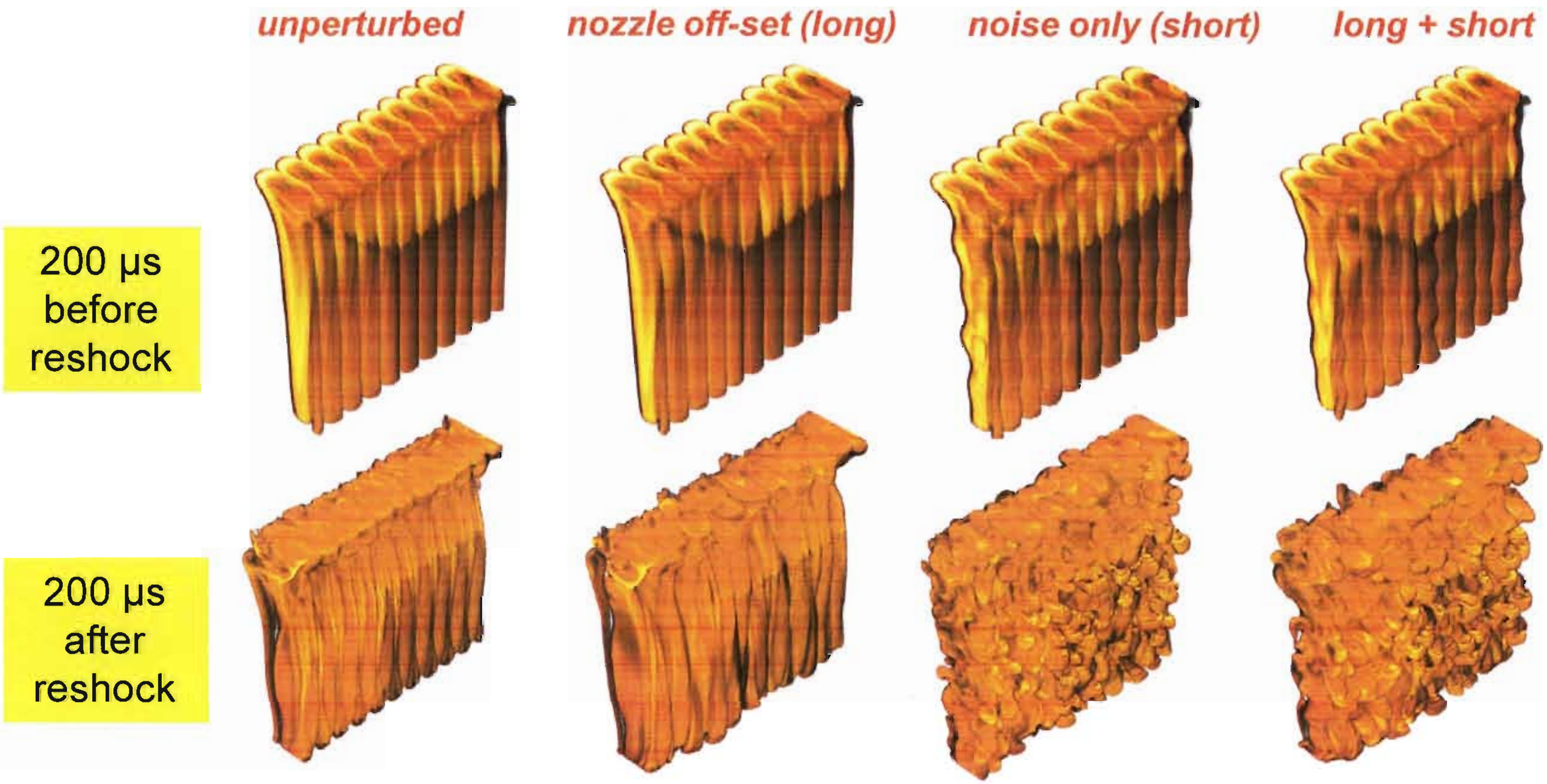

- Higher concentration gradients near the nozzles lead to more baroclinic vorticity production and results in substantially-3D flow features
- Structures for various cases look very similar before reshock,
- After reshock, small-scale perturbations break ballistic growth, trigger 3D mode-coupling, small-scale production, more isotropic flow features (suggestive of "transition") …

Consequences of Bipolar RM Behavior

low η_0 reshock effects achieved with high η_0 at first shock

Gowardhan, Ristorcelli, Grinstein; AIAA Paper June 2011 → in preparation for PoF

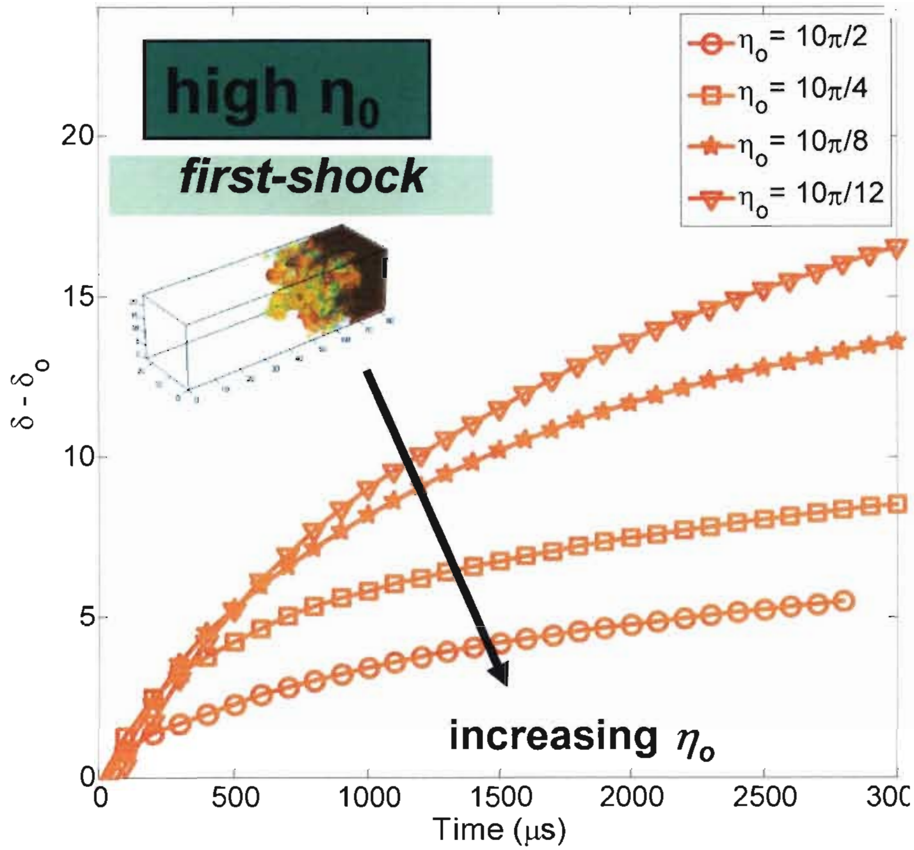

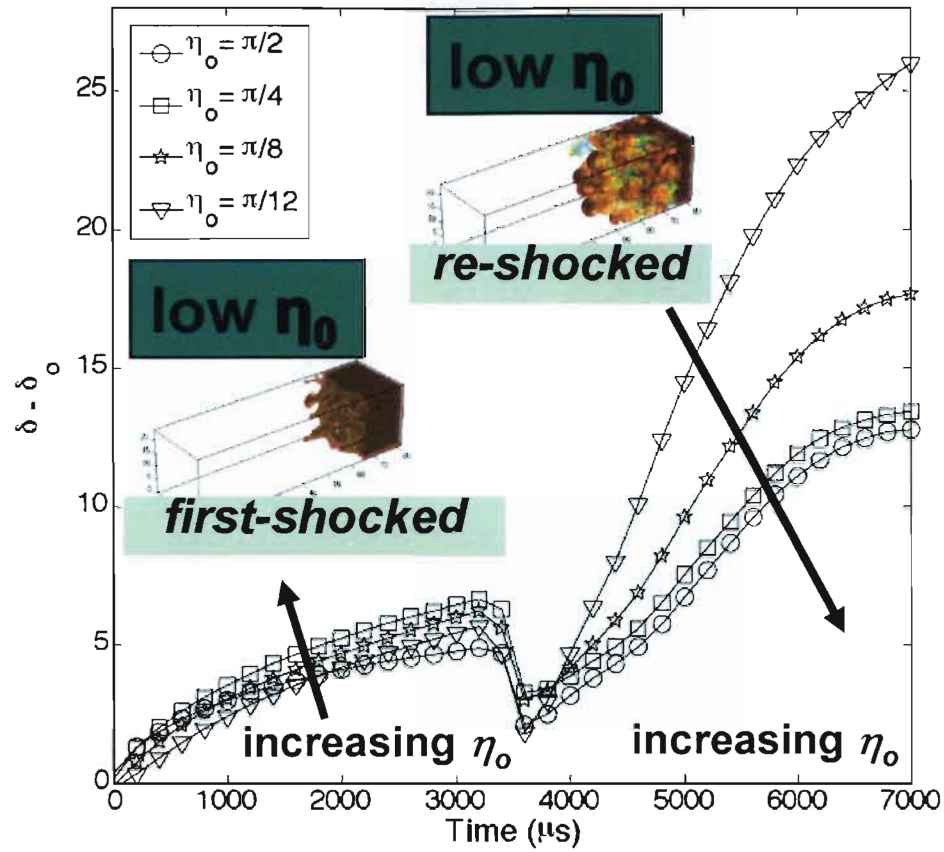

Modeler's (initial condition) challenge:

two different instabilities and growth trends (ballistic & mode-coupling, switch metrics at $\eta_0 \sim 1$ and subsequent late-time characteristics …

GC Width: Simulations *vs.* Expts.

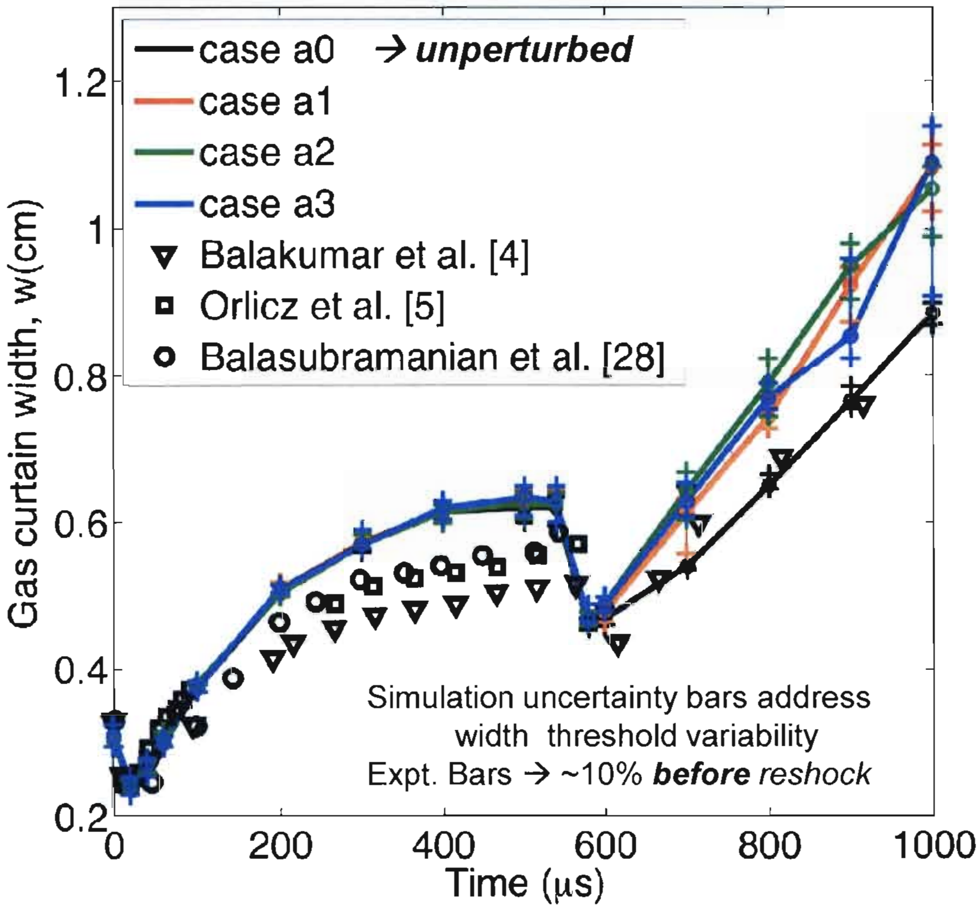

***GC* width is defined as shockwise distance over which $\chi(x) > \chi_h$ based on a selected threshold $\chi_h \sim 0.95$, where $\chi(x) = 4\zeta(x)(1-\zeta(x))$, and**

$$\zeta(x) = \frac{1}{L_y}\int_0^{L_y}\left(\frac{\rho_{SF6}(x,y,z=2)}{\rho(x,y,z=2)}\right)dy$$

- Simulated growth qualitatively consistent with expts.
- GC widths for all simulations are in close agreement **before reshock**; discrepancies between simulations & expts. mainly attributed to uncharacterized composition & fluctuations of SF_6 mixture in initial GC

After reshock, GC width growth rates are consistent but, "perturbed" significantly different from "unperturbed";
→ very sensitive to ICs and consequent interface conditions at reshock time causing problems for LES

Bipolar RM Behavior in Shocked Gas Curtains (no reshock) ?

- IC parameterization & additional GC cases
  - Data reduction
  - Bipolar RM behavior also for the shocked GC ?

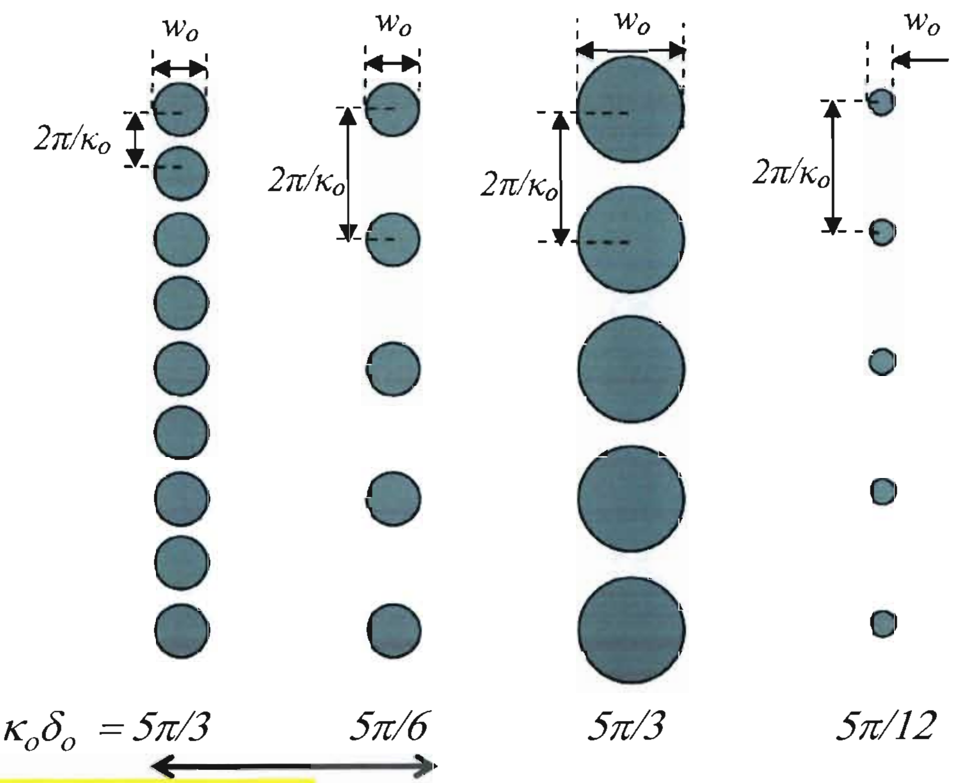

lab. expts. available only for these two cases

RM Behavior in Shocked GCs (no reshock)

Gowardhan and Grinstein, JoT 2011, under review

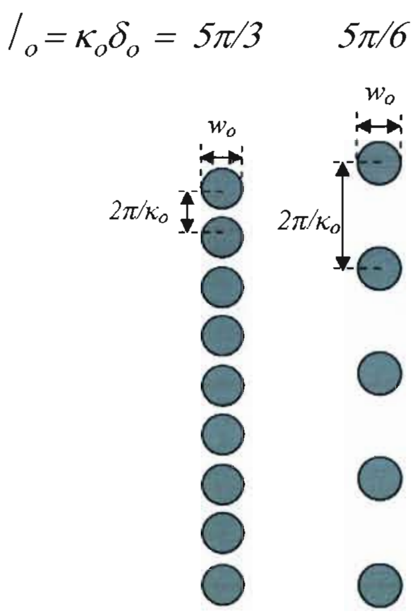

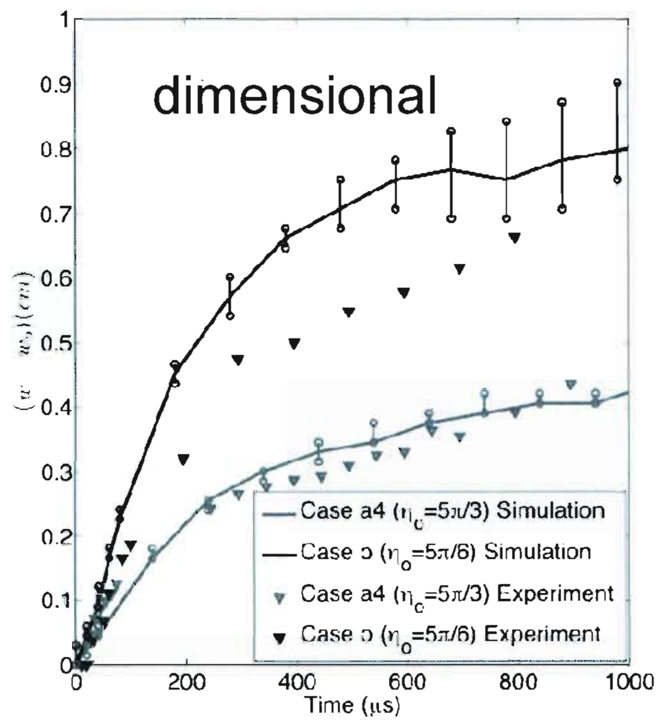

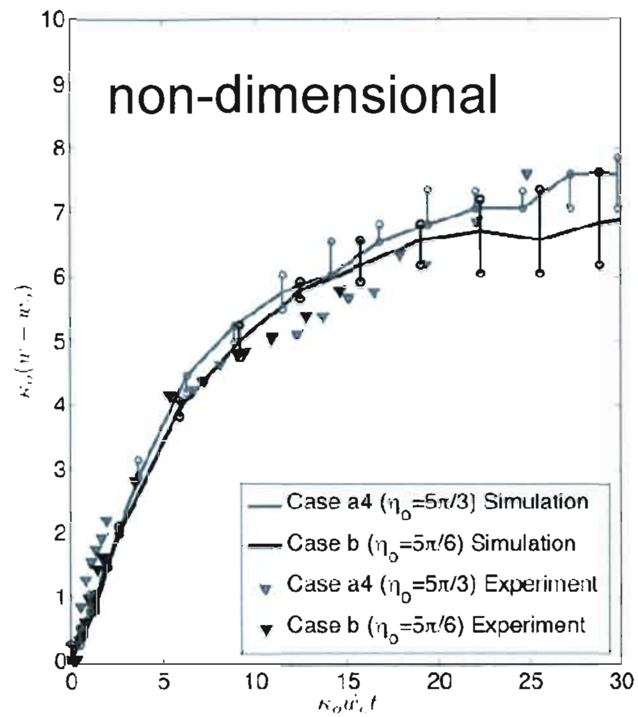

- Simulation results compare well with experiments for both GC cases.
- When non-dimensional GC widths are plotted against time scaled with initial width growth rates (*first proposed by Jacobs et al. 1996*) curves collapse well in "non-linear" regimes.

Los Alamos National Laboratory

X-Computational Physics Division

Bipolar RM Behavior in Shocked GCs (no reshock)

Gowardhan and Grinstein, JoT 2011, under review

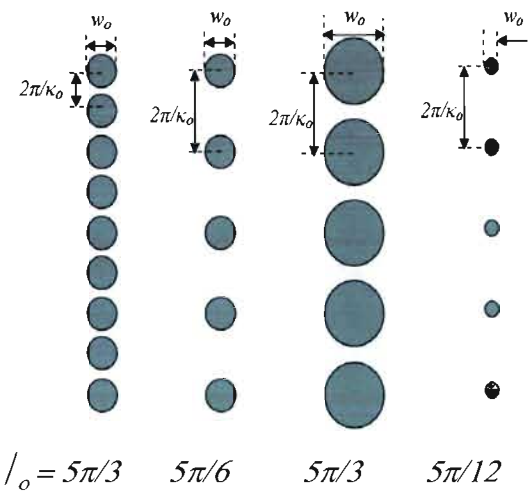

dimensional

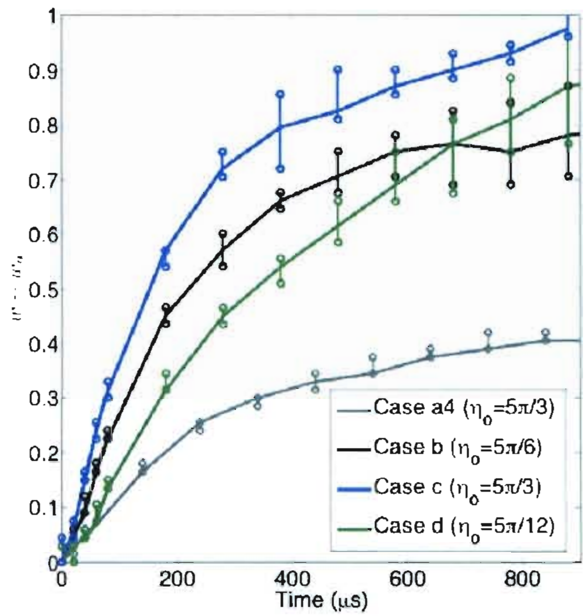

non-dimensional

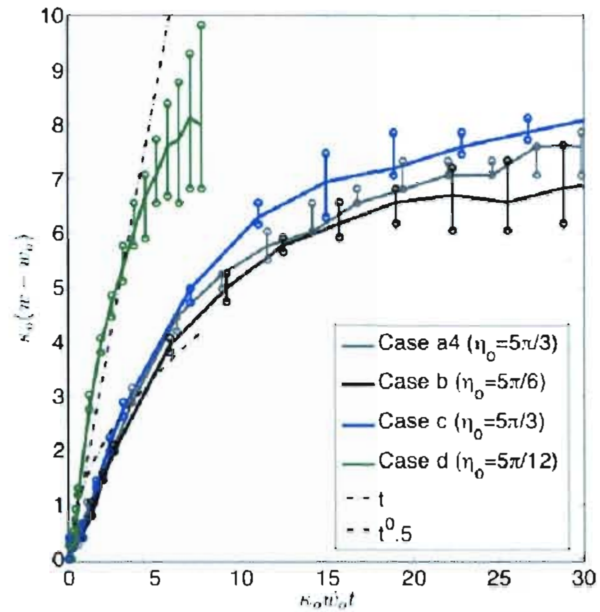

- When non-dimensional mixing widths are plotted against non-dimensional time, cases with initial *rms* slope greater than π/2 collapse in the non linear regime and the case with initial *rms* slope less than π/2 collapses on the linear region.
- **This demonstrates the bipolar RM behavior also in the shocked GC.**

Main Conclusions

The modeler's (initial condition) challenge

- **IC parameter (η_o) controls RM bipolar behavior**
- RM Instability behavior switches for $\eta_o \sim 1$

- **Two very different instabilities & growth trends**
- **low η_o** : ***linear, ballistic***

$$\rightarrow as\ \eta_o \uparrow \quad enstrophy \uparrow \quad isotropy \uparrow \quad TKE \uparrow \quad mix-width \uparrow$$

- **high η_o** : ***non-linear, mode coupling***

$$\rightarrow as\ \eta_o \uparrow \quad enstrophy \uparrow \quad isotropy \uparrow \quad TKE \downarrow \quad mix-width \downarrow$$

- **Reshock effects emulated with first shock, if η_o > 1**
- **Bipolar RM demonstrated also for (2-interface) GC**

Direct Numerical Simulations of variable-density mixing

- **Code used: CFDNS (Livescu et al LA-CC-09-100).**
- **For this problem, mixed FFTs - 6th order compact finite differences.**
- **Main difficulty: Density variations lead to a variable coefficient Poisson equation (Livescu and Ristorcelli, J. Fluid Mech. 2007).**
  - Closed form solution for the gradient component of $\nabla p/\rho$, responsible for mass conservation
  - Iterative solver for the curl component of $\nabla p/\rho$, related to the baroclinic production of vorticity (Livescu and Ristiorcelli, J. Fluid Mech. 2007 and Chung and Pullin, J. Fluid Mech. 2010).
- **Extensive resolution studies performed to ensure the accuracy and convergence of the solution.**
- **2-D simulations (up to $16{,}384^2$) performed at LANL and on Jaguar, ORNL.**
- **3-D simulations (up to $4096^2 \times 4032$ RT) performed on Dawn, LLNL; Jaguar, ORNL; and LANL.**

Single-mode RTI: Growth stages

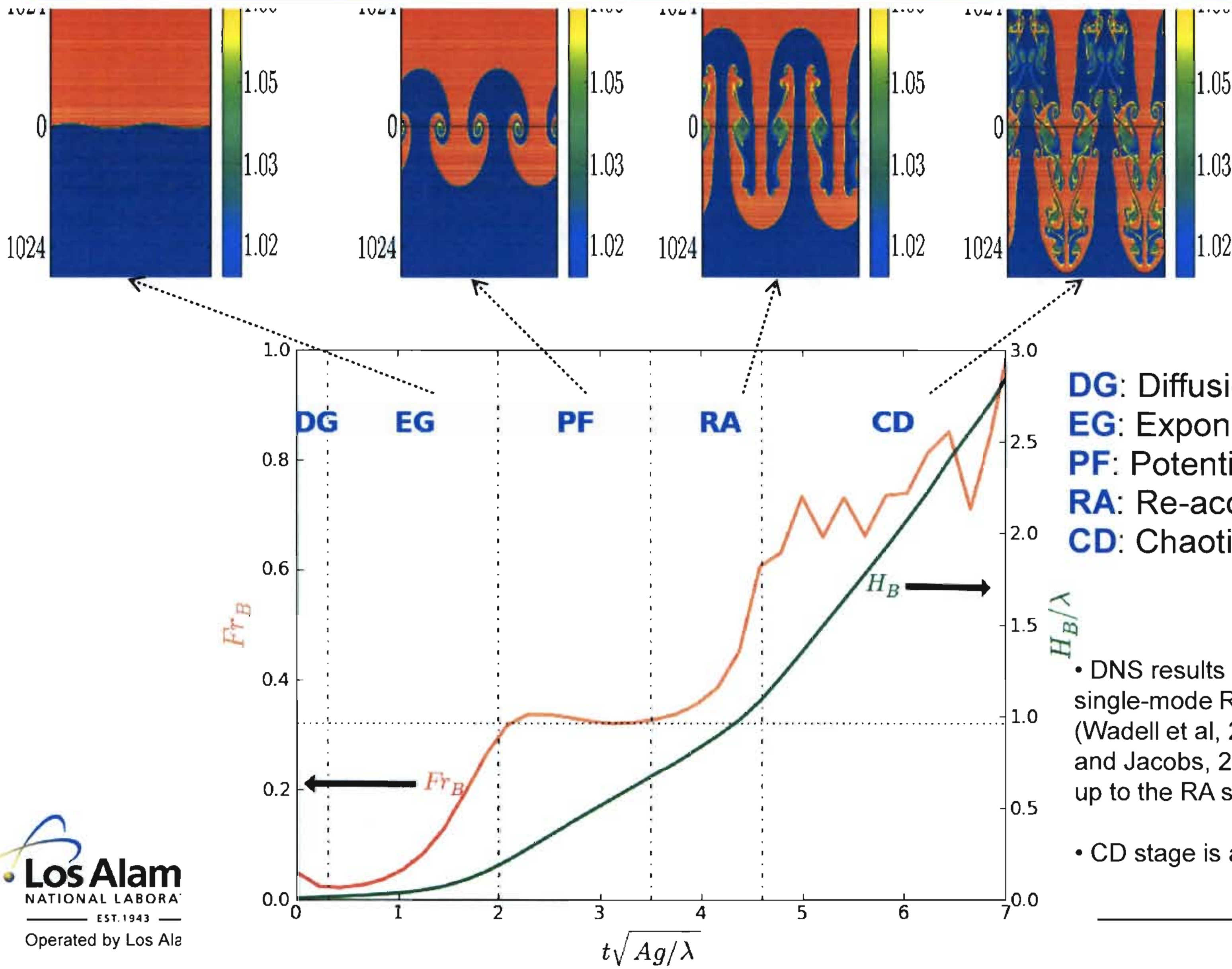

DG: Diffusional growth
EG: Exponential growth
PF: Potential flow
RA: Re-acceleration
CD: Chaotic development

- DNS results match the available single-mode RTI experiments (Wadell et al, 2001, and Willkinson and Jacobs, 2007) which extend up to the RA stage.

- CD stage is a new finding.

Multi-mode Rayleigh-Taylor instability: A=0.75, grid size 4096^2 x4032

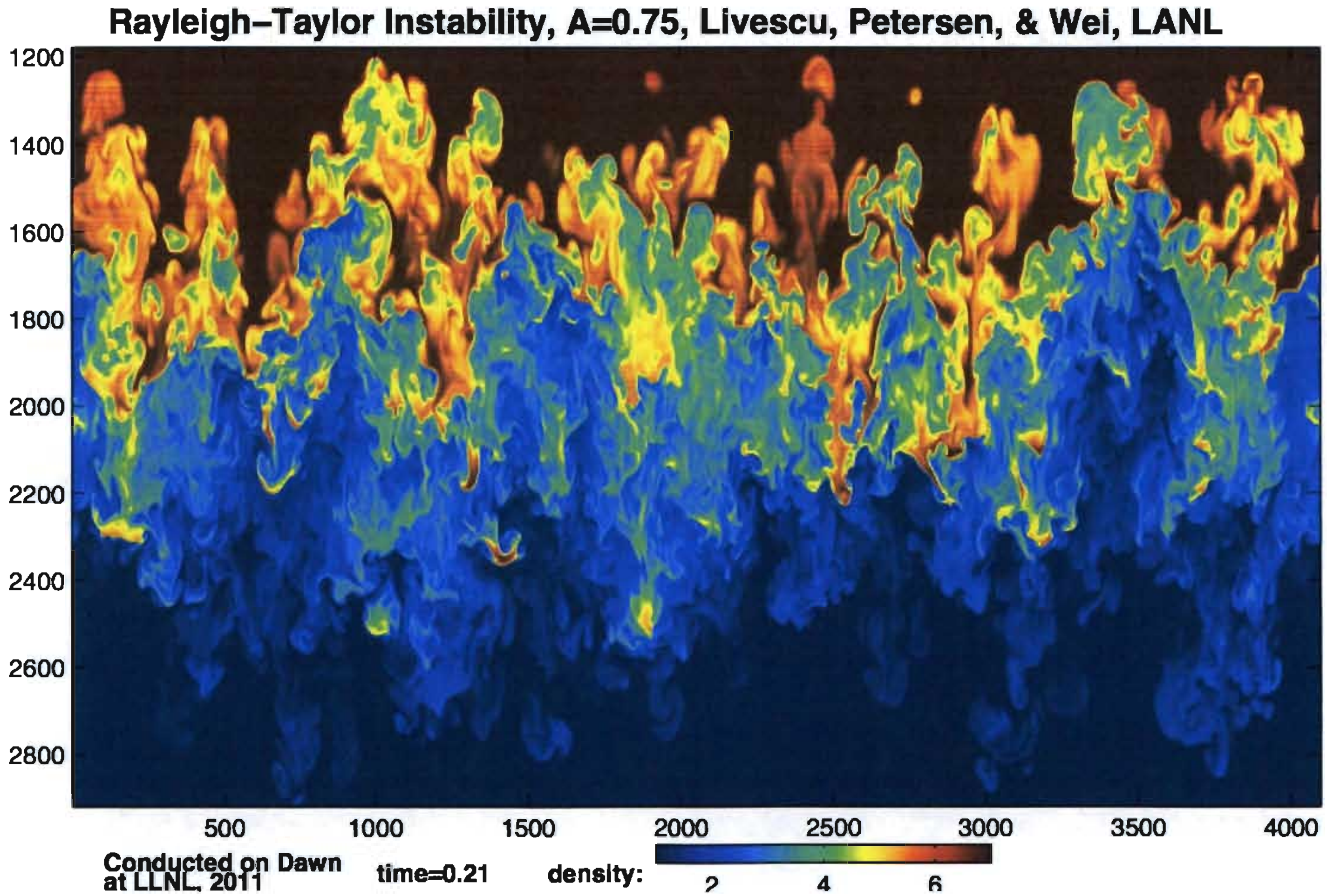

Global measures: mixing layer growth for different perturbation spectra

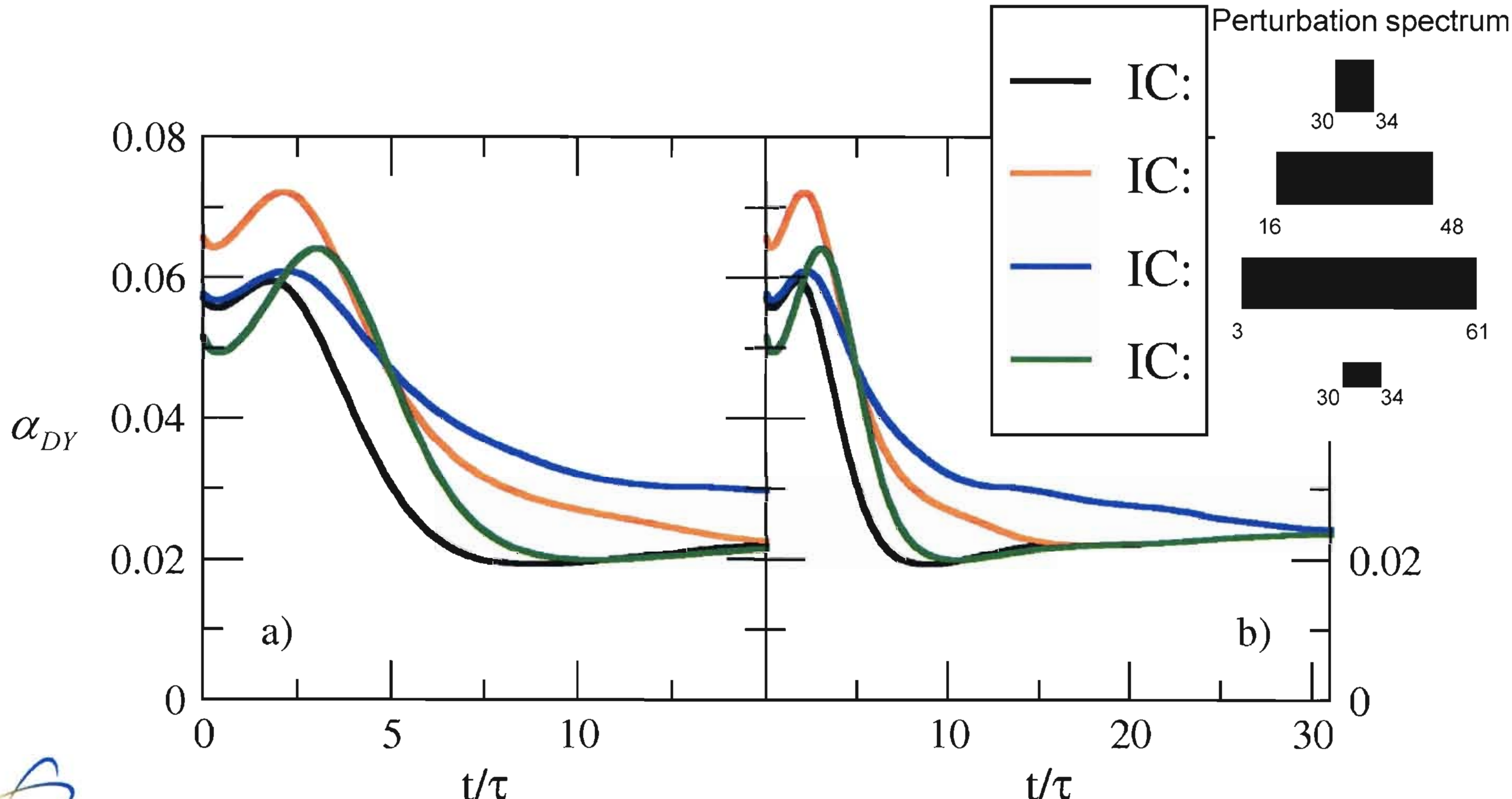

Summary and conclusions

- An overview of initial condition dependence on transition to turbulence in single-, two, and multi-mode RTI using data from high resolution DNS has been given.

- A new stage has been found in the single-mode RTI evolution, with complex vortical interactions and chaotic growth. This stage can be seen only at high Reynolds numbers; corresponding simulations require high resolution .

- A new mechanism for instability growth, by material ejections due to the induced velocity generated by vortex pair interactions, has been found. In two-mode RTI, this mechanism can effectively be controlled through symmetries, or lack thereof, in IC.

- Material ejections are strongest in the single-mode RTI. Multi-mode RTI with long wavelength perturbations or confined RTI also exhibits this growth mechanism resulting in increased growth rate, alpha.

Single Mode Model Results

$$\eta_2 = -\frac{k}{8} + \left(\frac{k}{8} + \eta_2(0)\right) e^{-2k(\eta_0 - \eta_0(0))}$$

$$\ddot{\eta}_0 \frac{k^2 - 4A_T k\eta_2 - 32A_T\eta_2^2}{4(k - 8\eta_2)} + \dot{\eta}_0^2 k^2 \frac{(5A_T - 4)k^2 + 16(2A_T - 3)k\eta_2 + 64A_T\eta_2^2}{8(k - 8\eta_2)^2} + A_T g\eta_2 = 0$$

$$\eta_2(t \to \infty) = -\frac{k}{8} \qquad U = \sqrt{\frac{2A_T}{1 + A_T}\frac{g}{k}}$$

For spikes

$$\eta \to -\eta \qquad A_T \to -A_T \qquad g \to -g$$

The Goncharov model predicts the bubble growth up to first saturation

Multi-mode Study Using Ballistic ODE's to Predict the Envelope of the RT Bubble Mix Region

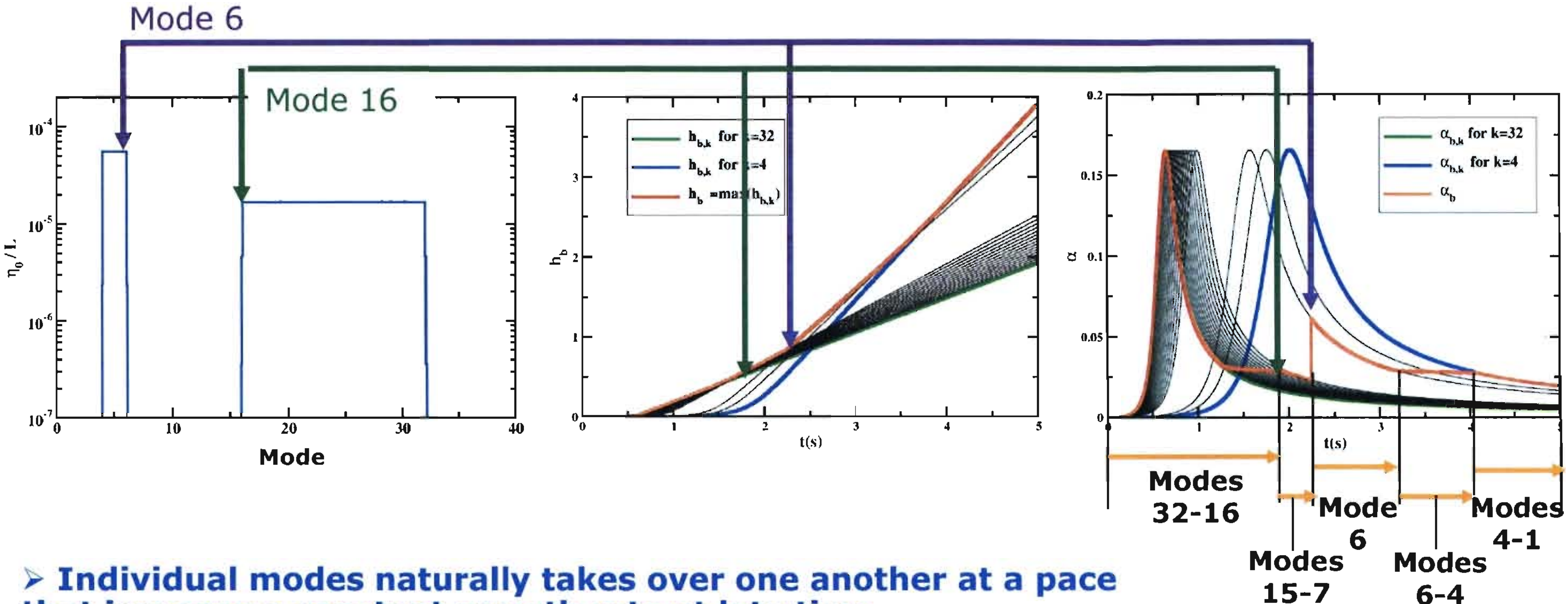

- Individual modes naturally takes over one another at a pace that imposes a constant growth rate at late time
- Each band of the initial spectrum is 'seen' in the growth rate
- At late time, h_b is governed by the longest wavelength evolution
- Our ballistic model cannot be used after the longest wavelength of the initial perturbation spectrum has become dominant

$$\alpha = \frac{U^2}{4Agh}$$

A Weakly Nonlinear Model for Multimode Perturbation

Haan's model:

$$\Delta\phi^{h/l} = 0$$

$$Z(\vec{x},t) = \sum_{\vec{k}} Z_k(t) e^{i\vec{k}\cdot\vec{x}}$$

$$\partial_t Z + \partial_x Z \cdot \partial_x \phi\big|_Z + \partial_y Z \cdot \partial_y \phi\big|_Z = \partial_z \phi\big|_Z$$

$$\phi^h(\vec{x},z,t) = \sum_{\vec{k}} \phi_k^h(t) e^{-kz} e^{i\vec{k}\cdot\vec{x}}$$

$$\left[\rho\left(\partial_t\phi + \frac{1}{2}v^2 + gZ\right)\right] = P$$

$$\phi^l(\vec{x},z,t) = \sum_{\vec{k}} \phi_k^l(t) e^{kz} e^{i\vec{k}\cdot\vec{x}}$$

$$\ddot{Z}_k = \gamma(k)^2 Z_k + A_T k \sum_{\vec{m}} \left\{ \ddot{Z}_m Z_n \left(1 - \hat{m}\cdot\hat{k}\right) + \dot{Z}_m \dot{Z}_n \left(\frac{1}{2} - \hat{m}\cdot\hat{k} - \frac{1}{2}\hat{m}\cdot\hat{n}\right)\right\}$$

Mode coupling term

$$\vec{n} = \vec{k} - \vec{m} \qquad \gamma(k) = \sqrt{A_T g k}$$

Haan's model allow mode generation